PhD degree in Molecular Medicine (curriculum Molecular Oncology)
European School of Molecular Medicine (SEMM)
University of Milan and University of Naples "Federico II"
Settore disciplinare: Med/04

Mechanistic investigation of BRD4 inhibition in MYC dependent tumors

Elisa Donato
IIT@SEMM, Milan
Matricola n. R09849

Supervisor: *Dr. Stefano Campaner*
IIT@SEMM, Milan

Anno accademico 2014-2015

Table of contents

Contents

List of abbreviations

4-OHT
4-Hydroxytamoxifen, 31
4-sU
4-thioUridine, 95
AchR
Acetylcholine Receptor, 53
AML
Acute Myeloid Leukemias, 12
A-PE
Anti-Pause Enhancer, 18
ASOs
AntiSense Oligonucleotides, 14
BD
Bromodomain, 15
BET
Bromo and ExtraTerminal domain containing proteins, 15
BL
Burkitt's Lymphomas, 12
BM
Bone Marrow, 23
BR
Basic Region, 3
BrdU
Bromo deoxy Uridine, 32
BSA
Bovine Serum Albumin, 32
CDK
Cyclin Dependent Kinase, 11
CDK7
Cyclin Dependent Kinase 7, 9
CDK9
Cyclin Dependent Kinase 9, 9
ChIPqPCR
Chromatin ImmunoPrecipitation followed by quantitative Polymerase Chain Reaction, 52
ChIPseq
Chromatin ImmunoPrecipitation followed by highthroughput sequencing, 57
CTD
Carboxy Terminal Domain, 9
DDR
DNA Damage Response, 20
DEGs
Differentially Expressed Genes, 69
DLBCL
Diffuse Large B Cell Lymphomas, 23
DMSO
Dimethyl Sulfoxide, 32
DMVs
DNA Methylation Valleys, 23
DNA
Deoxyribonucleic Acid, 3
DOWN
Downregulated, 83
DSIF
DRB Sensitive Inducing Factor, 9
EMT
Epithelial to Mesenchymal Transition, 19
ER
Estrogen Receptor, 77
ET
Extra-terminal domain, 15
EtOH
Ethanol, 32
FA
Formaldehyde, 62
GLUT
Glutaraldehyde, 62
GO
Gene Ontology, 69
GSEA
Gene Set Enrichment Analysis, 69
HATs
Histone Acetyl Transferases, 7
HLH-LZ
Helix Loop Helix- Leucine Zipper, 3
HSCs
Hematopoietic Stem Cells, 23
IgH
ImmunoGlobulin Heavy chain, 26
Inr
Initiator, 4
JMJD6
Jumonji Domain containing 6, 18
KI
Knock In, 81
LCRs
Locus Control Regions, 23
MB
Myc homology boxes, 3
MEFs
Murine Embrionic Fibroblasts, 29
mESCs
murine Embrionic Stem Cells, 22
MM
Multiple Myeloma, 12
mRNA
messenger RNA, 5
MSigDB
Molecular Signature DataBase, 69
NELF
Negative Elongation Factor, 9

Figure Index

I. Abstract

The *c-myc* gene encodes for a transcription factor involved in the regulation of different cellular mechanisms, ranging from cell cycle control and apoptosis to cellular metabolism. Myc is frequently altered in human cancer either by genomic rearrangement or by alteration of upstream regulatory pathways. Myc crucial role both in tumor formation and maintenance makes it an attractive molecular target for cancer therapy. Unfortunately, Myc is intrinsically resilient to direct pharmacological targeting using small molecules.

To overcome this issue, alternative therapeutic avenues have been explored. In the last years, independent groups showed that BET proteins inhibition leads to a strong Myc downregulation in Multiple Myelomas and Acute Myeloid Leukemias, with consequent cell cycle arrest and tumor regression. To support the hypothesis of a direct and specific effect on Myc levels mediated by BET proteins, two different working models were proposed depending on *c-myc* location (translocated versus endogenous).

In order to extend these observations and improve our understanding of the mechanism of action of BETs inhibitors, we evaluated global transcriptional alteration and chromatin profiles in Burkitt's Lymphomas in response to JQ1.

Our results demonstrate that BETs inhibitors efficacy is dependent on global alteration of RNA PolII dynamics, due to the role of BRD4 in regulating elongation. Yet, despite a pervasive eviction of BRD4 from chromatin and the global effect on RNA PolII observed following BETs inhibition, the transcriptional alterations are limited to a subset of genes. These genes are characterized by promoter regions heavily marked by H3K27Ac, high binding of BRD4 and Transcription Factors (Myc and E2F1) and RNA PolII. These JQ1 sensitive genes are consistent among different cell lines and characterized by high expression levels.

Prominent promoter saturation and high RNA PolII pausing render their expression rate-limited by transcriptional elongation. Indeed the same genes are selectively targeted by pharmacological treatments affecting components of the elongation machinery. Thus, selective transcriptional effects following JQ1 treatment are linked to BETs role in regulating transcriptional elongation. These observations highlight the role of BETs protein in regulating gene expression and provide a rationale to explain how broad inhibition of elongation may lead to a selective transcriptional response.

II. Introduction

MYC

The *myc* gene was first identified as the avian retroviral oncogene *v-myc* responsible of the transforming capacity of the MC29 avian virus (Sheiness and Bishop, 1979), only later its cellular counterpart was identified (Vennstrom et al., 1982). *c-myc* is a member of a larger family comprising also L-Myc and N-Myc. All the family members share high structural homology and exert their transcriptional function by binding to the cofactor Max (Blackwood and Eisenman, 1991). The c-Myc protein is characterized by different N-terminal Myc homology Boxes (MB), which are also conserved in the other family members. In particular, the most relevant for Myc function are MBI and MBII, that respectively contain key phosphorylation sites (Thr58 and Ser62) and binding domains for co-activators as TRRAP. The Myc protein contains also a Transactivator Domain (TAD), needed for the activation of transcription, and a Nuclear Localization Signal (NLS), necessary for the proper subcellular localization. The helix-loop-helix-leucine-zipper domain (HLH-LZ) and the basic region (BR) are located at the C-terminus and are necessary for the dimerization with Max and for the binding to specific DNA sequences, respectively.

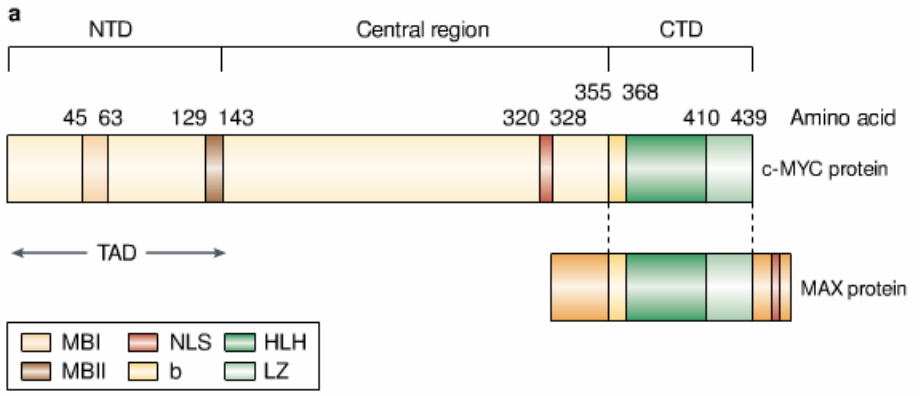

Fig. 1 Myc protein structure
Schematic representation of the Myc protein structure where an N-terminal Domain (NTD), a central region and a C-terminal Domain (CTD) are highlighted. The NTD contains the Trans-Activator Domain (TAD), necessary for gene activation, and the Myc homology Boxes (MB). In particular MBI and MBII are depicted: MBI contains key phospho-sites (Thr58 and Ser62), while MBII contains protein-protein interaction domain. In the central region is located the Nuclear Localization Signal (NLS). Finally, the CTD contains the Helix-Loop-Helix-Leucine-Zipper (HLH-LZ) domain, necessary for the dimerization with Max, and the Basic region (b) needed for the binding to the DNA.
Figure adapted from "c-myc: more than just a matter of life and death." (Pelengaris et al., 2002)

Transcriptional and post-translational regulation of Myc

Since Myc is involved in different cellular processes and its deregulation is associated to tumor formation, Myc expression is tightly regulated at different levels, ranging from the transcriptional control to protein degradation.

The *c-myc* gene is characterized by the presence of at least 4 different promoters (P0, P1, P2 and P3) located before the second exon, which contains the starting codon. The most used promoter is P2 that, together with P1, contains both TATA boxes and Initiator (Inr) sequences. P0 and P3 are less used and they are TATA-less promoters (Wierstra and Alves, 2008).

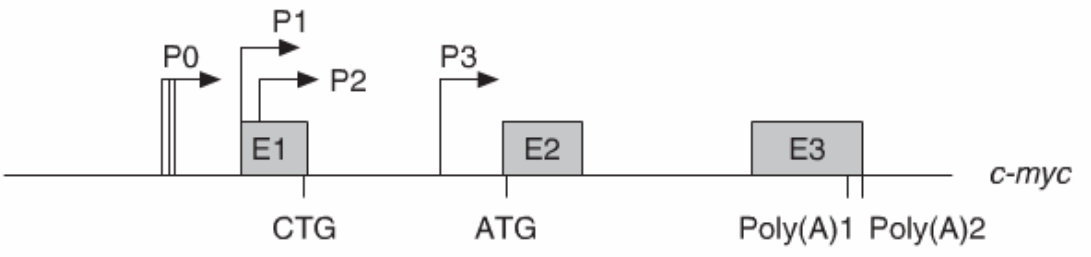

Fig. 2 The *c-myc* gene structure
The *c-myc* gene is composed by 3 exons, with the starting codon located in the second exon. At least 4 different promoters, located upstream of the second exon, were identified so far.
Figure adapted from "The c-myc Promoter: Still MysterY and Challenge" (Wierstra and Alves, 2008)

In Myc promoter a plethora of binding sites for different TFs were identified (Wierstra and Alves, 2008). Evidences were provided for the positive regulation of *c-myc* transcription mediated by WNT (He et al., 1998; Sansom et al., 2007), JAK/STAT (Bromberg et al., 1999; Kiuchi et al., 1999), Notch (Palomero et al., 2006; Sharma et al., 2006; Weng et al., 2006) and Hedgehog (Berman et al., 2002; Sicklick et al., 2006), while TGFβ represses *c-myc* transcription (Chen et al., 2002; Frederick et al., 2004).

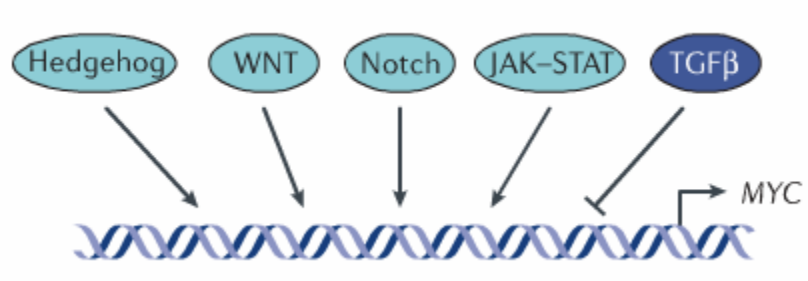

Fig. 3 Transcriptional regulation of the *c-myc* gene
c-myc transcription is regulated by a plethora of different signaling pathways. Among the most relevant, activating signals are mediated by Hedgehog, WNT, Notch, JAK-STAT pathways, while negative regulation is exerted by TGFβ signaling.
Figure adapted from "MYC: connecting selective transcriptional control to global RNA production" (Kress et al., 2015)

Myc is one of the first genes for which the regulation of the elongation step and the presence of RNA PolII paused at the promoter were observed. Indeed, Myc is not expressed in quiescent cells but its transcription is immediately activated in response to mitogenic stimuli. This immediate response is favored by the presence of promoter-proximal paused RNA PolII, ready to be released as soon as the stimulus is triggered (Bentley and Groudine, 1986; Nepveu and Marcu, 1986). Once Myc is transcribed, it could be regulated both at the post-transcriptional and post-translational levels. Indeed both, Myc mRNA and protein have a very short half life (20-30 minutes) due to active mechanisms that shorten the mRNA or destabilize the protein through phosphorylation of key residues. In particular, mitogenic stimuli induce the phosphorylation on Ser62, necessary for the stabilization and activation of Myc protein. At the same time, phospho-Ser62 serves as a scaffold for the recruitment of GSK3β that in turn phosphorylates Thr58, thus causing the subsequent ubiquitination and degradation of the Myc protein (Meyer and Penn, 2008; Vervoorts et al., 2006).

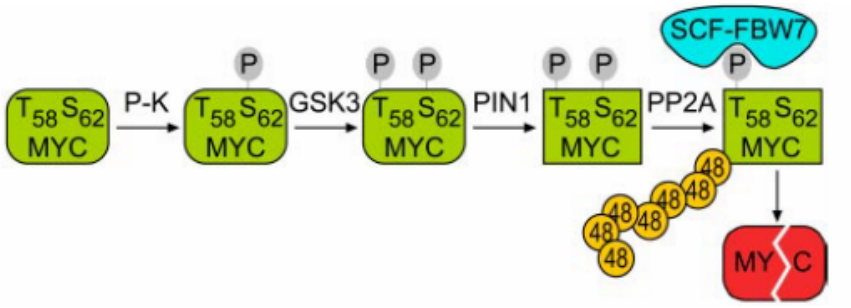

Fig. 4 Schematic representation of Myc protein degradation
Two critical residues are responsible of Myc protein degradation: Thr58 and Ser62. Ser62 is phosphorylated in response to mitogenic stimuli and, while enhancing Myc activity, creates a scaffold for the binding of GSK3β that leads to the phosphorylation of Thr58. After this second phosphorylation event, the oncosuppressor FBW7 is bound and it recruits SCF, favoring Myc ubiquitination and proteosomal degradation.
Figure adapted from "The Ins and Outs of MYC Regulation by Posttranslational Mechanisms" (Vervoorts et al., 2006) © 2006 by The American Society for Biochemistry and Molecular Biology, Inc.

Besides the direct regulation of Myc mRNA and protein, another layer of control is represented by the availability of Max. Indeed, Myc recognition of the DNA target sequences is mediated by the dimerization with its partner Max (Amati et al., 1992). Differently from Myc, Max is constitutively expressed and it could dimerize also with other HLH-LZ proteins as Mad, a Myc antagonist that, recognizing Myc target sequences, represses genes that are usually activated by Myc. Thus, the amount of free Max and the balance of Myc-Max and Mad-Max dimers represent an additional step in the control of Myc activity (Grandori et al., 2000).

Myc as transcription activator

The Myc-Max heterodimer shows a preference for specific DNA sequences, called E boxes (CACGTG). Its binding to chromatin allows the recruitment of different co-activators and chromatin remodeling factors such as pTEFb (Rahl et al., 2010) TRRAP (McMahon et al., 1998) CBP and p300 (Vervoorts et al., 2003), as well as RNA PolII itself (Koch et al., 2007). Indeed, the function of Myc as transcription activator could be simplistically summarized as a first step of recruitment of chromatin modifiers, favoring the deposition of marks of transcriptional activation, and a second step of enhancement of elongation, favoring the release of promoter paused RNA PolII. Different evidences

showed that Myc, via its MBII domain, could directly bind TRRAP (McMahon et al., 1998) and recruits on the promoter Histone Acetyl Transferases (HATs) (McMahon et al., 2000). Finally, after inducing chromatin acetylation at promoters, Myc could recruit RNA PolII and pTEFb to enhance the release of the stalled RNA PolII and induce the transcriptional elongation (Eberhardy and Farnham, 2002; Rahl et al., 2010). Myc is not a pioneer factor, meaning that it is not able to bind closed chromatin and cannot recognize target sequences when they are buried into the nucleosome structure. Indeed, it was demonstrated in reprogramming experiments that, while Oct4, Sox2, Klf4 (OSK) were able to act as pioneer factors by binding closed chromatin and unwinding the DNA, Myc only bound the DNA subsequently to OSK (Soufi et al., 2012).

Moreover, Myc binding to its target sequences required the presence of specific chromatin modifications characteristic of active regulatory regions as H3K4me1, H3K4me2, H3K4me3, H3K27Ac. Furthermore, DNA sequences bound by Myc are usually located in regions enriched for CpG islands (Sabò et al., 2014).

Different mechanisms have been proposed for Myc recognition and binding to its target sequences: one above all better summarizes what is known so far on Myc and predicts that target recognition occurs as a multistep process with a first phase of protein-protein interaction with the already assembled basal transcription machinery (Pre-Initiation Complex (PIC)) and with the chromatin "readers" that decipher the histone modifications. Once these regions are identified, the Myc-Max heterodimer makes contact with DNA and scans the open chromatin stretch in order to find high affinity regions to bind. The recognition of the E-boxes allows the transition from a low-affinity to a high-affinity binding among Myc-Max and the DNA, this interaction is further stabilized by the protein-protein contacts with the basal transcription machinery (Sabò and Amati, 2014).

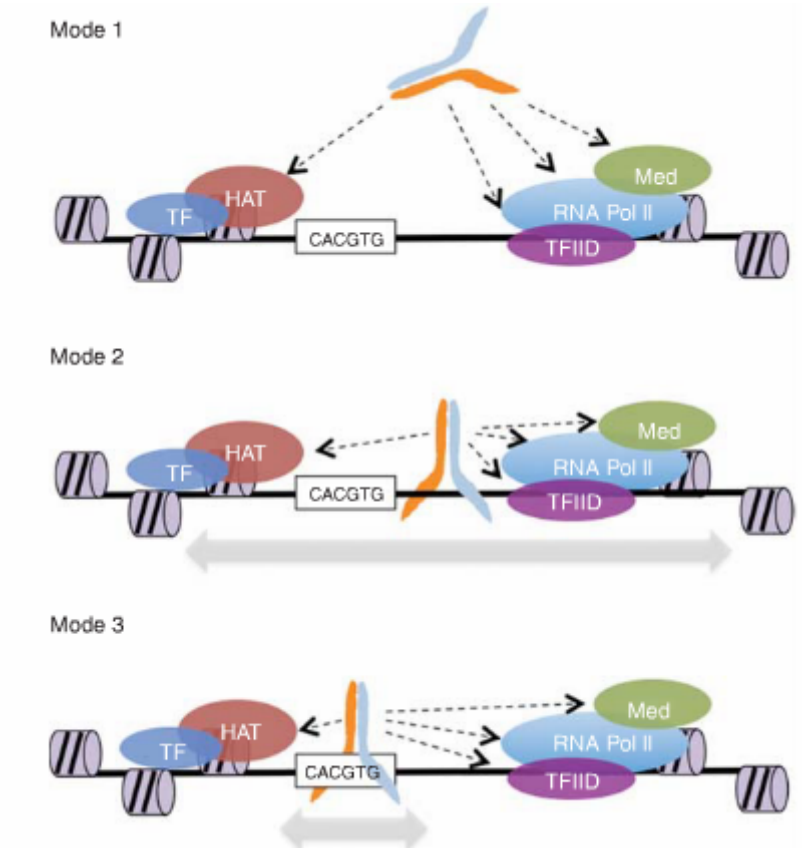

Fig. 5 Schematic model for Myc-Max dimer DNA recognition
The recognition of Myc target sequences, the E-boxes (CACGTG), follows the formation of Myc-Max dimer. Initially, Myc-Max dimer takes contacts with the basal transcription machinery (Pre-Initiation Complex (PIC)) and with chromatin readers. Subsequently, the dimer binds with low affinity and scans the DNA stretch, until the E-box is found and bound with high affinity.
Figure adapted from "Genome Recognition by Myc" (Sabò and Amati, 2014) Copyright © 2014 Cold Spring Harbor Laboratory Press; all rights reserved.

The intensity and the number of sites bound by Myc change strongly based on the cell line analyzed and depend on the endogenous Myc levels (Sabò and Amati, 2014). There is ample evidence showing that, when expressed at physiological levels, Myc binds only canonical E-boxes, preferentially at the promoter, with relative high affinity. In cells where Myc is deregulated and overexpressed, its binding is no longer restricted to specific DNA sequences, but can also occurs on not-canonical E-boxes present in distal regulatory regions. In this scenario, virtually all the regulatory regions are bound by Myc causing a phenomenon called "invasion" (Sabò et al., 2014).

Myc regulates transcriptional elongation

Myc can regulate the expression of its target genes either by activating or repressing them after the binding to regulatory regions usually located on the promoter. The promoter is defined as a DNA region surrounding the Transcription Start Site (TSS) and that is essential both for the assembly of the Pre-Initiation Complex (PIC) and for the recruitment of specific Transcription Factors (TFs) that ensure the fine regulation of the expression of the target genes. Similar to promoters for DNA composition and modular assembly of TFs binding sites, the enhancers can regulate the transcription of associated genes in an orientation- and distance-independent manner.

TFs and co-activators recruited to promoter associated regulatory regions can control gene expression by affecting different steps of the transcription process: initiation, elongation and termination. During the initiation step, RNA PolII and General Transcription Factors are recruited on the promoter. While first studies on gene transcription claimed that the recruitment of RNA PolII represented the limiting step in the regulation of gene expression, recent evidences demonstrated that RNA PolII, once on the TSS, is not immediately engaged in the transcription process, but instead it is retained on the promoter in a stalled condition (Krumm et al., 1992; Plet et al., 1995; Rasmussen and Lis, 1993; Rougvie and Lis, 1988; Strobl and Eick, 1992). Indeed, different modifications are required to prime RNA PolII and enhance its processivity, among which the most characterized are the phosphorylation on Serine 5 (Ser5) and Serine 2 (Ser2) of the Carboxy-Terminal Domain (CTD). The phospho-residue on Ser5 is needed for RNA PolII priming and it is added by CDK7, a component of the $TF_{II}H$ in the PIC complex (Sainsbury et al., 2015). Instead, the Ser2 is phosphorylated by CDK9 that, together with Cyclin T1, is part of the positive Elongation Factor (pTEFb). The phosphorylation on Ser2 is necessary for promoter clearance and the progression of transcription through the elongation step. pTEFb further pushes the RNA PolII toward the elongating form phosphorylating negative transcription regulators as NELF and DSIF, that in physiological

condition block RNA PolII in a promoter-proximal paused state (Buratowski, 2009; Jonkers and Lis, 2015). Finally, the transcription process ends as soon as RNA PolII encounters the Transcription End Sites (TES), that contain the information for its release from chromatin (Porrua and Libri, 2015).

Recent evidences show that Myc can actively enhance the elongation step by directly recruiting pTEFb on the promoter of its targets (Rahl et al., 2010). Accordingly, Myc-Max inhibition caused a strong reduction in the elongating and Ser2 phosphorylated RNA PolII, while no changes were observed on RNA PolII recruited on the promoter or on the amount of polymerase phosphorylated on Ser5 (Rahl et al., 2010).

Myc role in cell cycle progression and apoptosis

Myc regulates transcriptional programs involved in different aspects of cell life, ranging from the cell cycle control to regulation of cell growth, apoptosis, cell metabolism and ribosome biogenesis (Ponzielli et al., 2005).

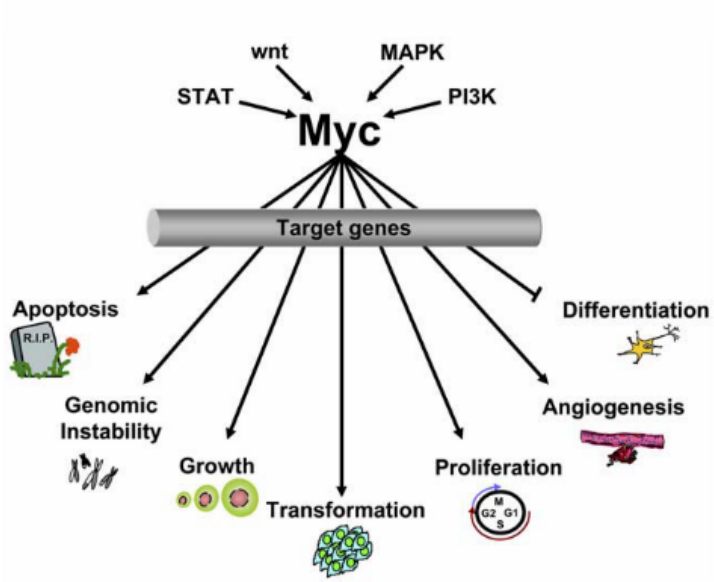

Fig. 6 Myc regulatory network
Myc is a key transcription factor involved in the regulation of different biological process, ranging from cell cycle progression and apoptosis to angiogenesis and cellular differentiation.
Figure adapted from "Cancer therapeutics; Targeting the dark side of Myc" (Ponzielli et al., 2005)

Since Myc is a transcription factor, it exerts its function through the regulation of key genes involved in different processes. Indeed, the positive effect exerted by Myc in the control of the cell cycle can be explained by the transcriptional activation mediated by Myc of genes essential for the cell cycle progression, such as Cyclin D1, D2, E1, CDC25A, E2F1, E2F2, CDK4 (Meyer and Penn, 2008; Obaya et al., 1999; Oster et al., 2002). Beside the transcription activator function, Myc can act as a transcriptional repressor, inhibiting the expression of specific genes. This is particularly relevant for cell cycle progression, where Myc importance is not only limited to the activation of the genes mentioned above, but it is critical also for the repression of cell cycle check point genes (GADD45 and GADD153) or for the inhibition of CDK inhibitors (Meyer and Penn, 2008). Myc is also involved in the regulation of apoptosis by acting on the ARF-MDM2-p53 axis, both activating ARF and concomitantly inhibiting p21. This aspect of Myc biology is particularly relevant in tumor onset: indeed, different publications clearly demonstrated that oncogenic Myc and concomitant inactivation of p53 or increased expression of anti-apoptotic factors as BCL2 led to an acceleration of tumor onset (Meyer and Penn, 2008; Strasser et al., 1990).

Myc in cancer

Given its crucial role in different aspects of cell life and in particular in the control of cell cycle and cell growth, Myc deregulation is associated to different types of cancer. Indeed, Myc expression is altered in a wide spectrum of tumors, ranging from hematological to solid tumors. The most common alteration of Myc expression involves gene translocation and amplification, while point mutations are more rare and usually lead to an increase in protein stability. In particular, Myc amplification is more frequent in solid tumors, indeed it is found in ~30% of Hepatocellular carcinoma, in 9-45% of Breast cancers and in 40% of Ovarian cancers; while Myc translocation is commonly associated to hematological disorders, in fact it is present in 100% of Burkitt's Lymphomas (BL) and ~15% of Multiple Myeloma (MM), where *c-myc* is translocated under the control of the Immunoglobulin regulatory regions (Vita and Henriksson, 2006). The translocation responsible of the onset of BL involves chromosome 8, in which *c-myc* is located, and chromosome 14, 2 or 22 where the regulatory regions for the immunoglobulin heavy and light chains are located (Molyneux et al., 2012).

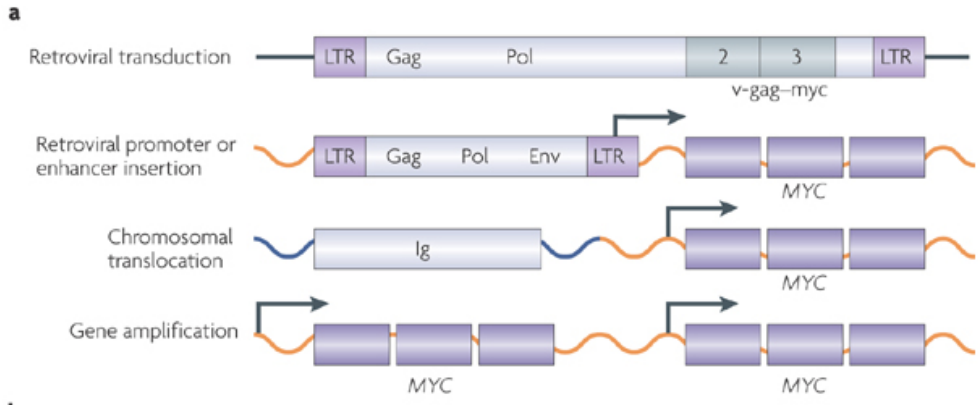

Fig. 7 Schematic representation of the *c-myc* gene rearrangement
Myc deregulation in cancer could be achieved by different mechanisms as gene amplification, typical of solid tumors, or genomic rearrangement, typical of hematopoietic malignancies. In particular 100% of BL and ~15% of MM are characterized by chromosomal translocation that juxtaposes the *c-myc* locus to the Immunoglobulin regulatory regions of the heavy, or more rarely of the light, chain.
Figure adapted from "Reflecting on 25 years with Myc" (Meyer and Penn, 2008)

Beside these gross genomic alterations, Myc expression can be deregulated also by the impairment of upstream pathways. One example is provided by Acute Myeloid Leukemia (AML) where the fusion oncoprotein MLL-AF4/9 directly activates *c-myc* transcription.

Furthermore, key Myc aminoacids could be mutated in cancer: one hotspot is represented by the residue Thr58 that when phosphorylated leads to Myc degradation via proteasome. Mutations on this residue not only ensure a longer protein half life, but also confer oncogenic properties separating the regulation of the cell cycle progression from the control of the apoptosis mediated by Myc. Indeed, mutant Myc on Thr58 is unable to induce BIM expression that inhibits BCL2, with the final result of the bypass of the apoptotic response and an acceleration of lymphomagenesis (Hemann et al., 2005).

Myc as a therapeutic target

As mentioned above, Myc is often associated to cancer since it is necessary both for tumor formation and tumor maintenance. The central role exerted by Myc in tumor maintenance was highlighted in experiments using conditional mice in which Myc expression could be modulated in a reversible way. In particular, if Myc expression was switched off in established tumors, tumor shrinkage and regression were observed, both in hepatocellular carcinoma (Shachaf et al., 2004) and in pancreatic cancer (Pelengaris et al., 2002a). It is worth to note that the response to Myc downregulation is tumor-type specific, since lymphomas undergo apoptosis, osteosarcoma cells are forced to differentiate while hepatocellular carcinomas show an heterogeneous response, indeed the vast majority of carcinoma cells die for apoptosis and few cells remain dormant and ready to re-establish a new tumor once Myc expression is restored (Gabay et al., 2014). The crucial role of Myc in tumor maintenance was demonstrated also in tumors driven by other oncogenes, as in Kras driven lung cancers (Soucek et al., 2008). Indeed, modulating the expression of a Myc dominant negative (Omomyc) (Soucek et al., 1998), and therefore blocking Myc transcriptional activity, was sufficient to cause strong regression also in already established Kras tumor. Since Myc is essential for the regulation of normal cell proliferation, this study assessed also the side effects of a systemic Myc inhibition. Indeed,

a prolonged Omomyc induction led to defects in spermatogenesis, hair production and epidermal thickness. However, these effects were well tolerated and reversible, since the animals did not show any weight loss and, after Myc restoration, the proliferation in the normal tissues was reinstated (Soucek et al., 2008).

Due to its involvement both in tumor formation and maintenance and since its downregulation is clearly associated to tumor regression and cellular differentiation, the possibility to target Myc represents a tempting therapeutic option. Unfortunately, Myc, as other transcription factor, does not possess a ternary structure suitable for direct drug targeting. Thus, different approaches have been used in order to overcome this obstacle: the main strategies evaluated so far range from inhibition of *c-myc* expression, using AntiSense Oligonucleotides (ASOs), to transcription inhibition thanks to the use of Triple helix Forming Oligonucleotides (TFOs) or porphyrins that create a physical obstacle for RNA PolII. Another promising alternative is represented by the possibility to prevent the dimerization with Max, through the use of Myc dominant negative, as Omomyc (Soucek et al., 1998, 2002). Each of these approaches shows limitations in particular for clinical applications, concerning molecules stability, half-life and feasibility to reach the right target (Ponzielli et al., 2005).

BET proteins

BET family

Chromatin is a target of several Post-Translation Modifications (PTMs), ranging from acetylation to ubiquitination, which are produced by a class of proteins collectively called "writers". These modifications are thought to provide a "code", which contains epigenetic information. This code is deciphered by proteins called "readers" which are able to recognize specific PTMs, and eventually reset by "erasers", proteins capable of removing PMTs. (Filippakopoulos and Knapp, 2014).

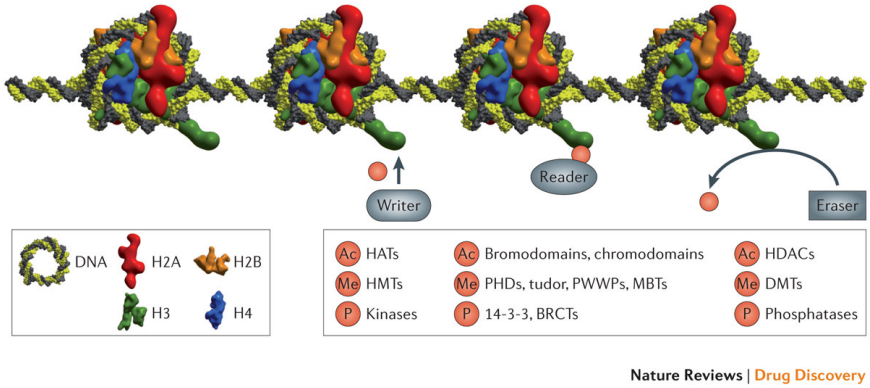

Fig. 8 Histone modifications and proteins involved in histone modification
Histone proteins usually are subjected to post translation modification mediated by "writers" that are devoted to add phospho, methyl, acetyl or other groups. This code is read by a specific class of proteins called "readers" and eventually removed by "erasers". Histone Acetyl Transferares, Kinases and Histone Methyl Transferases are members of the writer class; among the readers are included bromodomain and chromodomain, while Histone Deacetylases, Phosphatases and Demethylases composed the eraser class.
Figure adapted from "Targeting bromodomains: epigenetic readers of lysine acetylation" (Filippakopoulos and Knapp, 2014)

In particular, the acetyl group is added to lysines by the Histone Acetyl Transferases (HATs) and is detected by bromodomain containing proteins, such as those belonging to the BET family (Bromodomain and Extra-Terminal containing proteins). The BET family is composed of 4 different nuclear proteins (BRD2, BRD3, BRD4 and BRDT) characterized by two tandem bromodomains (BD) and an Extra-terminal (ET) domain.

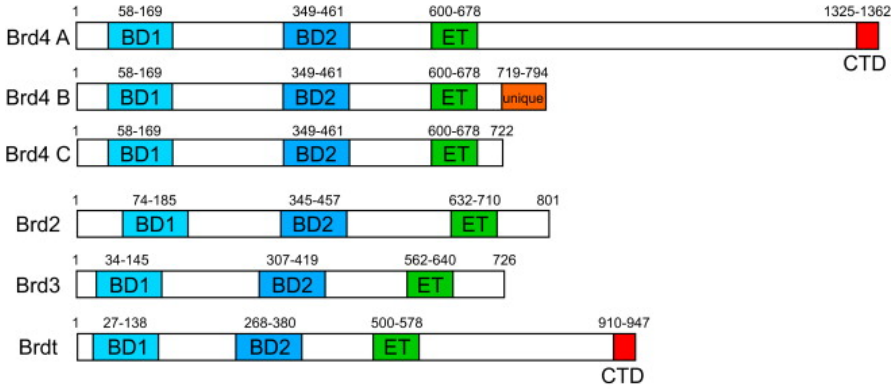

Fig. 9 Schematic representation of BETs proteins
The BET family is composed of 4 different members: BRD2, BRD3, BRD4 and BRDT. All the members are characterized by 2 N-terminal bromodomains (BD) and one Extra-Terminal domain (ET). While for BRD2, BRD3 and BRDT only one isoform is known, for BRD4 3 different isoforms exist.
Figure from "The Mechanisms behind the Therapeutic Activity of BET Bromodomain Inhibition" (Shi and Vakoc, 2014) ©2014 Elsevier Inc.

The bromodomain was first identified in the Drosophila *brahma* gene and is composed by 4 α-helices and 2 loops that create a hydrophobic pocket where the acetylated lysines are bound. In the human genome 61 bromodomains have been identified, distributed in 46 different proteins that cluster in 8 different families.

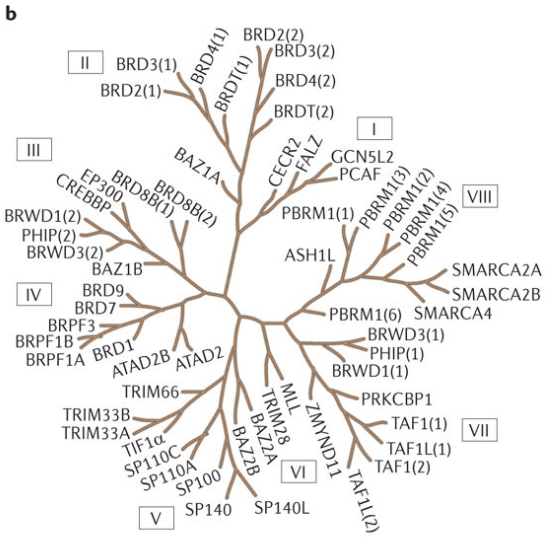

Fig. 10 Phylogenetic for bromodomain proteins
In humans the bromodomain containing proteins are divided in 8 different classes, based on protein structure. In total, 61 different bromodomains organized in 46 different proteins were indentified.
Figure adapted from "Targeting bromodomains: epigenetic readers of lysine acetylation" (Filippakopoulos and Knapp, 2014) © 2014 Macmillan Publishers Limited. All Rights Reserved.

Thanks to its peculiar 3D structure, the bromodomain pocket is amenable to small molecule targeting. Indeed, in the recent years different BET protein inhibitors, mimicking the acetyl lysines or blocking the bromodomain pocket, have been synthesized (Filippakopoulos and Knapp, 2014). The scientific community has extensively taken

advantage of BET inhibitors in order to study BETs mechanism of action and their involvement in different pathologies.

BETs as cell cycle progression regulators

BRD2 and BRD4 are the BET proteins better characterized. They are ubiquitously expressed, while BRDT expression is limited to the testis. Less is known about BRD3.

Both BRD2 and BRD4 are involved in the cell cycle control and progression, since BRD2 interacts with E2F proteins, necessary for S phase genes transcription, and BRD4 is recruited on the promoter of G1 genes and it is essential for their expression, since BRD4 silencing prevents the progression through the cell cycle after serum starvation (Mochizuki et al., 2008). Furthermore, BRD4 is also critical for G1/S progression since its overexpression led to a block in G1 due to the binding and the sequestration of RFC, a component of DNA replication machinery (Maruyama et al., 2002). Involvement of BRD4 was also demonstrated for the G2/M progression, where it is critical the interaction with SPA-1, a GAP protein (Farina et al., 2004). Indeed, not only BRD4 could bind SPA-1 and enhance its GAP activity, but also SPA-1 could regulate BRD4 subcellular localization, since SPA-1 overexpression led to BRD4 mislocalization in the cytoplasm, blocking G2/M transition (Farina et al., 2004). Furthermore, both BRD2 (Shang et al., 2009) and BRD4 (Houzelstein et al., 2002) deficient mice are not viable, showing severe defects in the development and *in utero* death, respectively. Attempts were made to produce BRD2 hypomorphic mice that are still viable but show severe defects in organogenesis (Wang et al., 2010). The drastic *in vivo* effects caused by deletion of either BRD2 or BRD4 clearly suggested that, even though the two proteins share high level of homology both in the bromodomains and in the extra-terminal domain, BET proteins cannot compensate for the absence of the other family members, thus suggesting that each BET protein may have specific and unique functions.

BETs as transcriptional co-activators

BET proteins are also involved in transcriptional regulation since they can function as co-activators. BRD4 is involved in the release of the promoter-proximal paused RNA PolII, thanks to its ability to recruit pTEFb on the TSS, via the direct binding to Cyclin T1 (Jang et al., 2005; Yang et al., 2005). Recent evidences suggested that BRD4 is an atypical kinase able to phosphorylate RNA PolII on Ser2. In particular, this activity seems to be essential for the first round of RNA PolII phosphorylation, when CDK9 is still repressed (Devaiah et al., 2012). Yet, the lack of a clear kinase-like domain in BRD4 protein may call into question this atypical BRD4 function.

BRD4 affects gene transcription both at the promoter-proximal level, thanks to pTEFb recruitment, and at distal regulatory regions, through the binding with Jumonji Domain containing 6 (JMJD6) (Liu et al., 2013). The interaction and the cooperation among BRD4 and JMJD6 takes place at a subset of distal regulatory regions called anti-pause enhancers (A-PE). The looping of A-PE in the proximity of gene promoters, mediated by the Mediator complex, ensures the activation of gene transcription thanks to the release of promoter-paused RNA PolII. The triggering signal for the release of the RNA PolII is mediated by JMJD6, a de-methylase that removes the methyl group from H4R3me2 and 7SK, thus causing the destabilization of 7SK and the release (and activation) of pTEFb (Liu et al., 2013) (Fig.11).

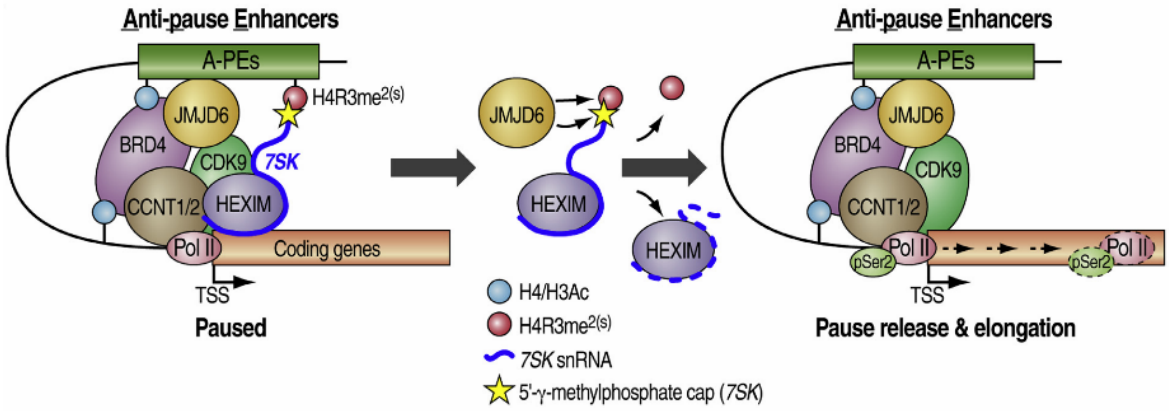

Fig. 11 Model for RNA PolII pause release caused by BRD4-JMJD6 interaction
pTEFb is sequestered in an inactive complex by HEXIM1 and 7SK. When BRD4 and JMJD6, following histone acetylation, are recruited on distal regulatory regions, called anti-pause enhancers (A-PE), JMJD6 enzymatic activity leads to demethylation of both H4R3me2 and 7SK, with the consequent disruption of the inhibitory complex.
Figure adapted from "BRD4 and JMJD6-Associated Anti-Pause Enhancers in Regulation of Transcriptional Pause Release" (Liu et al., 2013) © 2013 Elsevier Inc.

Beside the recognition of acetylated histones, the recruitment of BRD4 on promoters could be mediated also by the interaction with specific transcription factors. This TF mediated BRD4 recruitment was demonstrated for TWIST target genes (Shi et al., 2014). Indeed, TWIST could recruit BRD4 on the regulatory regions of its targets thanks to the binding of TWIST acetylated lysines to BRD4 bromodomains. Once the complex is formed and recruited on the chromatin, BRD4 could enhance the transcription of TWIST targets recruiting pTEFb (Shi et al., 2014). In particular, evidences were provided for genes involved in the Epithelial to Mesenchymal Transition (EMT) and in tumor progression (e.g. WNT5A) (Shi et al., 2014). Furthermore, BRD4 activates the transcription of inflammatory genes thanks to interaction with acetylated RelA, a subunit of NFkB. This interaction is particularly relevant in tumor where BRD4 stabilizes NFkB in the nucleus, allowing the transcription of NFkB targets (Huang et al., 2009). The involvement of BRD4 in the regulation of inflammatory response genes is further supported by the demonstration that treatment with BET inhibitors reduces the graft-versus-host disease after bone marrow transplantation (Sun et al., 2015).

In the scenario of gene transcription regulation, BRD4 can also interact with Nuclear SET Domain-Containing Protein 3 (NSD3) via its ET domain (Rahman et al., 2011). NSD3 is

a methyltransferase that belong to the SET family and that is responsible of the methylation of the histone H3K36, a histone modification typical of active transcription.

BRD4 is implicated in DNA condensation and gene bookmarking

Beside its involvement in gene regulation, BRD4 may also have a structural role in regulating chromatin condensation. Indeed, studies in which BRD4 was silenced, or displaced from the chromatin thanks to the use of a dominant negative isoform, highlighted a global chromatin unfolding with a consequent enlargement of the nuclei and chromatin fragmentation (Wang et al., 2012). This effect on chromatin condensation was recently connected to a BRD4 role in DNA Damage Response (DDR). Indeed, it was demonstrated that BRD4 isoform B is responsible for the maintenance of high order chromatin structure and its silencing was associated to an increased γH2AX signal after irradiation. The BRD4 isoform B structural function and regulation of DDR seems to be mediated by the Condensin II complex and in particular by SMC2 and SMC4, that by compacting chromatin can prevent the onset of DDR signaling (Floyd et al., 2013) .

Beside the involvement in the transcriptional process and in chromatin structure maintenance, BRD4 is also implicated in the transmission of mitotic memory since it is constantly bound to chromatin, even during mitosis. BRD4 bookmarking is possible thanks to histone acetylation and the consequent binding mediated by the bromodomains. Recent publication demonstrated that BRD4 preferentially bound M/G1 genes that showed high levels of promoter acetylation. This bookmarking ensures a rapid transcription of G1 genes soon after the end of mitosis (Dey et al., 2009; Zhao et al., 2011). The relevance of this bookmarking is further supported by BRD4 silencing or inhibition experiments where post-mitotic transcription is strongly reduced when BRD4 is evicted from the chromatin (Dey et al., 2009; Zhao et al., 2011).

Super-enhancers

In the last few years a new class of distal regulatory regions has been identified: the Super-Enhancers (SEs). Different features characterize these regions: (1) they are larger than canonical enhancers, (2) they are highly acetylated, (3) they show high occupancy of transcriptional co-factors such as Mediator complex and BRD4 (4) they are depleted in promoters (Lovén et al., 2013).

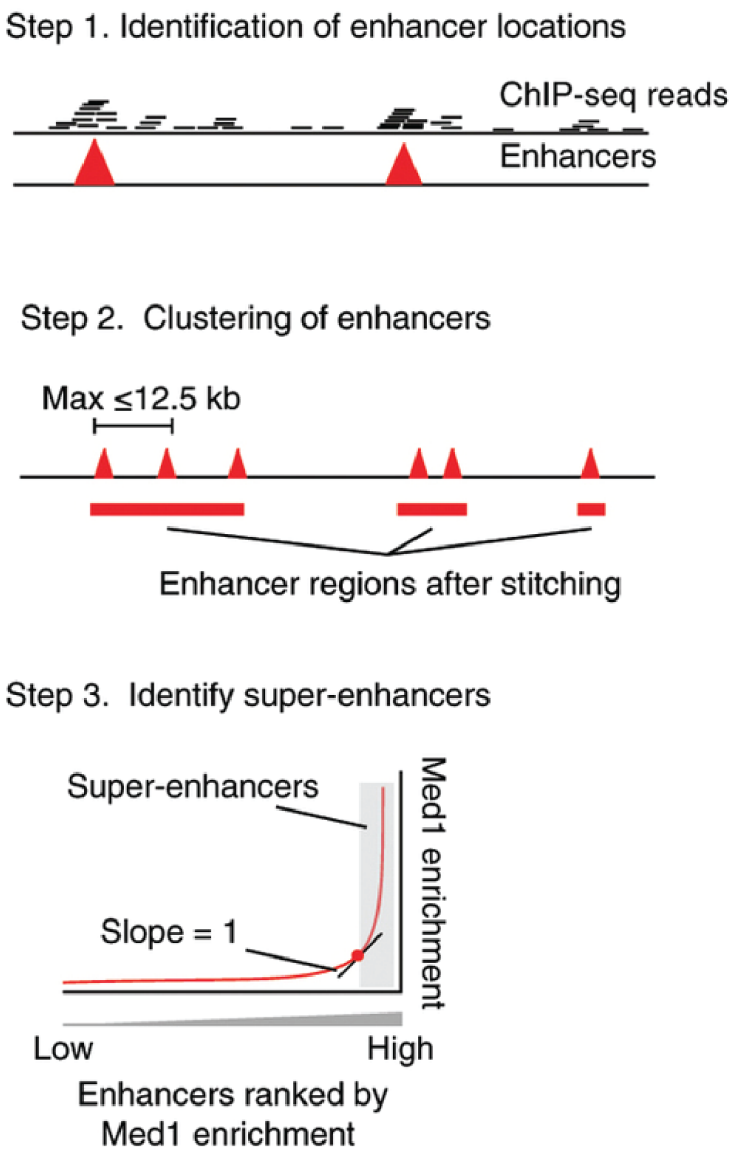

Fig. 12 Pipeline to define Super Enhancers
Super Enhancers are defined as broad distal regulatory regions that are particularly enriched for BRD4 and MED1 binding, they are highly acetylated and devoid of promoters. After the canonical peak calling pipeline, peaks closer than 12.5 kb were stitched together and finally all the stitched peaks are ranked based on Med1 enrichment: only the most enriched ones are defined as Super Enanchers.
Figure adapted from "What are super-enhancers?" (Pott and Lieb, 2015)

SEs have been computationally identified in different cellular systems and found in the proximity of cell identity genes in Embrionic Stem Cells (mESCs) (Hnisz et al., 2013; Whyte et al., 2013) as well as in other differentiated cellular models (pro-B cells (Meng et al., 2014; Qian et al., 2014), adipocytes (Schmidt et al., 2015). Disruption of the SEs-promoter loop, through the silencing of Mediator components or by the treatment with BRD4 inhibitors, results in the downregulation of these cell type specific genes. SEs can be identified not only in physiological conditions but also in cancer cells, where actually they were first discovered. In the tumor context, SEs regulate the expression of key

oncogenes, as in the MM (Lovén et al., 2013) or Diffuse Large B Cell Lymphomas (DLBCL) (Chapuy et al., 2013).

The mechanism of action and the consequent relevance of SEs are still under debate (Pott and Lieb, 2015). The first point of debate is the novelty connected to the SEs since broad regulatory regions with enhancer characteristics have been already described as DNA Methylation Valleys (DMVs) (Xie et al., 2013) or Locus Control Regions (LCRs) (Li et al., 2002). Comparison of SEs with DMVs or LCRs showed a high level of overlap, and more precisely all the SEs were included in the other categories (Hnisz et al., 2013). The only difference among the distinct classes of the above mentioned distal regulatory regions is the number of elements identified, since usually SEs are in the order of hundreds, while the others are in the tune of thousands: this difference is probably related to the different method used for the identification. Also the approach used to identify SEs is under debate, since arbitrary thresholds were used to set the most enriched Med1 stitched peaks. Furthermore, functional studies validating the SEs identified are still missing, with the consequent confusion about the putative mechanism of action, since it is not clear yet if SEs are special regulatory regions with unique characteristics or if their activity is just the result of the merging of adjacent canonical enhancers.

BETs misregulation and cancer

As other factors involved in the cell cycle control, also BRD2 and BRD4 overexpression or misregulation is associated with cancer. Indeed, transgenic mice where BRD2 gene is placed under the control of the Eμ- enhancer, with a consequent overexpression of the gene in the hematopoietic system, are characterized by the onset of lymphomas resembling human DLBCL (Greenwald, 2003). The pro-proliferative effect of BRD2 was also confirmed by bone marrow (BM) reconstitution experiments, where mice sub-lethally irradiated were subjected to BM transplantation with Hematopoietic Stem Cells (HSCs)

previously infected with control, overexpressing vectors or silencing vectors for BRD2 (Belkina et al., 2014). These experiments demonstrated that BRD2 overexpression could provide selective advantages to donor B cells and ensured a higher proliferative response of mature B cells after stimulation *in vitro*, while HSCs in which BRD2 was silenced were not able to properly engraft and proliferate in the recipient mice (Belkina et al., 2014).

Misregulation of BRD4 was first identified in the poorly differentiated squamous cell carcinoma, the human NUT midline carcinoma (NMC tumors) (French et al., 2003) where a chromosomal translocation caused the formation of an oncogenic fusion protein with BRD4, or most rarely BRD3 (French et al., 2008), and NUT, a nuclear protein normally expressed only in testis. This fusion protein is composed of the complete NUT protein and the N-terminal domain of BET proteins, including the two bromodomains (Filippakopoulos and Knapp, 2014).

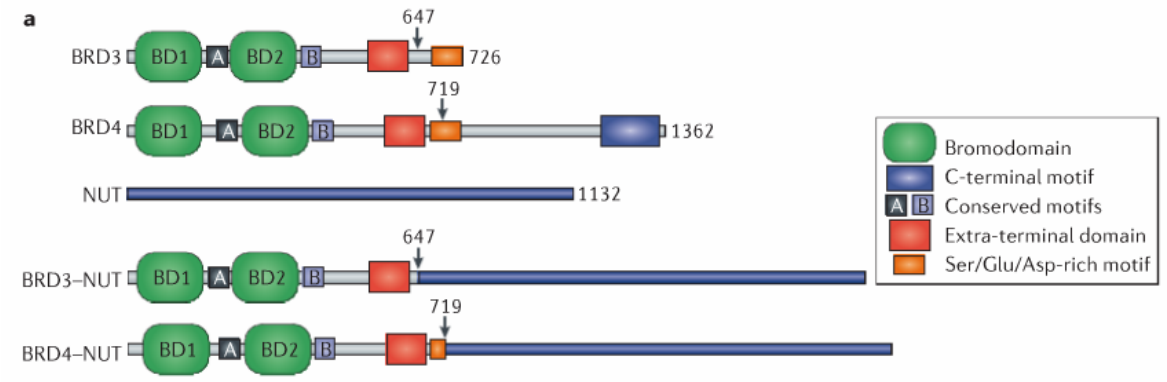

Fig. 13 Structure of the BRD-NUT oncogene
NUT Midline Carcinoma is a poorly differentiated squamous cell carcinoma where BRD4 NTD, comprising the 2 bromodomains, is fused to the complete sequence of the NUT protein. More rarely the oncogenic fusion protein is composed by BRD3 NTD and NUT protein.
Figure adapted from "Targeting bromodomains: epigenetic readers of lysine acetylation" (Filippakopoulos and Knapp, 2014)

Recently, a model for "chromatin-driven carcinogenesis" for NMC onset has been proposed thanks to the identification of very large regulatory regions called Megadomains (Alekseyenko et al., 2015). Briefly, once the BRD-NUT oncoprotein is formed, it binds already acetylated regulatory regions that act as "seed" and from which start a feed-forward loop of acetylation and recruitment of further BRD-NUT proteins, causing the spreading of the acetylation and the formation of the Megadomains, whose limits are

defined by the Transcription Activation Domains (TADs). The Megadomains are associated to enhanced transcription of genes among which are included genes, or non coding RNAs, essential for the maintenance of the undifferentiated state characteristic of NMC tumors, as Tp63, MED24 and PVT1. These Megadomains differ from the previous described SEs (Lovén et al., 2013) for location and origin, since Megadomains are generated from the expansion of already pre-marked and existing canonical enhancers and they are an order of magnitude larger than SEs.

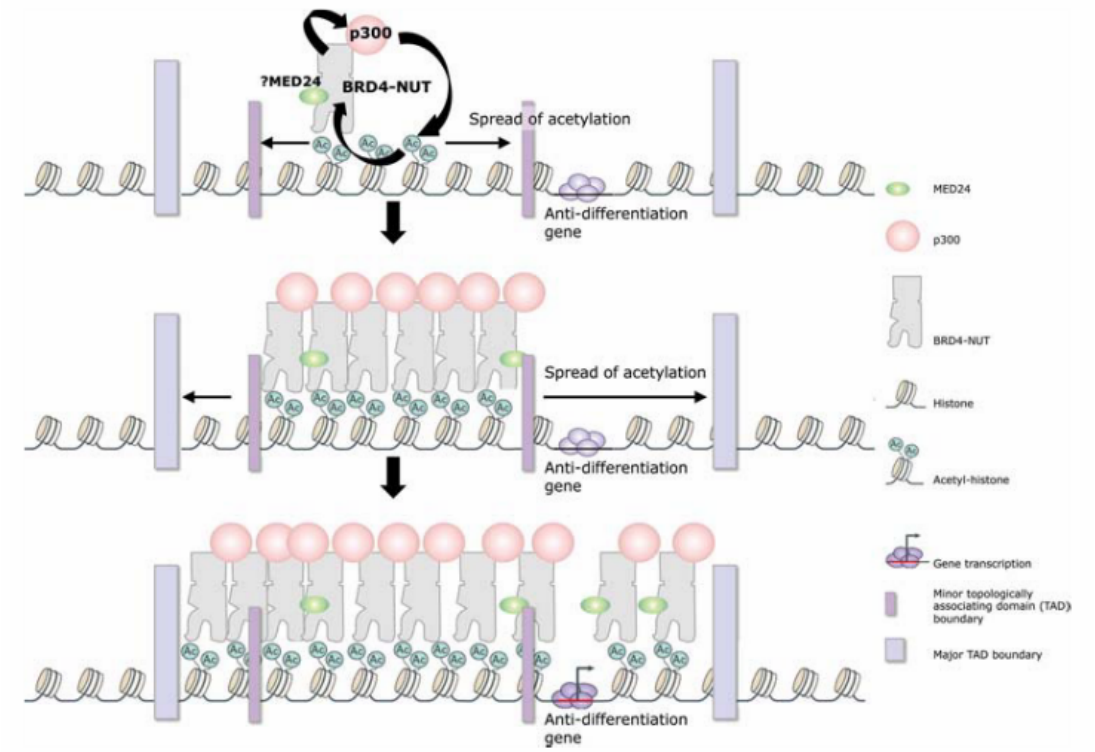

Fig. 14 Model for Megadomain formation
The oncogenic fusion protein BRD4-NUT, after the recruitment on already acetylated chromatin, induces further histone acetylation thanks to the binding with p300. The increase in the acetylation levels causes a following recruitment of BRD4-NUT protein, the spreading of the acetylation and the formation of the megadomain that is limited only by TAD boundaries.
Figure adapted from "The oncogenic BRD4-NUT chromatin regulator drives aberrant transcription within large topological domains" (Alekseyenko et al., 2015) © 2015 Alekseyenko et al.; Published by Cold Spring Harbor Laboratory Press.

Inhibiting BET proteins to indirectly targeting Myc

In the last years an exploding interest on BET proteins rose due to the development of small molecules that, preventing the binding of BET proteins to their targets, lead to the block of cell proliferation *in vitro* and tumor regression *in vivo*. Different reports

suggested that Myc downregulation was the principal target of BETs inhibitors, ensuring a specificity of action restricted to tumors in which Myc is deregulated (Dawson et al., 2011; Delmore et al., 2011; Mertz et al., 2011; Zuber et al., 2011). Since the cellular models used in these reports were characterized by different mechanisms accounting for Myc deregulation, two distinct models were proposed to explain the specificity of action in these different tumor contexts. If *c-myc* is translocated under the control of the Immunoglobulin Heavy chain enhancers (IgH), which are regulatory regions highly decorated with BRD4, the reduction in *c-myc* transcription could be explained by the displacement of BRD4 from the IgH enhancers mediated by BETs inhibitors (Lovén et al., 2013).

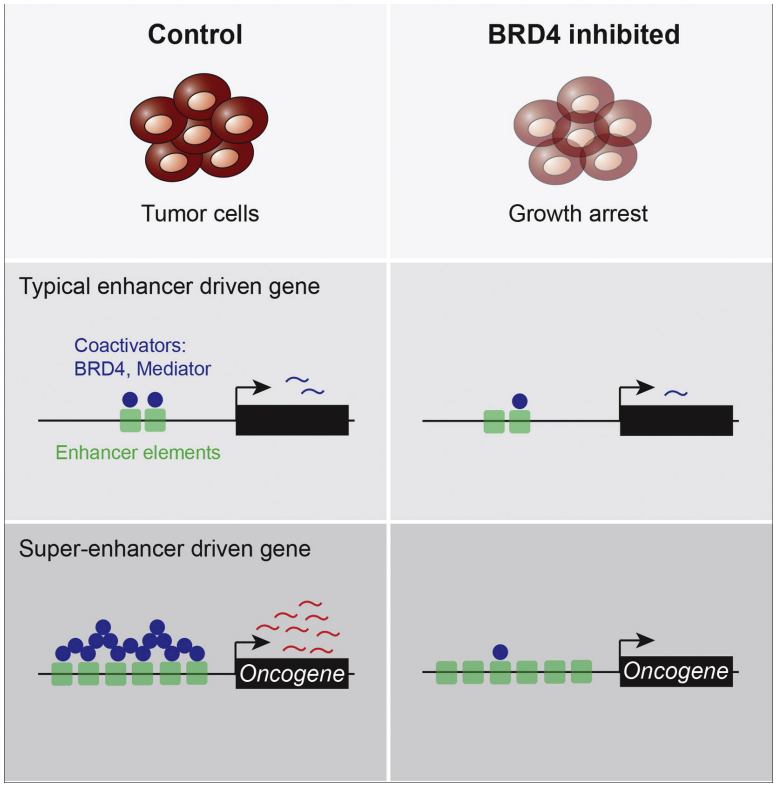

Fig. 15 Model for Myc downregulation mediated by BETs inhibitors in *c-myc* translocated tumors
In Multiple Myeloma, as well as in many other hematological malignancies, *c-myc* is translocated under the control of the Immunoglobulin (Ig) regulatory elements. Recently, it was demonstrated that Ig regulatory regions are highly decorated with BRD4 and Mediator complex and they differ from the canonical enhancers for their length. These new regulatory elements, called IgH Super-enhancers (IgH-SEs), are particularly sensitive to BETs inhibition, that evicting BRD4 from IgH SEs, causes a specific switching off of Myc expression.
Figure from "Selective inhibition of tumor oncogenes by disruption of Super-enhancers" (Lovén et al., 2013).

When *c-myc* is not translocated, as in the Acute Myeloid Leukemia, its expression is driven by MLL/AF9 oncoprotein that binds the promoter via BET proteins: in this scenario the reduction of Myc expression mediated by BETs inhibitors is due to the lack of recruitment of the MLL fusion protein to its promoter.

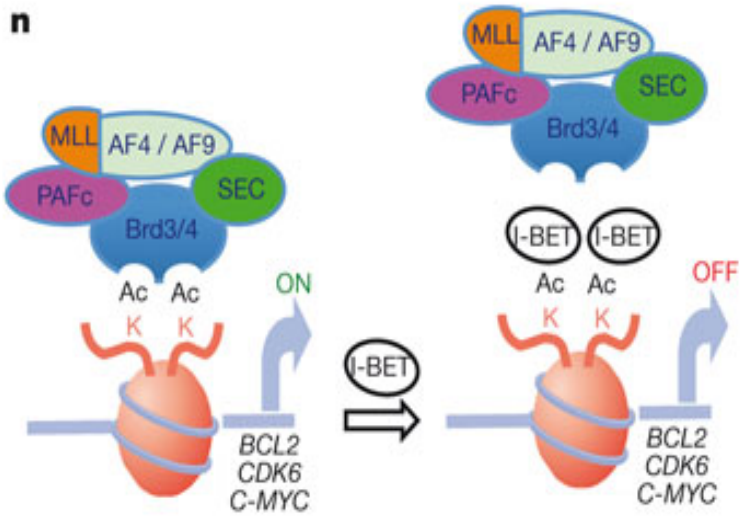

Fig. 16 Model for Myc downregulation in response to BETs inhibition when *c-myc* expression is dependent on other oncogene

In Acute Myeloid Leukemia the MLL/AF9 fusion protein is the driven oncogene responsible for the transcription of genes involved in proliferation and apoptosis as *c-myc*, BCL2 and others. MLL fusion proteins are recruited on the promoters of their targets by BETs proteins. In this context, BETs inhibitors, preventing the binding of BET proteins to the acetylated histones, impair MLL fusion proteins transcription program.

Figure adapted from "Inhibition of BET recruitment to chromatin as an effective treatment for MLL-fusion leukaemia" (Dawson et al., 2011)

Among all the inhibitors produced, the most used in preclinical studies are the ones that, mimicking the acetylated lysines, bind the bromodomain with the consequent detachment of BET proteins from their interactors (i.e. acetylated histones), as JQ1 (Nicodeme et al., 2010) and I-BET (Filippakopoulos et al., 2010).

III. Materials and methods

Cell culture

Burkitt's Lymphoma (BL-2, BL-28, DAUDI, P3HR1, RAJI and RAMOS) and Acute Myeloid Leukemia (MV4.11 and THP.1) cell lines were purchased from ATCC. The Multiple Myeloma cell lines were kindly provided by Dr. G. Tonon. The Eμ-Myc lymphomas cells were obtained smashing lymphomas derived from Eμ-Myc mice. Murine Embryonic Fibroblast (MEFs) were derived from 13.5 day post coitum C57/BL6 or MycER knock in embryos. BL, AML and MM were cultured in RPMI medium supplemented with 10% Fetal Bovine Serum, 2mM L-Glutammine, 1% penicillin/streptomycin. Eμ-Myc Lymphoma cells were cultured in DMEM and IMDM (ratio 1:1) supplemented with 10% Fetal Bovine Serum, 2mM L-Glutammine, 1% penicillin/streptomycin, 25 μM β-mercaptoethanol, 1% Non Essential Aminoacids. MEFs were cultures with DMEM medium supplemented with 10% Fetal Bovine Serum, 2mM L-Glutammine, 1% penicillin/streptomycin, 25 μM β-mercaptoethanol, 1% Non Essential Aminoacids. All the cells were grown at 37°C and 5% CO_2, except for MEFs that were grown at 37°C in low oxygen.

For the production of viral particles carrying vectors for constitutive expression, Hek293T or AMPHO packaging cells were cultured with DMEM with 10% Fetal Bovine Serum, 2mM L-Glutammine, 1% penicillin/streptomycin. On the contrary, for the production of viral particles carrying vectors for inducible silencing, Hek293T packaging cells were cultured with DMEM with 10% Tet-FREE Fetal Bovine Serum, 2mM L-Glutammine, 1% penicillin/streptomycin.

BETs inhibitor JQ1 was kindly provided by Dr. J. Bradner. For the treatment with the drug, 250000 cells/mL were cultured in fresh medium with different concentration of JQ1 (0, 50, 100, 250 or 500 nM).

PHA-767491 (Calbiochem, Cat# 217707) and 5,6-Dichlorobenzimidazole 1-β-D-ribofuranoside (DRB, Sigma-Aldrich, D1916) were used to inhibit CDK9. 250000 cells/mL were cultured in fresh medium and treated with PHA-767491 (0-0.1-1-10-50 μM) or DRB (0-0.1-1-10-100 μM) for 24 or 3 hours, respectively.

Cell transfection, viral production and infection

Hek293T or AMPHO packaging cells were transfected according to CaCl2 protocol. Briefly, for each 10 cm plate of packaging cells, 10 µg of DNA of interest were mixed with 3 µg of helper plasmids (VSVG and Δ8.2 for lentiviral production and pKAT or pCL-Eco for retroviral production for human or murine cells infection, respectively), 61 µL of CaCl2, 423 µL of H2O and 500 µL of HBS 2x. The mixture was incubated for 10 minutes at room temperature and then added to packaging cells with 9 mL of complete DMEM medium. After O/N incubation, the medium was replaced with 5 mL of fresh complete DMEM. The virus was collected 48h and 72h after the transfection.

BL cells were infected using spin infection protocol. Briefly, $2*10^6$ cells were resuspended in 2 mL of virus with 8 µg/mL of Polybrene. The cells were spinned at 1800 RPM for 1:30h and then let in the incubator at 37°C for 3h. The medium was replaced for the O/N recovery with 2mL of fresh complete medium. 24h after the infection, the cells were selected with 2.5 µg/mL of Puromycin.

When Doxycycline inducible vectors were used, transfection, virus production and cell infected culture were performed using medium supplemented with 10% of Fetal Bovine Serum Tet-FREE. The induction of the inducible vectors was performed adding 2 µg/µL of Doxycycline.

Plasmids

LT3GEPIR shREN and RT3GEN shBRD4 were kindly provided by Dr. J. Zuber.

LT3GEPIR shBRD4 (602-1817-1838) vectors were obtained sub-cloning shRNA targeting BRD4 from RT3GEN to LT3GEPIR. Briefly, 5 µg of plasmids were digested O/N with XhoI and EcoRI restriction enzymes. The digested LT3GEPIR shREN was run on a 0.8% agarose gel, while the digested RT3GEN shBRD4 was run on a 2.5% agarose gel. A fragment of 10000 bp for LT3GEPIR digestion and one of 150 bp for R3GEN were purified from the gel and quantified by nanodrop. Ligation was performed for 3 hours at room temperature using a ratio vector/insert 1:3. The ligation was then transformed by heat shock in competent STBL3 bacteria, in order to avoid plasmid recombination, and plated on LB+Ampicillin plate. The day after, ~5 single colonies were picked and amplified in 5mL of LB+Ampicillin at 37°C over day. 4mL out of 5 mL for each bacterial growth were used for plasmid extraction with the NucleoSpin® Plasmid (No Lid)

(Macherey-Nagel) according to manufacturer's instructions. After checking the integrity of the plasmids on agarose gel, the vectors with the new insert was then checked by DNA Sanger sequencing.

pBP-CDK9 vector was obtained subcloning CDK9 CDS from pMX-CDK9, kindly provided by Dr. M. Esteban, into pBabePuro. Both pMX-CDK9 and pBabePURO were digested O/N with BamHI and EcoRI. The fragments were purified after agarose gel run and the ligation was performed with 1:3 vector/insert ratio. TOP10 bacteria were then transformed and plated on LB+Ampicillin plate for O/N growth. ~5 single colonies were picked and amplified in 5mL of liquid LB+Ampicillin at 37°C over day. The vectors were then extracted with the NucleoSpin® Plasmid (No Lid) (Macherey-Nagel) according to manufacturer's instructions. After checking the integrity of the plasmids on agarose gel, the vectors with the new insert was then checked by DNA Sanger sequencing.

pBabePURO-EV and pBabePURO-E2F1 were already available in the lab.

Cell growth Assay

The cell growth was measured using the CellTiterGlo Luminescent Cell Viability Assay (Promega).

For cells that grow in suspension (BL, AML, MM and Eμ-Myc lymphoma cells) 250000 cells/mL in a total volume of 4 mL were cultured in 6 well plate in presence of JQ1 (50, 100, 250, 500 nM) or DMSO for 4 days. The assay was performed in triplicate every 24h using 100 μL of cell suspension and 100 μL of CellTiterGlo. The luminescence was read in a white 96 well plate using a multiwell plate reader (Glomax, Promega).

For adherent cells (MEFs) 500 cells were plated in each well of a white 96 well plate, with a total volume of 100 μL. The cells were treated for up to 4 days with DMSO or JQ1 (100 or 250 nM) in combination with EtOH or 400 nM of 4-Hydroxytamoxifen (4-OHT). Each condition was plated in triplicate and the luminescence was read after the addition of 100 μL of CellTiterGlo using a multiwell plate reader (Glomax, Promega).

Cell cycle and dead cell discrimination analysis

The cell cycle progression was analyzed by Bromo deoxy Uridine (BrdU) incorporation. 250000 cells/mL of BL, AML, MM or Eμ-Myc lymphomas were cultured in a total volume of 15 mL in presence of DMSO or JQ1 (100 nM for BL, AML and MM and 50 nM for Eμ-Myc lymphomas) for 24h. BrdU (33 μM) was added to the culture during the last 20' of JQ1 treatment. The cells were then collected (1500 RPM for 5'), resuspended with 250 μL of PBS and fixed with 750 μL of cold ethanol (100%) dropwise. 500000 cells/ 10 cm plate of MEFs were cultured with DMSO or different concentration of JQ1 (100 or 250 nM) in combination with EtOH or 400 nM 4-OHT for 48h. BrdU (33 μM) was added to the culture during the last 20' of the treatment. Cells were then washed once with PBS, trypsinized and centrifugated at 1500 RPM for 5'. The pellet was resuspended with 250 μL of PBS and fixed with 750 μL of cold ethanol (100%) dropwise. For both suspension and adherent cells, the fixation step was carrying on O/N at 4°C. The cells were then washed once with PBS+1% BSA and then resuspended in 1mL of denaturing solution (2N HCl) and incubate at room temperature for 30'. The reaction was blocked with 3mL of 0.1M Sodium Borate (Na2B4O7 pH 8.5) for 2 min at room temperature. The cells were then collected at 1200 RPM for 10' and washed once with 1mL of PBS+1% BSA. The staining was performed using 100 μL of an anti-BrdU mouse antibody (1:5) in PBS 1% BSA for 1h at room temperature and light protected. Cells were washed once with 1mL of PBS+1% BSA and resuspended in 100 μL of anti-mouse FITC (1:50) or anti-mouse Alexa 648 (1:50) in PBS 1% BSA and incubate for 1h at room temperature, light protected. After one washing step in 1ml PBS 1% BSA, cells were incubated O/N at 4°C in 1mL of PBS+PI (2.5 μg/mL) +RNaseA. The acquisitions were performed with FACS Calibur. The analysis was performed with FlowJo software.

The discrimination of dead cells was performed on live BL, AML, MM cells (250000 cells/mL, total volume= 10 mL) treated or not with JQ1 (100 nM) for 24h. Cells were collected and washed once with 1mL of PBS+1% BSA. Cells were then resuspended in 500 μL of PBS. 2 μL of PI (50 μg/ml in PBS) were added and incubated for 5' at room temperature. The acquisitions were performed with FACS Calibur. The analyses were performed with FlowJo software.

Western blot

For western blot analysis, 250000 cells/mL of BL, AML, MM and Eμ-Myc lymphoma cells were cultured in a total volume of 20 mL. 24h after the plating different concentrations of JQ1 (0, 50, 100, 250, 500 nM) were added to the culture for either 6 or 24h. Cells were collected by centrifugation at 1500 RPM for 5' and washed once in PBS. Cells were lysed in an adequate volume of lysis buffer (20 mM HEPES pH7.5, 100 mM NaCl, 5 mM EDTA, 10% Glycerol, 1% Triton X-100) supplemented with MINI-complete Protease Inhibitor Cocktail Tablets (Roche) and phosphatase inhibition (0.4 mM ortovanadate, 10 mM NaF) for 10' on ice. The cell lysate was then sonicated for 20'' with 10% of amplitude with Branson sonicator and cleared by centrifugation at full speed at 4°C. Proteins were quantified by Bradford assay. 20-30 μg of proteins were boiled at 95°C with Laemmli sample buffer and loaded on Mini-PROTEAN® TGX™ Gel (Bio-rad). Proteins were transferred to Trans-Blot® Turbo™ Nitrocellulose Transfer Packs (Bio-rad) using Trans-Blot® Turbo™ Transfer System (Bio-rad). Blocking was performed with TBS 1X+5% of not fat milk or with TBS 1X+ 5% of BSA. The primary antibodies used were: Myc (1:10000, Y69 Abcam ab32072), vinculin (1:10000, Sigma, V9264), tubulin (1:1000, Santa Cruz), BRD4 (1:1000, Bethyl A301-985A100), RNA PolII (1:1000, Santa Cruz N-20, sc-899), RNA PolIIS5p (1:1000, Abcam ab5131), RNA PolIIS2p (1:500, Chromotek 3e10), HEXIM1 (1:1000, Abcam ab25388), CDK9 (1:500, Santa Cruz H-169, sc-8338).

The secondary antibodies used were: anti-mouse (1:5000, homemade), anti-rabbit (1:5000, homemade), anti-rat (1:5000, Cell signaling). The blot were developed with ECL (amsharm) using ChemiDoc System (Bio-rad).

RNA extraction and expression quantification

For expression analysis, 250000 cells/mL of BL, AML, MM and Eμ-Myc lymphoma cells were cultured in a total volume of 20 mL, while 500000 cells/10 cm plate were plated for MEFs. 24h after the plating different concentrations of JQ1 (0, 50, 100, 250, 500 nM) were added to the culture for either 6 or 24h. Cells that grow in suspension were collected by centrifugation at 1500 RPM for 5' and washed once in PBS, while adherent cells were trypsinized, centrifugated at 1500 RPM for 5' and washed once in PBS. RNA was extracted using RNeasy columns (Qiagen) and

treated on-column with DNase (Qiagen). 1 µg of RNA was retrotranscribed using the ImPromII kit (Promega) according to the manufacture's instruction. 10 ng of cDNA were used to perform real-time qPCR using FAST SYBR Green Master Mix (Applied Biosystems).

Primers:

Human:

BRD4 from (Floyd et al., 2013)

CDC25A FW:	CACATGGAAGAAGAGGTTGA
CDC25A REV:	ATACAGCTCAGGGTAGTGGA
E2F1 FW:	TCCAAGAACCACATCCAGTG
E2F1 REV:	CTGGGTCAACCCCTCAAG
GINS3 FW:	AGTCCCGAGAATGCAGACAT
GINS3 REV:	GCGAAAACGTCCGATAAAAG
KIF2C FW:	AGGAGCATCTGGTTAACTCTGC
KIF2C REV:	TCTGCCCAGAGGTTCTGC
MCM2 FW:	CGAAACCTGGTTGTTGCTG
MCM2 REV:	GGTGAAGGATTCCGATGATTC
MYC FW:	TCAAGAGGTGCCACGTCTCC
MYC REV:	TCTTGGCAGCAGGATAGTCCTT
PARK7 FW:	GGGGTGAGTGGTACCCAAC
PARK7 REV:	TGGAAGCCATTTTTATGTTATATGTTT
RPL36 FW:	GGGCCCTCAAATTTATCAAGA
RPL36 REV:	GTCTTTCTTGGCAGCAGCTT
RPPO FW:	TTCATTGTGGGAGCAGAC
RPPO REV:	CAGCAGTTTCTCCAGAGC
RRM2 FW:	GCGATTTAGCCAAGAAGTTCAGAT
RRM2 REV:	CCCAGTCTGCCTTCTTCTTGA

SLC16A1 FW:	GTGACCATTGTGGAATGCTG
SLC16A1 REV	CATGTCATTGAGCCGACCTA
TOMM20 FW:	CTGCAGGTCTTACAGCAAACTC
TOMM20 REV:	TCAGCCAAGCTCTGAGCAC

Murine:

Arrsd1 FW:	GCAGAGGCTGTGGAAACC
Arrsd1 REV:	TTCTTCCCTGCTCCTTTGC
BRD4 FW:	CCCCATCTCAACCAGCAT
BRD4 REV:	AGAGCAGCAGCTCGGTTACT
Cabp4 FW:	GCTGATAAGCCCAAAGCTGA
Cabp4 REV:	CATCCCTGTCCTTGTCAAACT
Cct3 FW:	TTAGCTCAGCACTACCTCATGC
Cct3 REV:	CTCAGGTCGGCTGACTATCC
Dusp6 FW:	AAATTCCTATCTCGGATCACTGG
Dusp6 REV:	CATCTATGAAAGAAATGGCCTCA
Endou FW:	GACGGCTGTCATGAAGGAAC
Endou REV:	TCGTCCACAAACTCTTGTTCTG
Fam26f FW:	AGCCTGGTGACCCTACTGAC
Fam26f REV:	ACTGGAACACCACTGAGGAGA
Fuca2 FW:	AGTCTGGGGGAAACAGAGGT
Fuca2 REV:	AGGTAACTCCACGGTGATGC
Il7r FW:	CGAAACTCCAGAACCCAAGA
Il7r REV:	AATGGTGACACTTGGCAAGAC
Msto1 FW:	TACAGAACAGGCCGGACAC
Msto1 REV:	GGTTACCTTCTTCTTTTAGAGTGTTCA
Myc FW:	CGTGAACTTCACCAACAGGAAC
Myc REV:	GAAATTCTCTTCCTCGTCGCAG

Myl4 FW:	CAAGCACATCATGTCTGGGTA
Myl4 REV:	TGGATCTCTTGCTTTCTCACG
Pax5 FW:	ACGCTGACAGGGATGGTG
Pax5 REV:	GGGGAACCTCCAAGAATCAT
Pcbp1 FW:	CAACAGCTCCATGACCAACA
Pcbp1 REV:	ACCAGCCGAAGTGTGACC
Pogk FW:	CCAGGGAGTAACCTTTGCAG
Pogk REV:	GTTGAGGAAAATGGGAGGTG
Prmt3 FW:	GAGGATGAGGATGGCGTCTA
Prmt3 REV:	ACTTTCTGTGCGTACTTTGTCCT
Pus7 FW:	CCCCAAGCATAAAATCAGTGAGG
Pus7 REV:	CCCCGATAAGGAGTAATCTCGAA
Reep6 FW:	AGCGCTTCGAACGTTTTCT
Reep6 REV:	TCTCTACACCGGTCCTTGCT
Rppo FW:	TTCATTGTGGGAGCAGAC
Rppo REV:	CAGCAGTTTCTCCAGAGC
Rsph9 FW:	ACCACGCAAGACGCTCTAC
Rsph9 REV:	AACGGCCACTCACCACAG
Slc16a13 FW:	ACCTGAGTATTGGGCTGCTG
Slc16a13 REV:	GCCATGGTCGGAGTGAAG

For Microarray assay, 250000 cells/mL of RAJI cells were cultured in a total volume of 40 mL. 24h after the plating DMSO or 100 nM of JQ1 were added to the culture for 24h. Total RNA from 10^7 RAJI was purified using TRIzol reagent (Invitrogen) according to manufacturer's instructions, treated with TurboDNase (Ambion) and processed for oligonucleotide microarray profile through Affymetrix Human Gene 1.0 ST arrays platform.

For RNAseq assay, 250000 cells/mL of Eμ-Myc lymphoma cells (ly9644, ly27805, ly28514) were cultured in a total volume of 40 mL. 24h after the plating DMSO or 50 nM of JQ1 were added to the culture for additional 24h. Total RNA was extracted from 10^7 Eμ-Myc lymphoma cells using

miRNeasy Mini Kit (QIAGEN) according to manufacturer's instructions. Digestion with DNase I was performed on column. 1 µg of RNA was used for RNAseq strand specific library preparation (Illumina) according to TruSeq Stranded Total RNA Sample Preparation Guide. Ribosomal RNA was removed using rRNA removal Mix, present in the kit. The index used to mark the different samples was decided according to TruSeq Sample Preparation Pooling Guide (Illumina): since we multiplexed 2 samples per lane, we used AR006 and AR012 to mark DMSO and JQ1 samples, respectively. The efficacy of rRNA depletion and the quality of the library preparation were tested using Agilent Technologies 2100 Bioanalyzer using Eukaryote Total RNA Nano or High Sensitivity DNA Assay, respectively.

Nanostring® assay was performed using a codeset designed including genes deregulated by Myc. Briefly, 250000 cells/mL of Eµ-Myc lymphoma cells (ly9644, ly27805, ly28514) were cultured in a total volume of 40 mL. 24h after the plating DMSO or 50 nM of JQ1 were added to the culture for additional 24h. Total RNA was extracted from 10^7 Eµ-Myc lymphoma cells using TRIZOL reagent (Invitrogen) according to manufacturer's instructions and treated with TurboDNase (Ambion).100 ng of total RNA was used to proceed with the probe hybridization according to manufacturer's instructions.

4-sU labeling

4-thiouridine (4-sU) labeling was performed as previously described (Rabani et al., 2011) with minor modifications. RAJI (300000 cells/mL) were cultured in 100 mL of complete medium. 24h after the plating, cells were treated with vehicle (DMSO) or JQ1 (100 nM) for 24h. A pulse of 30' of 4-sU (300 µM) was performed. The reaction was immediately blocked with 4 volumes of cold PBS and cells were centrifugated at 1800 RPM for 15' at +4°C. RNA was extracted with the Qiagen miRNeasy kit according to the manufacturer's instructions and DNase I digestion was performed. 40 µg of total RNA was used for the biotinylation reaction. RNA was diluted in 100 µl of RNase-free water. 100 µl of biotinylation buffer (2.53 stock: 25 mM Tris pH 7.4, 2.5 mM EDTA) and 50 µl of EZ-link biotin-HPDP (1 mg/ ml in DMF; Pierce/Thermo Scientific 21341) were added and incubated for 2 h at 25°C. RNA was precipitated and unbound biotin-HPDP was removed by a combination of chloroform/isoamylalcohol (24:1) precipitation with purification

using MaXtract high density tubes from Qiagen. Biotinylated RNA was purified using Dynabeads MyOne Streptavidin T1 (Invitrogen). Before addition of RNA, 50 µL of beads were washed twice in washing buffer A (100 mM NaOH, 50 mM NaCl) and once in washing buffer B (100 mM NaCl). Beads were resuspended in 100 µL of buffer C (2 M NaCl, 10 mM Tris pH 7.5, 1 mM EDTA, 0.1% Tween-20) to a final concentration of 5 µg/µL. RNA was added in an equal volume and rotated at room temperature for 15'. Beads were washed 3 times with washing buffer C. RNA was eluted from the beads in 100 µL of 10 mM EDTA in 95% formamide (65 °C, 10'). RNA was extracted with the RNeasy MinElute Spin columns from Qiagen according to the manufacturer and eluted in 14 µL of RNase-free water. RNA was retrotranscribed with SuperScript® VILO cDNA Synthesis Kit, according to manufacturer's instruction. Real-time qPCR was performed using FAST SYBR Green Master Mix (Applied Biosystems).

Primers:

MCM2 FW	AAGGGGATTGTCTTGGGGAG	2°intron
MCM2 REV	TGCCTATGGTCGCTCTGTAG	2° intron
MCM2 FW	CCATTCTTGTCGGTCTCCCT	7°intron-8°exon
MCM2 REV	CCAGGCCTCTCTTGATGTCT	7°intron-8°exon
RPL36 FW	TACTCACCTCCGCCCCTT	1° exon
RPL36 REV	CACTTTGTGGCCCTTGTTGA	1° exon
RPL36 FW	CGCGAGAGAAGCTGCTTAAC	2°intron-3°exon
RPL36 REV	GTGTTTGGTCAGACGCTAGG	2°intron-3°exon
RRM2 FW	AGTGGTGTGATCTTGGCTCA	4°intron
RRM2 REV	ACTCATGAGGCTGAGGTTGG	4°intron
RRM2 FW	TGTGACTTCCGAACCTCAGG	3°intron-4°exon

RRM2 REV	CTCCTCGGGTTTCAGGGATT	3°intron-4°exon
SYVN1 FW	CTGGAACCTGGGTCAGTCTT	1° intron
SYVN1 REV	TGCAGCTTTTCCTCATCACC	1° intron
SYVN1 FW	ATTCAAGGCACATGTGGGGT	6°exon-7°intron
SYVN1 REV	CTGGTGTTTGGCTTTGAGGT	6°exon-7°intron
TOMM20 FW	AGCCTGGTTGATACGGTGAA	1° intron
TOMM20 REV	GCCTCTCGAGTAGCTAGGAC	1° intron
TOMM20 FW	GATGGTCTACGCCCTTCTCA	3°intro-4°exon
TOMM20 REV	CCAAGGCTTTTCAGGTTACATG	3°intro-4°exon
ZNF367 FW	CCAGCCCCAGTGAAGAAGTA	1°intron
ZNF367 REV	CAAGTTGTTCCAAGGCTCCC	1°intron
ZNF367 FW	CACAGATAGGGCCTCTCACC	2°intron-3°exon
ZNF367 REV	CCCTCCTCTTCTGGCCTTAT	2°intron-3°exon

Chromatin Immunoprecipitation

BL, MM or Eμ-Myc lymphoma cells (250000 cells/mL) were plated and DMSO or JQ1 (100 nM for the cell lines, 50 nM for Eμ-Myc lymphomas) were added 24h after the initial plating. After 24h of drug treatment, cells were counted and washed once with PBS. 10^8 cells were resuspended in 10 mL PBS and fixed. For Myc, Histone Marks, RNA PolII and E2F1 ChIP the cells were fixed using formaldehyde (final concentration of 1%), for BRD4 ChIP the cells were fixed using either glutaraldehyde (final concentration 1%) or formaldehyde (final concentration of 1%). The fixation step was carried out at room temperature for 10' and quenched with 0.125 M Glycine for 5' at

room temperature. Cells were washed twice with PBS and stored at -80°C as pellet. 10^8 cells were resuspended in 5 mL of LB1 buffer (50 mM HEPES pH 7.5, 140 mM NaCl, 1 mM EDTA, 10% Glycerol, 0.5% NP-40, 0.25% Triton X-100), kept on ice for 10' and then centrifugated at 1350 xg for 5' at +4°C. The supernatant was eliminated and the cells were gently rocked at room temperature for 10' in 5 mL of LB2 buffer (10 mM tris-HCl pH 8, 200 mM NaCl, 1 mM EDTA, 0.5 mM EGTA). At this point, the nuclei were extracted and pelleted by spinning at 1350 xg for 5' at +4°C. The pellet was resuspended in 3 mL of LB3 buffer (10 mM Tris-HCl pH 8, 100 mM NaCl, 1 mM EDTA, 0.5 mM EGTA, 0.1 % Na-Deoxycholate, 0.5% N-lauroylsarcosine) and sonicated in order to obtain DNA fragment of 300-100 bp. For BRD4, Myc, E2F1, total RNA PolII and RNA PolII-S5p ChIP, the lysate from $50*10^6$ cells was incubated with 10 µg of antibody previously bound to protein G Dynabeads (Invitrogen) in PBS+0.5% BSA. For Histone Marks ChIP, $20*10^6$ cells were incubated with 5 µg of the antibody previously bound to protein G Dynabeads (Invitrogen) in PBS+0.5% BSA. For RNA PolII-S2p ChIP, the lysate corresponding to $10*10^7$ cells was incubated with 60 µL of hybridoma O/N on the rotating wheel at +4°C. Concomitantly, 4.5 µL of anti-rat were incubated with 50 µL of protein G Dynabeads O/N on the rotating wheel at +4°C. The day after the chromatin+primary antibody was mixed to the secondary antibody+protein G Dynabeads for 3h on rotating wheel at +4°C. After the incubation with the antibody, the beads were collected using the DynaMag™ magnet and washed 6 times with 1 mL of RIPA buffer (50 mM HEPES pH 7.5, 500 mM LiCl, 1 mM EDTA, 1% NP-40, 0.7% Na-Deoxycholate). Beads were then washed with 1 mL f TE 1X+50 mM NaCl before the elution step (de-crosslinking). For cells fixed with formaldehyde, de-crosslinking was performed O/N at 65°C with 150 µL of TE1X+2% SDS. For cells fixed with glutaraldehyde, de-crosslinking was performed with 150 µL of TE+1% SDS+ 100 mM $NaHCO_3$. The sample were first treated for 1h with RNaseA at 37°C, then Proteinase K was added and the de-crosslink reaction was incubated at 65°C O/N. DNA was purified with PCR Qiaquick columns (Qiagen) and quantified using PicoGreen (Invitrogen) or QUBIT (Invitrogen).

For ChIPqPCR, 6 µL of DNA diluted 1:6 was used to perform real-time PCR using FAST SYBR Green Master Mix (Applied Biosystems).

Primers:

Human:

AchR FW:	CCTTCATTGGGATCACCACG
AchR REV:	AGGAGATGAGTACCAGCAGGTTG
IFRD2 FW:	CGTGCCCCAGCAGTCATT
IFRD2 REV:	GCAGTGGGCAGCGAGC

IgH_E1, IgH_E2, IgH_E3, IgH_E4 primers were taken from (Delmore et al., 2011)

NCL FW:	TTTTGCGACGCGTACGAG
NCL REV:	ACTAGGGCCGATACCGCC
NME1 FW:	GGGAGTGGGTTAGGTGAGGAGT
NME1 REV:	CGTCGCGGTCTGACGAG

Murine:

AchR FW:	AGTGCCCCCTGCTGTCAGT
AchR REV:	CCCTTTCCTGGTGCCAAGA
D7 FW:	CGGCTCGGCCAGCAGAAG
D7 REV:	TAGTCCACATGGCGGCGC
Nucleolin FW:	GAGTGTCTGTAGTACCCCGGAAA
Nucleolin REV:	CCACGCTGCCGTCCC
Pus7 FW:	GCTGCACCGCGTGGAGAC
Pus7 REV:	GGCTGGTGGGATAACCCGT

For ChIPseq, 2–10 ng ChIP DNA was prepared for HiSeq2000 sequencing with TruSeq ChIP Sample Prep Kit (Illumina) following the manufacturer's instructions.

NGS data filtering and quality assessment

ChIP-seq reads sequenced with the Illumina HiSeq2000 were filtered using the fastq_quality_ trimmer (setting the options to -Q33 -t 20 -l 10) and fastq_masker (setting the options to -q 20 -r

N) tools of the FASTX-Toolkit suite (http://hannonlab. cshl.edu/fastx_toolkit/). Their quality was evaluated and confirmed using the FastQC application (http://www.bioinformatics.babraham.ac.uk/projects/fastqc/).

Analysis of ChIP-seq data

ChIP-seq NGS reads were aligned with the BWA tool (Li H. (2013) Aligning sequence reads, clone sequences and assembly contigs with BWA-MEM.arXiv:1303.3997v2 [q-bio.GN].) using default settings using the mm9, hg19 and hg18 genomes for Eμ-*myc*, Raji and MM1.S and OC-LY1 data, respectively. Peaks were called with the MACS v1.4 software (Zhang et al., 2008) . Peaks' p-value threshold was set to 10^{-8} for Raji data and 10^{-9} for MM1.S data. FDR (false discovery rate), determined as the ratio between the negative and the positive peaks, was set to 5% for all the data. Negative peaks were found by MACS on the input samples, using the ChIP as reference.

Normalized reads count within a genomic region was determined as the number of reads per million of library aligned reads (rpm), that were subtracted by the input normalized reads. Peak read density (reads per million of reads per base pair) for a particular region was determined as the ratio between the normalized reads count and the length of the region in base pair.

Definition of promoter, intragenic and intergenic regions

In order to assess if a specific ChIP-seq peak is in a promoter, in a genebody or is intergenic, the following criteria were applied. Regions that overlap with at least one bp with any promoter (defined as genomic region [-2000; +1000] bp spanning TSSs, transcription start sites), were considered as belonging to promoters; regions that weren't promoters but had at least 1 bp overlapping with any genebody were considered intragenic. The remaining regions (that did not overlap either with promoters or genebodies) were considered intergenic. Annotations were performed with the R annotation packages TxDb.Hsapiens.UCSC.hg19.knownGene and TxDb.Hsapiens.UCSC.hg18.knownGene or TxDb.Mmusculus.UCSC.mm9.KnownGene of Bioconductor(Marc Carlson (). TxDb.Hsapiens.UCSC.hg18.knownGene: Annotation package for

TranscriptDb object(s). R package version 2.14.0.; Marc Carlson (). TxDb.Hsapiens.UCSC.hg19.knownGene: Annotation package for transcriptDb object(s). R package version 2.14.0.).

RNA PolII stalling index

The RNA polymerase II stalling index (SI, also called elongation rate) (Rahl et al., 2010; Zeitlinger et al., 2007) was calculated as SI = Prom/GB; prom refers to the read counts on the promoter (TSS ± 300 bp interval) and GB to the read counts in the gene body (the interval between TSS +301 and 3,000 bp after the TSS). These values were normalized both to library size (total number of reads) and to the length of the interval, and only genes with GB > 600 and with a RNAPII ChIP-seq peak in the promoter region were considered. PolII signal in genebodies was plotted using the same criteria that were used in SI calculation; genes were expanded by 20% upstream and 20% downstream, in order to have a better overview of the neighborhood. They were then divided into 150 bins, for which the input-subtracted reads were counted and were normalized both by library size and gene length, using "GRcoverageInbins" function of compEpiTools R package (http://genomics.iit.it/groups/computational-epigenomics.html (2014). compEpiTools: tools for computational epigenomics. R package version 0.99.0.).

IV. Results

BET inhibition effects on cell viability and Myc levels

Previous publications already showed that BET inhibition strongly affects the proliferation of different tumor types (e.g. Multiple Myeloma (MM), Acute Myeloid Leukemia(AML)) both *in vitro* and *in vivo* (Dawson et al., 2011; Delmore et al., 2011; Mertz et al., 2011; Zuber et al., 2011). We focused our attention on human Burkitt's lymphoma (BL) cell lines and on Eμ-Myc lymphomas, a murine model for immature B cells malignancies (Adams et al., 1985). BL are characterized by a chromosomal rearrangement that put in close proximity the *c-myc* locus and the immunoglobulin distal regulatory regions. The most common recombination involves chromosome 8, where the *c-myc* gene is located, and chromosome 14, containing the regulatory regions for the immunoglobulin heavy chain (IgH). In a minor fraction of BL cases, *c-myc* is juxtaposed to the immunoglobulin light chain regulatory regions in chromosome 2 or 22 (Molyneux et al., 2012). The Eμ-Myc mouse model was engineered in the '80s to mimic human B cell malignancies: in this murine model, the chromosomal rearrangement found in the plasmacytoma ABPC17 (Corcoran et al., 1985) was reproduced fusing the IgH enhancer upstream of the first exon of the *c-myc* gene. In this model, c-*myc* misregulation leads to the development of B cell lymphoma with a short latency of around 3 months and high penetrance.

As a first step, we assessed the sensitivity of BL and Eμ-Myc lymphomas cells to BET inhibition, by evaluating cell growth in samples treated with increasing doses of JQ1, ranging from 50 nM to 500 nM. As positive controls, we used AML (MV4.11, THP.1) and MM cells (MM.1S, OPM1, KMS11) for which the sensitivity to BETs inhibitors has already been reported. As shown in Fig.17, all the BL cell lines (BL-2, BL-28, DAUDI, P3HR1, RAJI and RAMOS) and Eμ-Myc lymphoma cells were responsive to BET inhibition, showing growth arrest in a time- and dose-dependent manner. RAJI and Eμ-Myc lymphomas were the most sensitive cells, since they showed a strong decrease in cell viability already after 48h of treatment, at relatively low doses of JQ1 (100 nM and 50 nM, respectively).

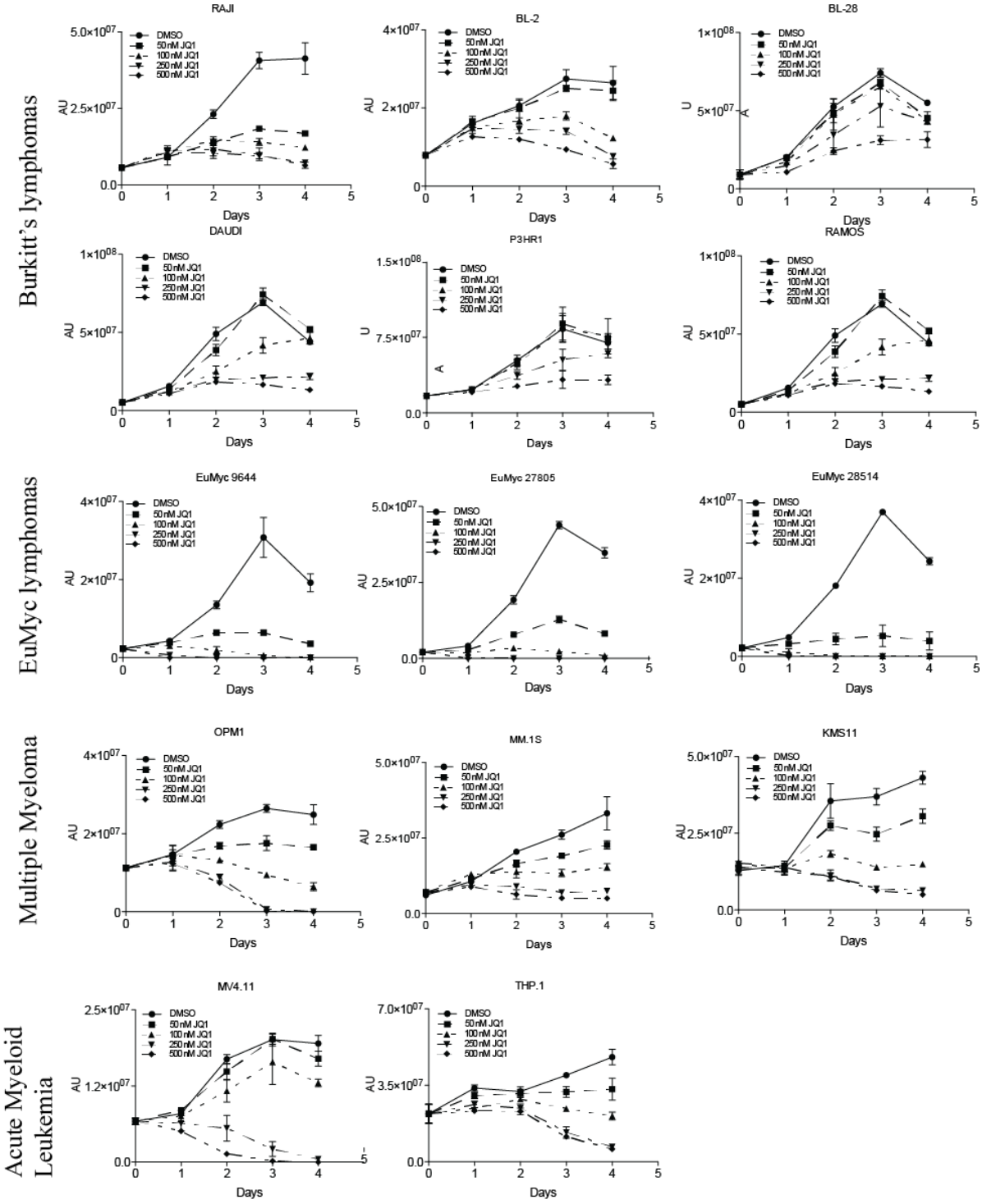

Fig. 17 BETs inhibition strongly affects cell growth

Cell growth assay using CellTiterGlo (Promega) on BL (BL-2, BL-28, DAUDI, P3HR1, RAJI and RAMOS), three independent Eμ-Myc lymphomas (9644, 27805 and 28514), MM (MM.1S, OPM1, KMS11) and AML (MV4.11, THP.1) cell lines after treatment with 0-50-100-250-500 nM JQ1 for up to 4 days. For each time point, the mean and the standard deviations of 3 technical replicates are reported.

Since BET inhibition caused a strong decrease in cell growth, we wondered whether this effect was due to a block in the cell cycle progression, to an increase in cell death or both. In order to discriminate among these possibilities and to evaluate short-term responses, we performed cell cycle analysis on cells treated for 24h using the lowest effective dose of JQ1, as determined in the

experiments mentioned above. In particular, 100 nM of BETs inhibitor was used to treat the human cell lines (BL, AML and MM), while 50 nM was used for Eμ-Myc lymphomas treatment. As shown in Fig.18, in BL and Eμ-Myc cells, BETs inhibition led to a decrease in the percentage of cells in S phase with a consequent increase in the G0/G1 population, suggesting a defect in G1/S progression. Also from this type of assay, RAJI and Eμ-Myc lymphomas resulted the most sensitive cell lines to BETs inhibition. Indeed, for RAJI cells the S-phase population dropped from 42% to 10%, while the G0/G1 population increased from 38% to 78%. Similar results were observed for Eμ-Myc lymphomas were the percentage of BrdU positive cells diminished from 68% to 40%, with a concomitant increase of G0/G1 population (from 23.5% to 45.2%). The reduction in the percentage of cycling cells was evident also in the other BL cell lines (BL-2, DAUDI, P3HR1 and RAMOS), even though they showed a milder cell cycle alteration with a ~20% reduction of the S-phase population respect to the control condition (from ~50-40% in DMSO sample to ~40-30% in JQ1 sample). The only exception was represented by BL-28 cells that, after 24h of treatment did not show any alteration in the cell cycle distribution. This was expected and coherent with the low sensitivity of BL-28 to BET inhibition observed in the cell growth assay.

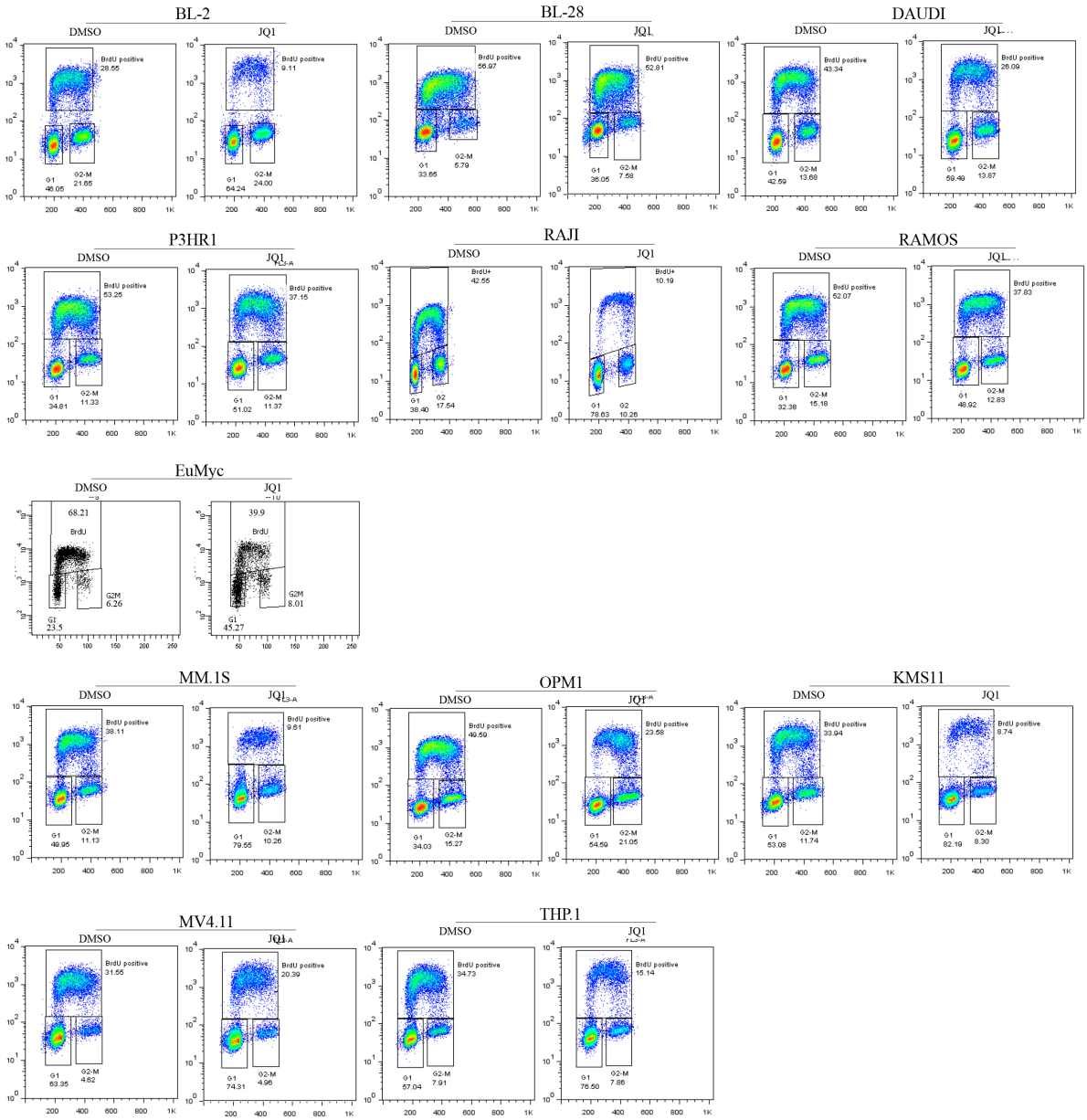

Fig. 18 BETs inhibition alters cell cycle progression

Cell cycle analysis by BrdU incorporation in BL (BL-2,BL-28, DAUDI, P3HR1, RAJI, RAMOS), Eμ-Myc lymphoma, MM (MM.1S, OPM1, KMS11) and AML (MV4.11, THP.1) cells after treatment for 24h with DMSO or JQ1 (100 nM for human cell lines or 50 nM JQ1 for Eμ-Myc cells). A BrdU pulse of 20' was performed. DNA content is evaluated by PI staining. For each cell line a single technical replicate was performed once.

In order to verify if the decrease in the percentage of cells engaged in active cell division was also associated to an increase in the amount of cellular death, we assessed cell vitality after 24h of treatment with BETs inhibitor, using Propidium Iodide (PI) staining as readout. As shown in the Fig.19, the different cell lines used showed a different percentage of PI positive cells in the control sample, reflecting intrinsic characteristics of each cell line. However, the treatment with JQ1 did not influence the amount of PI positive cells since it remained constant both in DMSO and JQ1

treated sample, suggesting the absence of any toxic effect mediated by BETs inhibition, at least in the first 24h.

Comprehensively, the analysis of cell growth and the vitality assay suggested that the first response to BETs inhibitors was mainly cytostatic with limited cytotoxic effects.

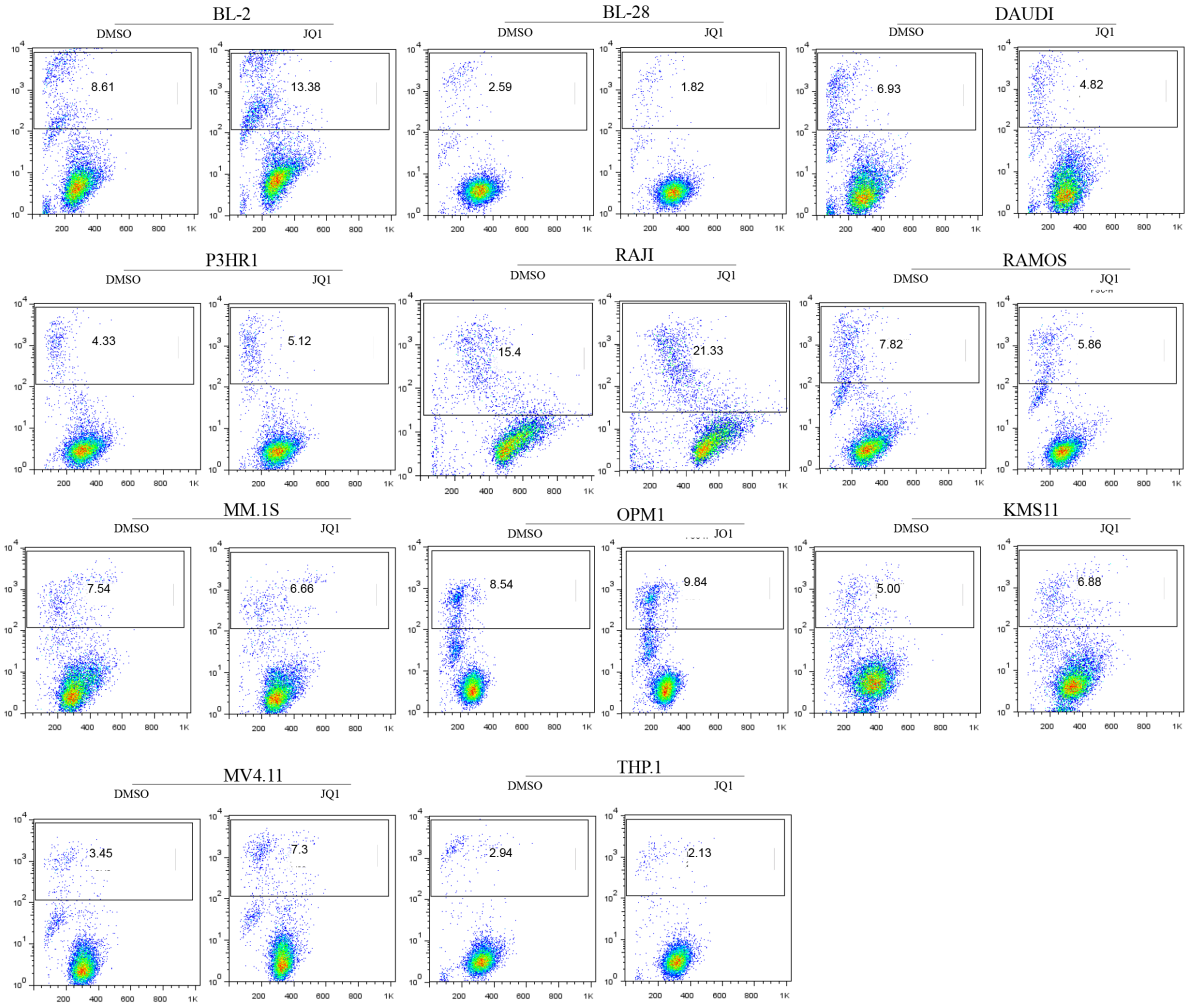

Fig. 19 BETs inhibition does not increase cellular death
Analysis of cell vitality on BL (BL-2, BL-28, DAUDI, P3HR1, RAJI, RAMOS), MM (MM.1S, OPM1, KMS11) and AML (MV4.11, THP.1) cells after treatment for 24h with DMSO or 100 nM JQ1 through PI incorporation. For each cell line a single technical replicate was performed.

The lack of a strong impact on cell death was further confirmed by experiments on Eμ-Myc cells infected with a constitutive vector encoding for BCL2, in order to make an apoptosis resistant version of these lymphomas. Two independent Eμ-Myc lymphomas infected with MSCV-BCL2 or MSCV-EV (as control) were treated with vehicle (DMSO) or 50 nM of JQ1 for up to 4 days and cell growth analysis was performed. As shown in Fig.20, the overexpression of BCL2, while providing increased fitness of the lymphomas, did not alter the effects of JQ1, since at all time point considered we observed a consistent inhibition of cell growth.

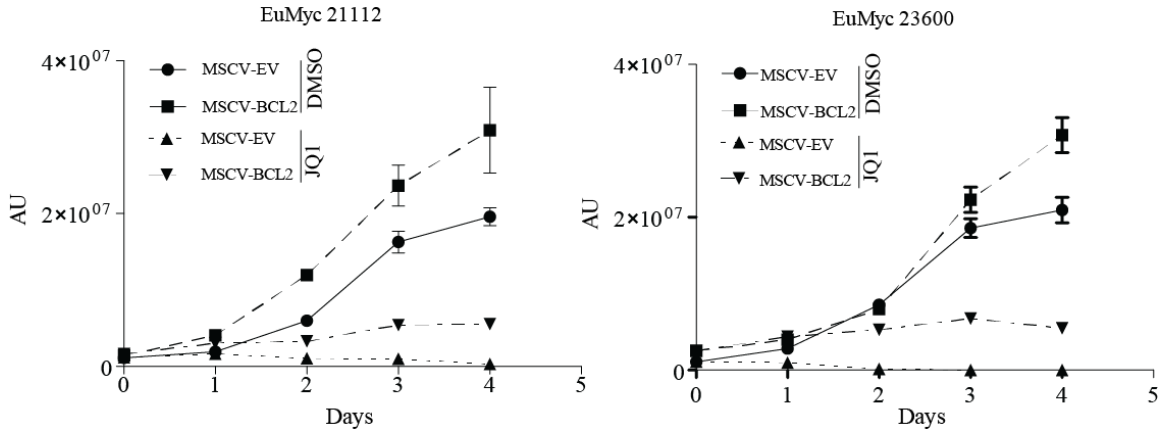

Fig. 20 BCL2 overexpression does not impact on the impairment of cell growth mediated by JQ1
Cell growth assay using CellTiterGlo (Promega) on two independent Eμ-Myc lymphomas (21112 and 23600) infected with MSCV-BCL2, or MSCV-EV as control, and treated with DMSO or 50 nM of JQ1 for up to 4 days. The mean and the standard deviations of 3 technical replicates are reported for each time point.

As expected, overexpression of BCL2 had no effect on cell cycle distribution: both control and BCL2 overexpressing lymphomas responded to BETs inhibition with a decrease in the percentage of S-phase cells (from ~60-50% in DMSO to ~30% in JQ1 sample) and a consequent increase in the amount of cells in G1 (from ~30-40% in DMSO to ~50-60% in JQ1) (Fig.21).

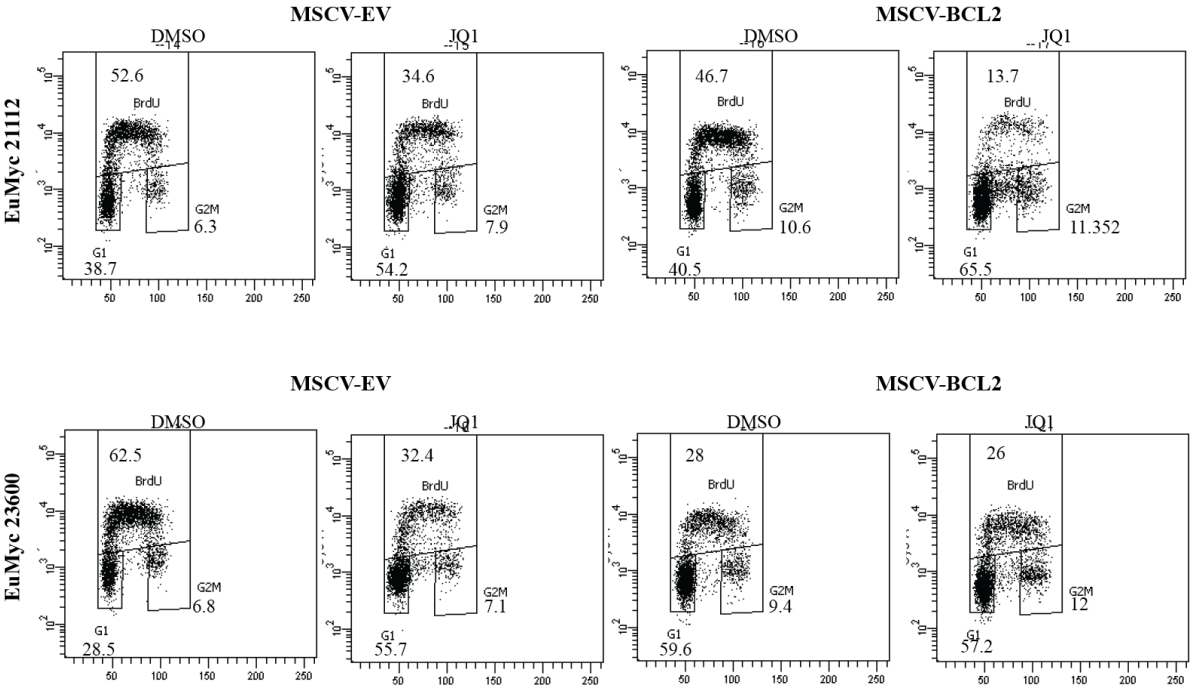

Fig. 21 Bypass of apoptosis is not influencing cell cycle distribution after BETs inhibition
Cell cycle analysis after BrdU incorporation in two independent Eμ-Myc lymphomas (21112 and 23600) infected MSCV-BCL2, or MSCV-EV as control, and treated with DMSO or 50 nM of JQ1 for 24h. DNA content is evaluated through PI staining. For each Eμ-Myc lymphoma a single technical replicate was performed.

The strong cytostatic effect observed is in line with what reported by studies on MM and AML (Delmore et al., 2011; Mertz et al., 2011; Zuber et al., 2011) where cell cycle arrest following BETs inhibition was linked to Myc downregulation. In order to verify if the decrease in *c-myc* expression after BETs inhibition was shared by different cellular systems, we analyzed Myc expression in BL and Eμ-Myc cells after JQ1 treatment, investigating both RNA and protein levels by RTqPCR and Western Blot, respectively. As previously reported (Delmore et al., 2011; Mertz et al., 2011; Zuber et al., 2011), we observed a substantial drop in Myc levels both at the RNA (Fig.22) and protein levels (Fig.23) either in MM and in AML cell lines. Myc downregulation was not consistently observed in all the BL cell lines analyzed: indeed, while BL-28, DAUDI and RAMOS showed a reduction in Myc transcription in a dose-dependent fashion; BL-2, P3HR1 and RAJI showed Myc mRNA changes only when treated with the highest concentration of JQ1 (500 nM) (Fig.22). The analysis of Myc protein levels phenocopied the expression data, since we observed Myc reduction in BL-2, P3HR1 and RAJI only after treatment with the highest concentration of drug (Fig.23). Similarly to what observed for some BL cell lines, also Eμ-Myc lymphomas did not show any changes in Myc mRNA (Fig.22) or protein (Fig.23) levels after 24h of BETs inhibitor treatment. These experiments suggested that JQ1 has growth inhibitory properties that can be separated from its effect on the modulation of Myc levels.

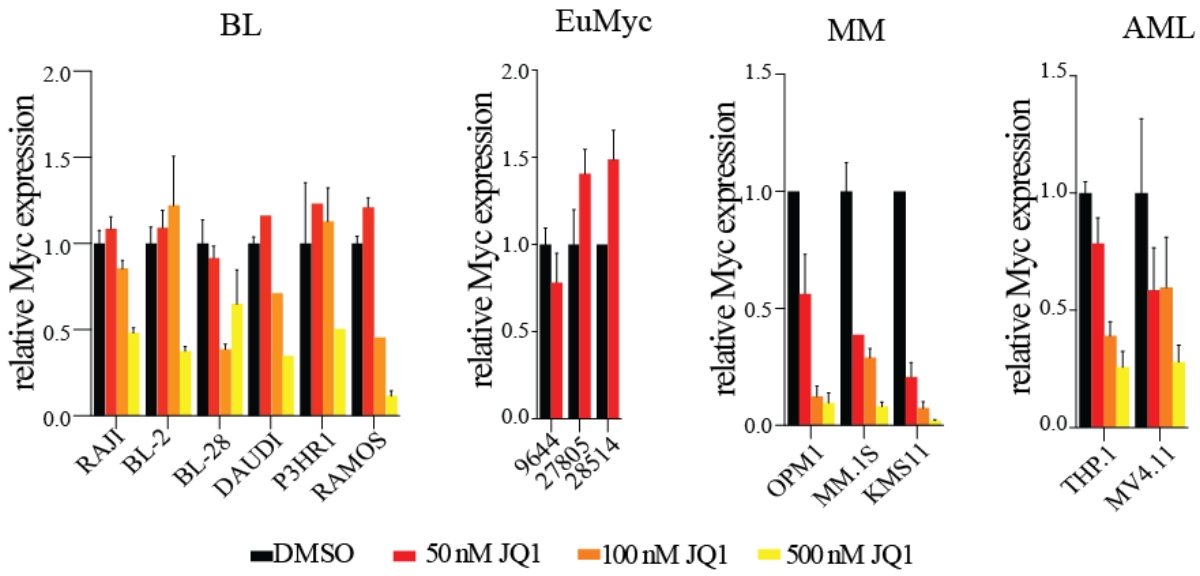

Fig. 22 BETs inhibition is not always associated to a reduction of Myc mRNA
Analysis of Myc expression levels by RTqPCR on BL (BL-2, BL-28, DAUDI, P3HR1, RAJI and RAMOS), three independent Eμ-Myc lymphomas (9644, 27805 and 28514), MM (MM.1S, OMP1, KMS11) and AML (THP.1, MV4.11) cells treated for 24h with different concentrations of JQ1 (black: DMSO, red: 50 nM, orange: 100 nM, yellow: 500 nM). The expression values are normalized on RPP0 and DMSO sample. The mean and the standard deviations of 3 technical replicates are reported.

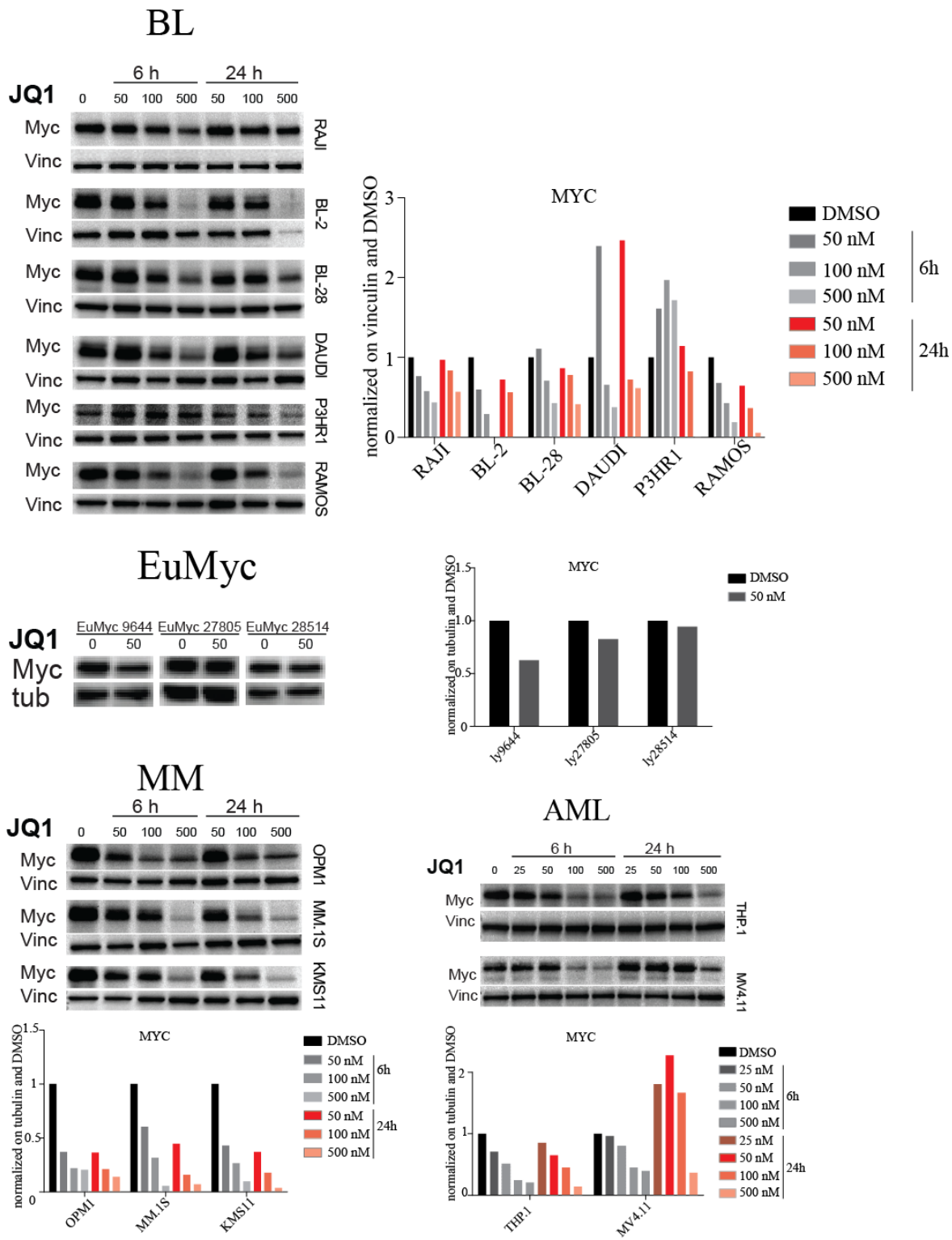

Fig. 23 BETs inhibition is not always associated to a reduction of Myc protein

Analysis of Myc protein levels by Western Blot analysis on BL (BL-2, BL-28, DAUDI, P3HR1, RAJI and RAMOS), three independent Eμ-Myc lymphomas (9644, 27805 and 28514), MM (MM.1S, OMP1, KMS11) and AML (THP.1, MV4.11) cells treated with different concentrations of JQ1 (0-50-100-500 nM) for 6 or 24h. Vinculin or tubulin is used as loading control. Quantification of Myc signal over Vinculin or Tubulin one is shown in the barplots. For RAJI cell line, 1 technical replicate for 3 independent biological replicates were performed and a representative western blot is shown. For the remaining cell lines, a single technical replicate was performed.

MM cell lines are characterized by a chromosomal translocation that juxtaposes the *c-myc* locus to the immunoglobulin heavy chain (IgH) regulatory regions. These IgH enhancers are characterized by extremely high BRD4 binding that positively regulates the transcription of the translocated *c-myc* (Lovén et al., 2013). In this light, Myc downregulation in response to JQ1 treatment could be explained as a consequence of BRD4 displacement from IgH enhancers. Since also BL are characterized by chromosomal rearrangement involving the *c-myc* gene and Ig regulatory elements, we asked if the lack of Myc downregulation in response to BETs inhibition, that we observed in some BL cell lines, could be dependent on different chromatin modifications of the IgH enhancers. To test this hypothesis, we performed Chromatin Immuno-Precipitation followed by quantitative PCR (ChIPqPCR) experiments on the IgH regulatory regions for H3K27Ac (Fig.24), commonly used as mark of open and active chromatin. The levels of acetylation were comparable among all the cell lines used, with the only exception for BL-28 that did not show any acetylation in the IgH enhancers (Fig.24).

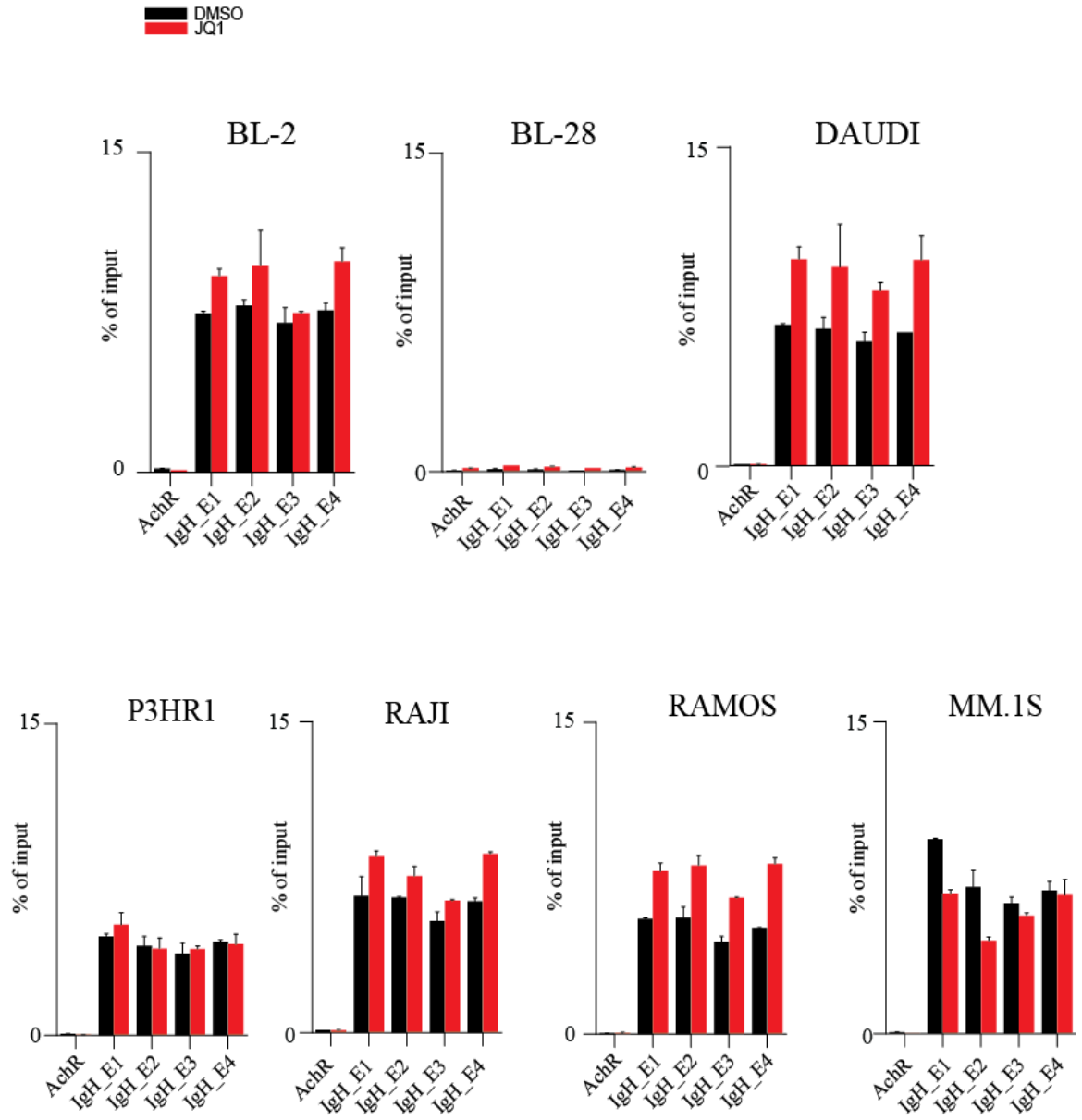

Fig. 24 Analysis of the acetylation levels on the IgH regulatory regions
Analysis of histone H3 acetylation levels on IgH regulatory regions by ChIPqPCR for H3K27Ac on BL (BL-2, BL-28, DAUDI, P3HR1, RAJI, RAMOS) and MM.1s treated with DMSO (black) or 100 nM of JQ1 (red) for 24h. The mean and the standard deviations of 3 technical replicates are reported. Acetylcholine Receptor (AchR) is used as negative control.

Since previous works on MM cells showed that IgH enhancers are particularly enriched for BRD4 binding, we verified if also BL IgH enhancers were decorated with BRD4 and if there were differences in terms of binding intensity or response to JQ1 treatment that could account for the absence of Myc downregulation observed in particular in RAJI. As it is shown in Fig.25, BL and MM cell lines were characterized by different levels of BRD4 binding to the IgH enhancers. In general, BL cells showed a lower BRD4 signal on the IgH enhancer regions compared to MM

lines. In particular, for 3 out of 6 BL cell lines used (BL-28, P3HR1, RAJI), BRD4 binding at the IgH enhancers was undetectable, while for the remaining 3 (BL-2, DAUDI, RAMOS) BL cell lines, BRD4 signal was barely enriched respect to the negative control, with a signal intensity that was from 5 to 10 times lower than the one determined in MM lines. Furthermore, BRD4 binding was strongly reduced in MM cells after JQ1 treatment, confirming the efficacy of the drug.

Interestingly, no BRD4 could be detected on the IgH enhancers of P3HR1 or RAJI, possibly accounting for their lack of Myc downregulation following BET inhibition.

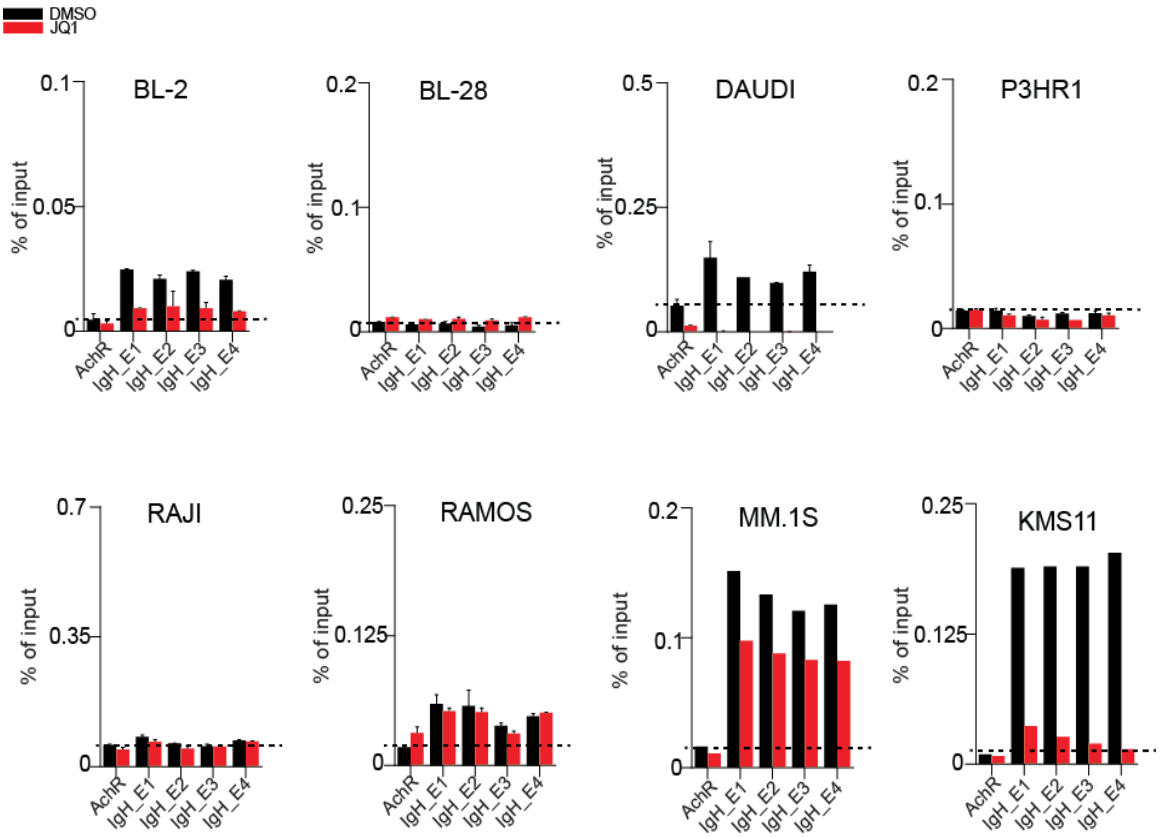

Fig. 25 BL cells are characterized by low levels of BRD4 binding on IgH enhancers
Analysis of BRD4 binding on IgH regulatory regions by ChIPqPCR for BRD4 on BL (BL-28,DAUDI, P3HR1, RAJI, RAMOS) and MM (MM.1S, KMS11) treated with DMSO (black) or 100 nM of JQ1 (red) for 24h. The mean and the standard deviations of 3 technical replicates are reported. Acetylcholine Receptor (AchR) is used as negative control.

The evidences collected so far suggested that MM and BL cell lines, despite the similar chromosomal rearrangement, control *c-myc* expression differently. Indeed, while the strong downregulation of Myc in MM cells could be explained by the massive depletion of BRD4 from the IgH enhancers, in BL cells other BRD4-independent regulatory mechanisms should account for Myc regulation, since the low BRD4 binding on IgH enhancers and the lack of transcriptional effect on Myc after JQ1 treatment.

JQ1 effects are mainly mediated by BRD4

While JQ1 shows high affinity for BRD4, it also has some potential activity on other members of the BET family (Filippakopoulos et al., 2010). To gain some insight regarding the intracellular target of JQ1, we first evaluated the expression of the 3 main BET proteins expressed in somatic tissue by RTqPCR. While BRD3 is barely expressed in all the cell lines analyzed (BL, MM and Eμ-Myc lymphomas), BRD4 is the predominant BET protein expressed in BL and MM cell lines. Instead, in the Eμ-Myc system, both BRD2 and BRD4 are present at comparable levels (Fig.26).

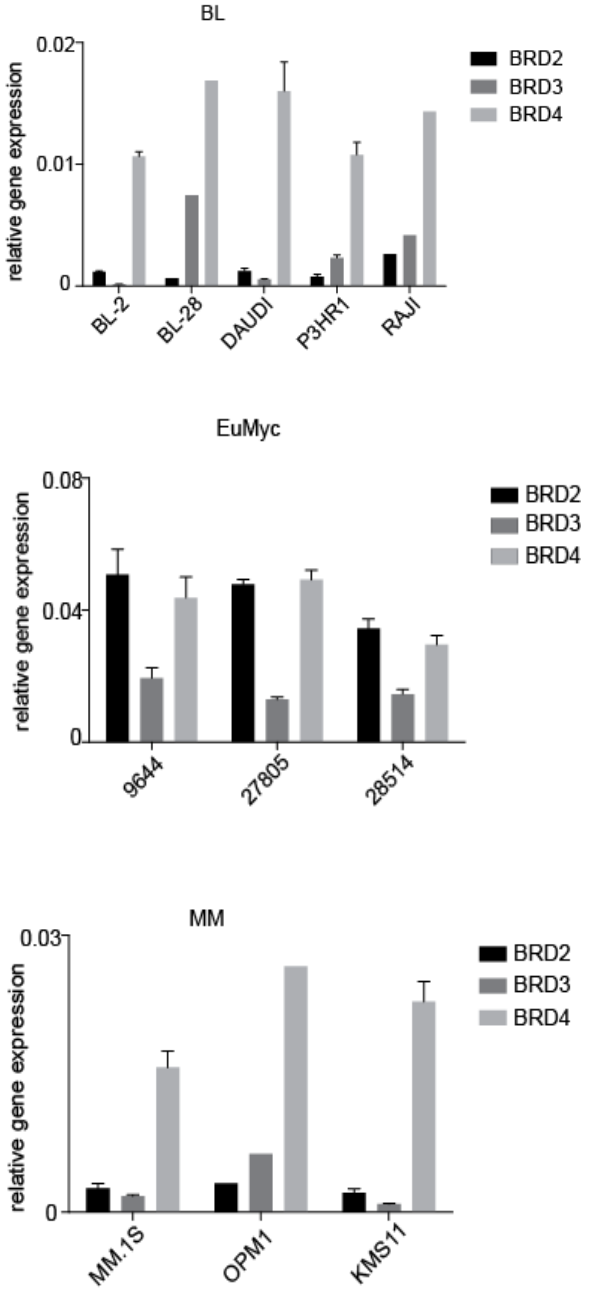

Fig. 26 BRD2 and BRD4, but not BRD3, are expressed in BL, Eμ-Myc lymphomas and MM
Analysis of BETs proteins expression levels by RTqPCR for BRD2 (black), BRD3 (dark grey) and BRD4 (light grey) in BL (BL-2, BL-28, DAUDI, P3HR1, RAJI), Eμ-Myc lymphomas (9644, 27805 and 28514) and MM (MM.1S, OPM1, KMS11). The expression values are normalized to RPP0 levels. The mean and the standard deviations of 3 technical replicates are reported.

Since JQ1 causes the displacement of its target from the acetylated histones, we evaluated the chromatin occupancy of BET proteins performing ChIPqPCR for BRD2, BRD3 and BRD4 on the TSS of genes selected (Fig.27). While both RAJI and Eμ-Myc cells showed no BRD3 enrichment compared to the negative control (Acetylcholine Receptor: AchR), as expected since the very low

expression level, the other two members of the family, BRD2 and BRD4, were bound to the TSS of the genes analyzed.

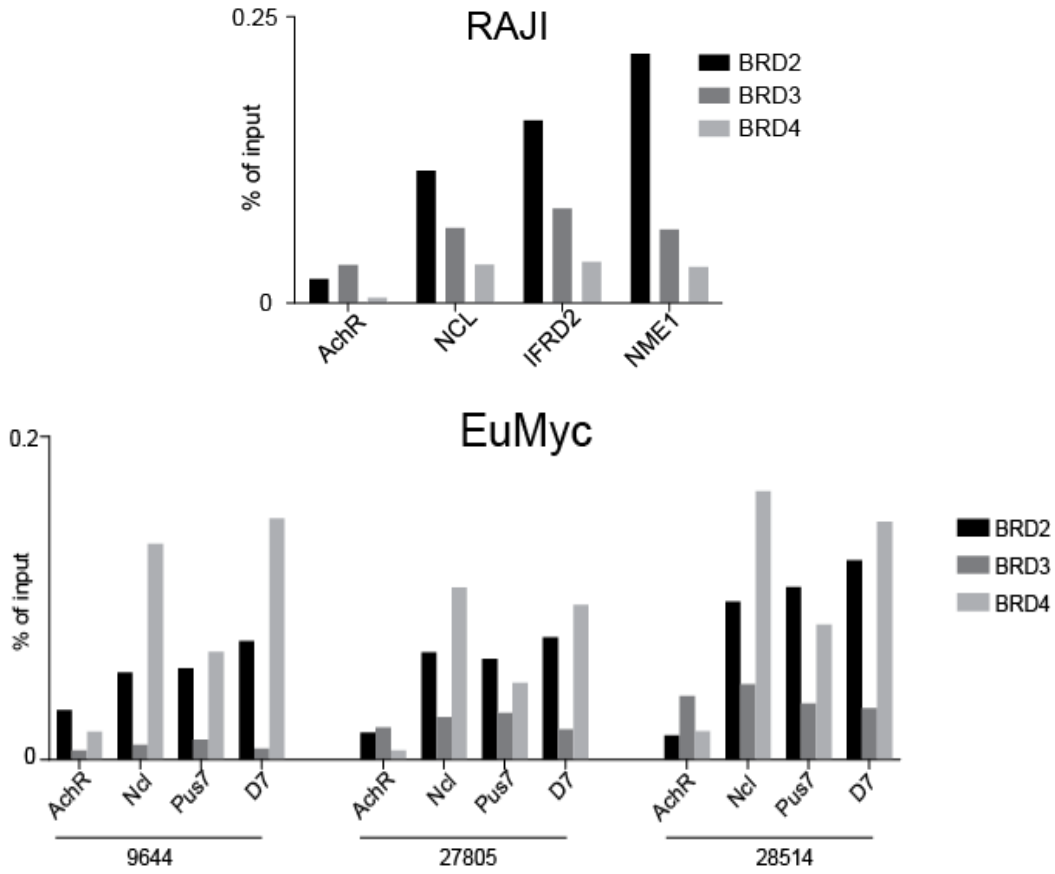

Fig. 27 BRD2 and BRD4, but not BRD3, bind promoters of active genes.
Analysis of BRD2 (black), BRD3 (dark grey) and BRD4 (light grey) chromatin binding by ChIPqPCR for on the promoter of expressed genes on RAJI or Eμ-Myc lymphomas. Acetylcholine Receptor (AchR) is used as negative control. For each cell line a single technical replicate was performed.

This results were in line with already published ChIPseq experiments on MM.1S cells for all the BET proteins (Anders et al., 2014). Indeed, these genome wide data showed that the 3 family members co-occupied the same genomic regions and furthermore, BRD4 signal was stronger and more abundant respect to BRD2 or BRD3 ones. After verifying the expression and the chromatin binding of BET proteins, we tested if BRD2 and BRD4 are equally affected by the treatment with JQ1, performing ChIPqPCR for BRD2 or BRD4 on RAJI or Eμ-Myc lymphomas after the treatment with DMSO or JQ1 for 24h (Fig.28). While BRD4 was consistently displaced after JQ1 treatment in all the cellular models analyzed, BRD2 response was more heterogeneous since just one Eμ-Myc lymphoma (28514) out of 3 showed a strong reduction in BRD2 enrichment after BET inhibition, thus suggesting that the cytostatic effect observed upon JQ1 administration was mainly due to BRD4 inhibition.

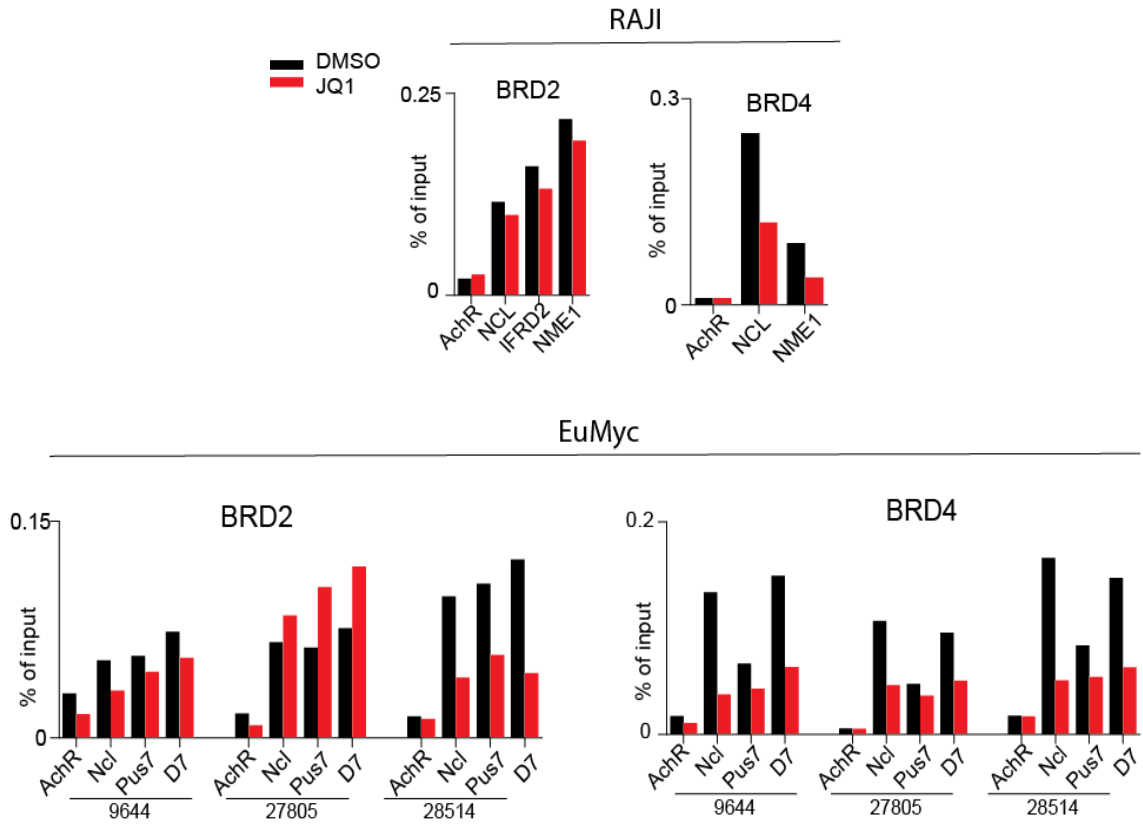

Fig. 28 JQ1 displaces BRD4, and less efficiently BRD2, from chromatin
Analysis of BRD2 or BRD4 binding to the chromatin after DMSO (black) or JQ1 (red) treatment through ChIPqPCR on RAJI or Eμ-Myc lymphomas (9644, 27805 and 28514). Acetylcholine Receptor (AchR) is used as negative control. For each cell line a single technical replicate was performed.

To further demonstrate the involvement of BRD4 in JQ1 response, we performed silencing experiments using specific shRNAs targeting BRD4. After a first attempt using a constitutive silencing vector, we took advantage of a conditional silencing system where the expression of a specific shRNA is induced by the addition of Doxycycline (Fellmann et al., 2013). All the 3 independent shRNAs used caused more than 80% reduction in BRD4 expression that was maintained for up to 3 days (Fig.29). The decrease of mRNA detected was mirrored by the reduction of protein production, suggesting the efficacy of the shRNA used (Fig.30).

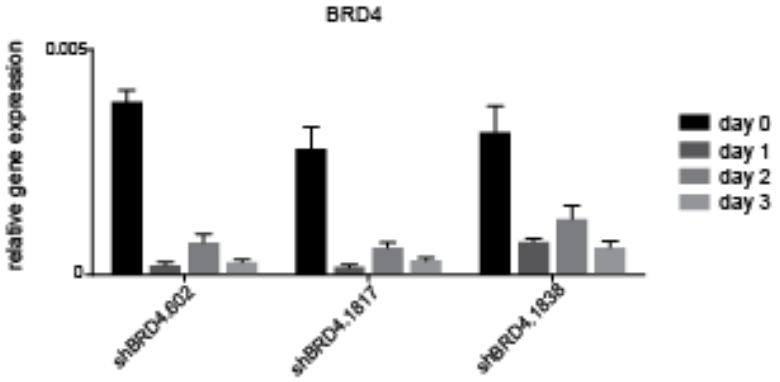

Fig. 29 shRNAs against BRD4 strongly reduce BRD4 mRNA production
Expression analysis by RTqPCR to evaluate the level of BRD4 knock down after 0 (black), 1 (dark grey), 2 (gray 50%) or 3 (light gray) days of shRNA induction through the administration of Doxycycline in RAJI. 3 independent shRNA are used: shBRD4.602, shBRD4.1817, shBRD4.1838. The expression values are normalized on RPP0 levels. The mean and the standard deviations of 3 technical replicates are reported.

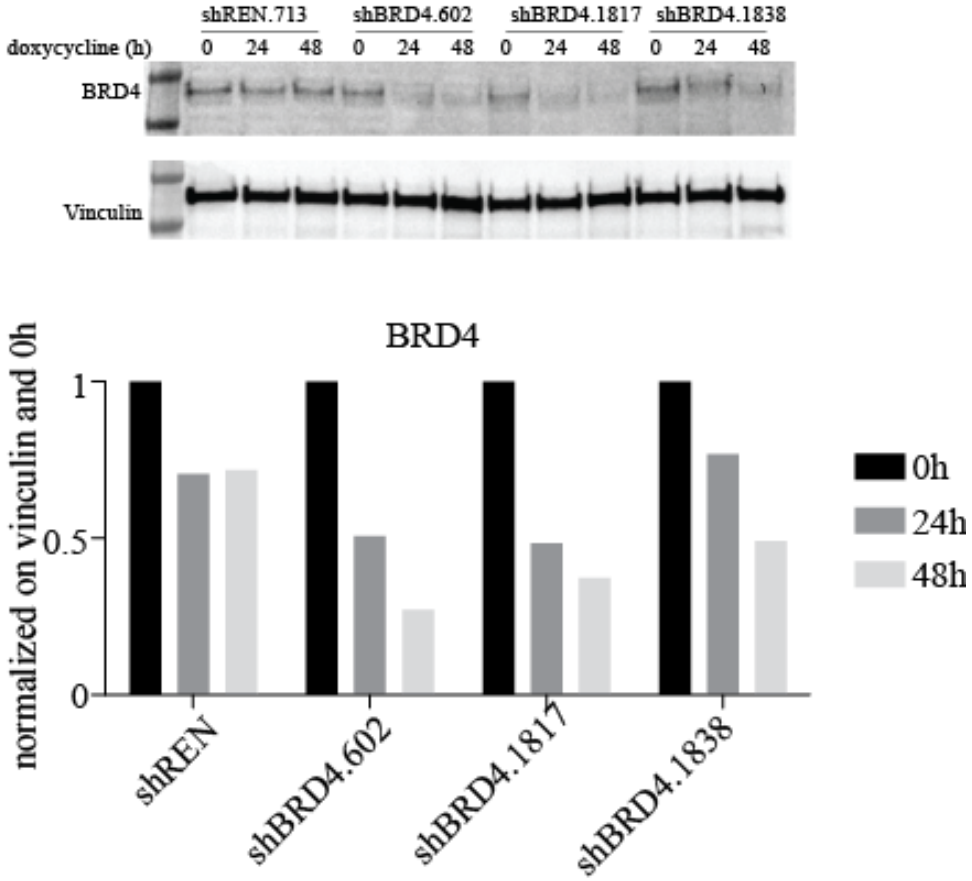

Fig. 30 shRNAs against BRD4 strongly reduce BRD4 protein levels
Analysis of BRD4 protein levels by Western Blot to evaluate the level of BRD4 downregulation after 0, 24 or 48h of shRNA induction through Doxycycline administration in RAJI. 3 independent shRNA are used: shBRD4.602, shBRD4.1817, shBRD4.1838. Vinculin is used as loading control. In the lower panel the barplot shows the quantification of the Western Blot: BRD4 signal (black: 0h, dark gray: 24h, light gray: 48h) is normalized on the Vinculin. Two technical replicates were performed and a representative western blot is shown.

In order to verify if BRD4 silencing could phenocopy BETs inhibitor response, we analyzed the cellular and transcriptional effect mediated by shRNAs against BRD4. Expression analysis by

RTqPCR demonstrated that BRD4 silencing strongly downregulated genes sensitive to JQ1 treatment, while the expression of genes insensitive to JQ1 remained constant up to 3 days after shRNA induction (Fig.31).

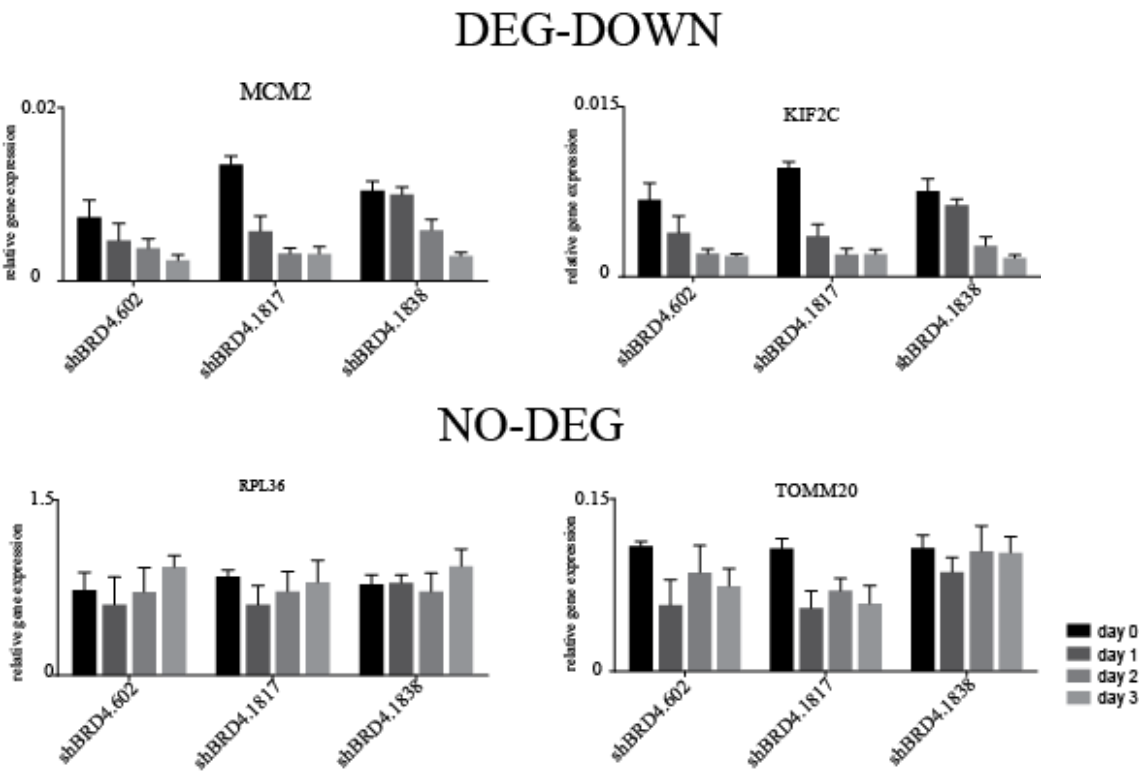

Fig. 31 BRD4 silencing recapitulates JQ1 transcriptional effects
Expression analysis by RTqPCR to evaluate the expression levels of genes sensitive or insensitive to JQ1 after 0 (black), 1 (dark grey), 2 (gray 50%) or 3 (light gray) days of BRD4 silencing through the administration of Doxycycline in RAJI. 3 independent shRNA are used: shBRD4.602, shBRD4.1817, shBRD4.1838. The expression values are normalized on RPP0 levels. The mean and the standard deviations of 3 technical replicates are reported.

Moreover, we performed cell cycle analysis to evaluate cytostatic effects following BRD4 silencing (Fig.32). Doxycycline administration caused an increase from ~40% to ~60-70% in the G0/G1 population already after 24h and the percentage of arrested cells further increased after 48h of silencing (from 50% to ~80%).

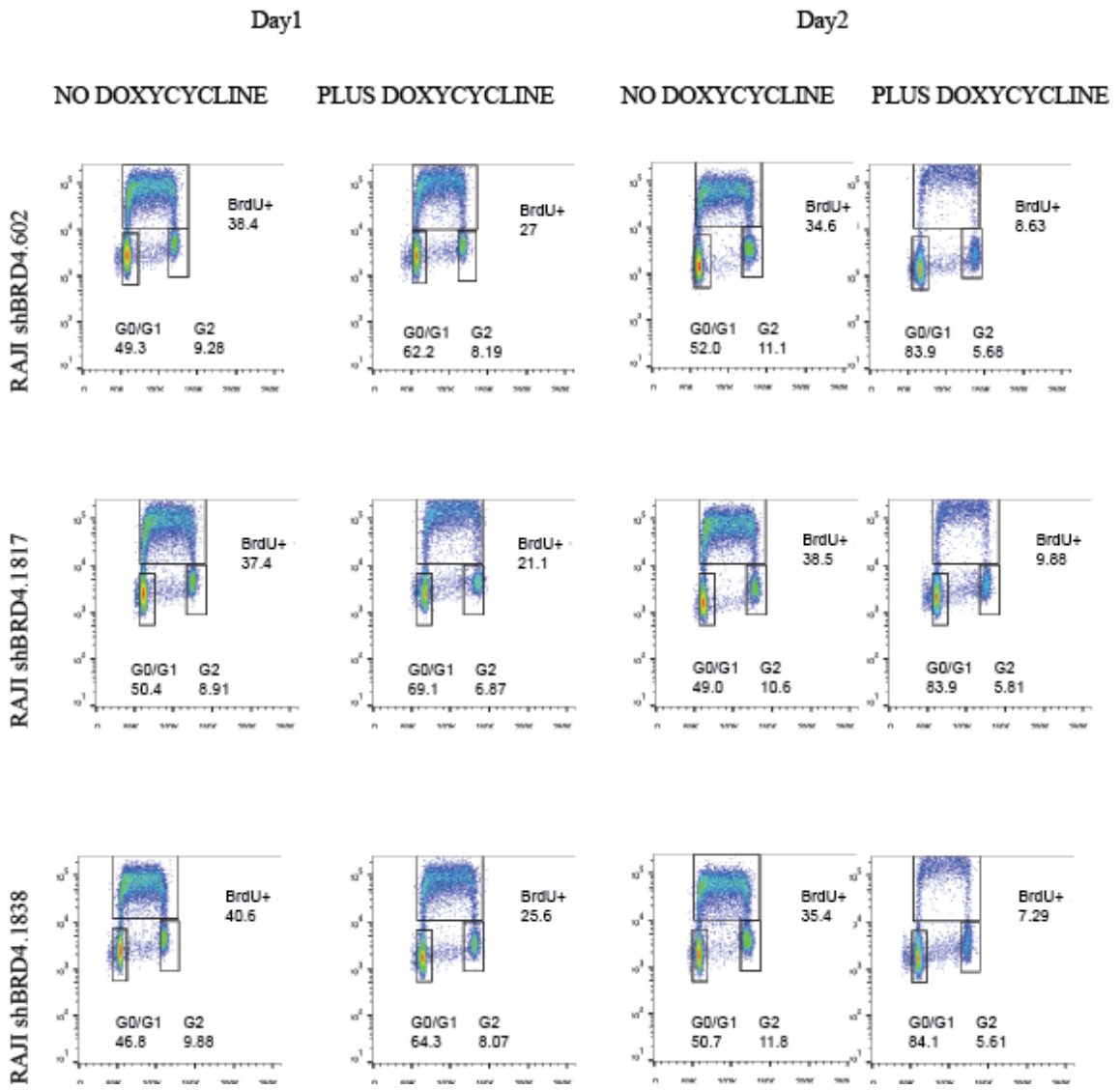

Fig. 32 BRD4 silencing recapitulates the block in the cell cycle progression induced by JQ1
Cell cycle analysis through BrdU incorporation (BrdU pulse: 20') after shBRD4 induction through Doxycycline administration for 24 or 48h. 3 different shRNAs against BRD4 are used: shBRD4.602, shBRD4.1817, shBRD4.1838. DNA content is evaluated through PI staining. For each cell line a single technical replicate was performed.

Whilst both BRD2 and BRD4 occupied the same genomic regions and JQ1 caused slight displacement of also BRD2 from the chromatin, we decided to use BRD4 as an approximation of the other BET members since the better quality of BRD4 ChIPseq data and the phenocopying effects of BRD4 silencing respect to JQ1 treatment.

Optimization of BET proteins Chromatin ImmunoPrecipitation

Having realized the poor performance, in our hands, of published protocol for BRD4 ChIP, we set out to optimize the procedure in order to obtain high resolution ChIPseq maps. Indeed, BRD4 ChIPseq experiments performed on RAJI using standard ChIP protocol with formaldehyde formaldehyde (FA) as fixative agent resulted in very low amount of immunopricipitated DNA. The quantity immunoprecipitated DNA strongly affected the quality of the ChIPseq library prepared, indeed ChIP signal was barely distinguishable from the background, with a consequent bad peak calling (only 884 BRD4 peaks were identified).

The implementation of the fixation step, using a fixative able to create covalent bonds among proteins not directly bound to DNA (i.e. glutaraldehyde: GLUT), allowed us to immunoprecipitate BRD4 more effectively. Indeed, the good quality of BRD4 ChIP signal was evident both in ChIPqPCR (Fig.33) and in ChIPseq (Fig.34) analysis, since the enrichment signal after the standard fixation protocol (FA) was undistinguishable from the negative control (AchR) while the use of an alternative fixative agent (GLUT) allowed 30 fold enrichment over the background. Furthermore, we verified that the use of a stronger fixative step did not cause the immunoprecipitation of non specific protein performing BRD4 ChIP after the treatment with JQ1 for 24h. Indeed we were still able to clearly detect BRD4 displacement from the chromatin (Fig.33-34).

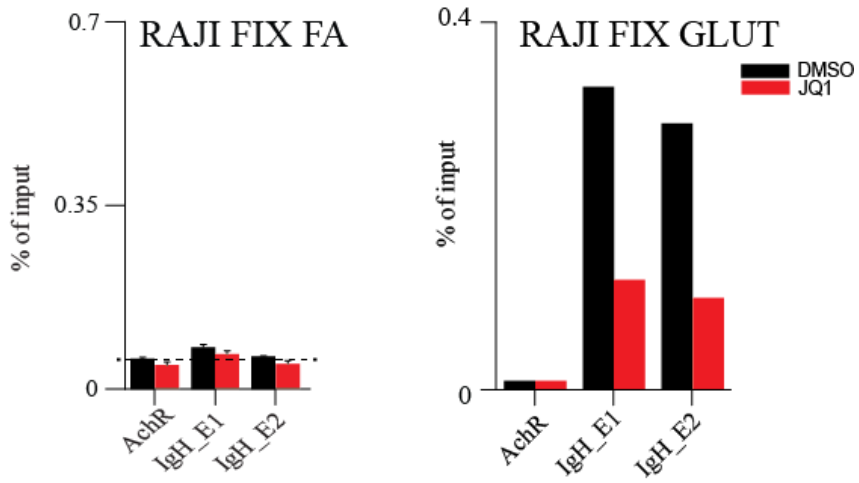

Fig. 33 Implementation of the fixation step increases the efficiency of BRD4 immunoprecipitation
Analysis of BRD4 binding on IgH regulatory regions by ChIPqPCR for BRD4 on RAJI fixed for 10' with formaldehyde or glutaraldehyde after treatment with DMSO (black) or 100 nM JQ1 (red) for 24h. Acetylcholine Receptor (AchR) is used as negative control. For RAJI fixed with FA the mean and the standard deviation of three technical replicates are reported; for RAJI fixed with GLUT a single replicate was performed.

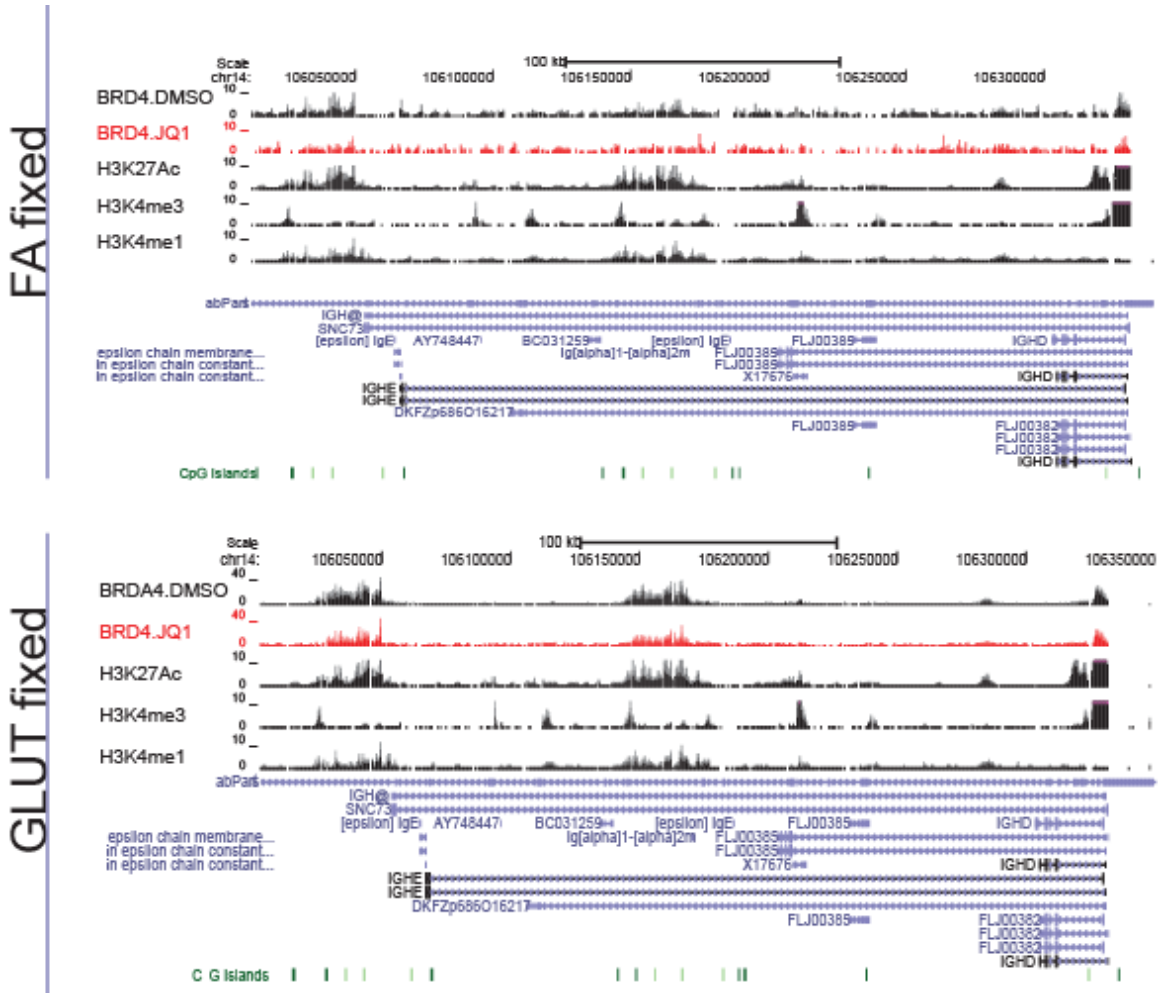

Fig. 34 Implementation of the fixation step increases the efficiency of BRD4 immunoprecipitation
Screenshot of BRD4 ChIPseq on RAJI fixed for 10' with formaldehyde or glutaraldehyde after treatment with DMSO (black) or 100 nM JQ1 (red) for 24h. H3K27Ac, H3K4me3, H3K4me1 are used to identify open and active chromatin. Each ChIP sample was sequenced once.

The improvement of signal to noise ratio was sufficient to properly proceed with further genome wide analyses, indeed we were able to identify 11915 different peaks. Furthermore, comparison of BRD4 peaks identified after standard or implemented fixation step showed that all the former peaks were include in the latter (Fig.35).

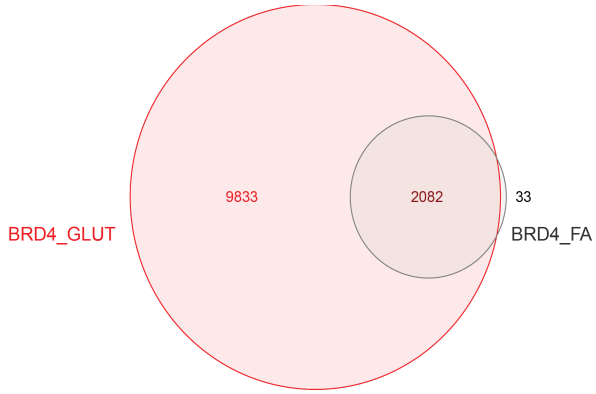

Fig. 35 The use of an alternative fixative enlarges the chromatin binding sites identified for BRD4
Analysis of genome wide BRD4 binding using different fixation protocols: FA (formaldehyde: gray), GLUT (glutaraldehyde: red). In the Venn Diagram the overlapping area (gray+red) shows the number of BRD4 common peaks, the red only and the gray only area represent the number of unique peaks identified after the fixation with GLUT or with FA, respectively. Each ChIP sample was sequenced once.

Genome Wide mapping of BRD4

To verify if the reduction in BRD4 binding mediated by JQ1 was limited to the genes analyzed by ChIPqPCR or instead if it was a common feature shared in a genome wide scale, we performed ChIPseq for BRD4 on cells treated with DMSO or JQ1 for 24h. As shown by the Venn Diagram in Fig.36, depicting the overlap between BRD4 ChIPseq in RAJI treated with DMSO or JQ1, the number of BRD4 peaks was strongly reduced after BETs inhibition, indeed only ¼ of peaks were still present in JQ1 sample (Fig.36). Furthermore, BRD4 peaks that were not displaced by JQ1 were already present in the DMSO sample (Fig.36). Similar results were also obtained using the primary Eμ-Myc lymphoma cells where only half of BRD4 peaks was still present after the treatment with JQ1 (Fig.36). Whilst BETs inhibition strongly reduced BRD4 occupancy both in BL and in Eμ-Myc lymphoma cells, a difference in percentage of JQ1-resistent BRD4 peaks was evident.

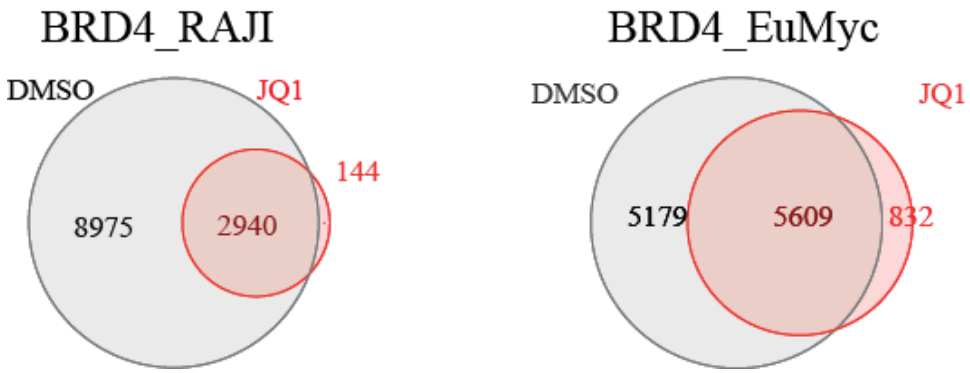

Fig. 36 BETs inhibition efficiently impairs BRD4 genome wide binding
Analysis of BRD4 chromatin binding in RAJI or Eμ-Myc lymphoma after treatment for 24h with DMSO (gray) or JQ1 (red). In the Venn diagram the overlapping regions (gray+red) represent the common BRD4 peaks identified both in DMSO and in JQ1 samples. The gray only and the red only regions represent the number of BRD4 peaks identified uniquely in DMSO and JQ1 samples, respectively. Each ChIP sample was sequenced once.

Nonetheless, the remaining BRD4 peaks in both RAJI and Eμ-Myc lymphoma cells were strongly less enriched than the DMSO counterpart, suggesting that JQ1 is exerting its activity on all BRD4 peaks, since the vast majority of them was displaced while the residual peaks showed a marked reduction in signal intensity (Fig.37)

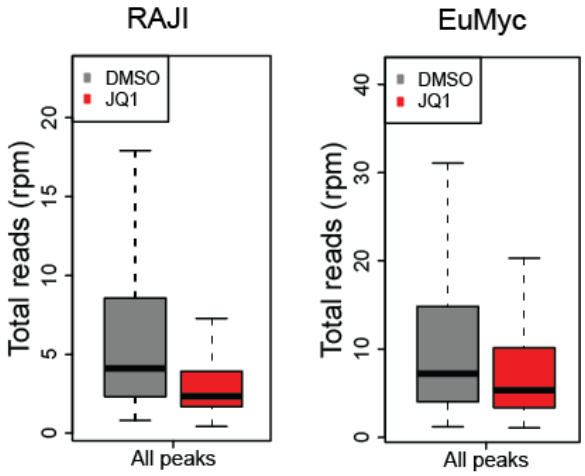

Fig. 37 BETs inhibition causes a strong reduction in BRD4 intensity binding
Quantification of reads associated to BRD4 peaks (rpm: reads per million) in RAJI or Eμ-Myc lymphomas after 24h treatment with DMSO (gray) or JQ1 (red).

In order to have more insight into BRD4 chromatin binding, we performed a genomic distribution analysis of BRD4 peaks. As shown by the pie chart in Fig. 38, BRD4 peaks were equally distributed among promoter, intragenic and intergenic regions in RAJI. Moreover the allocation of BRD4 peaks was not strongly influenced by JQ1 treatment, since the percentage of peaks associated to promoter, intragenic and intergenic regions was comparable among DMSO and JQ1

samples, suggesting the absence of a preferential displacement from a specific genomic location (Fig.38). Similar results were obtained also in Eμ-Myc lymphomas, where BRD4 occupied regions were equally assigned to genes or intergenic locations (Fig.38).

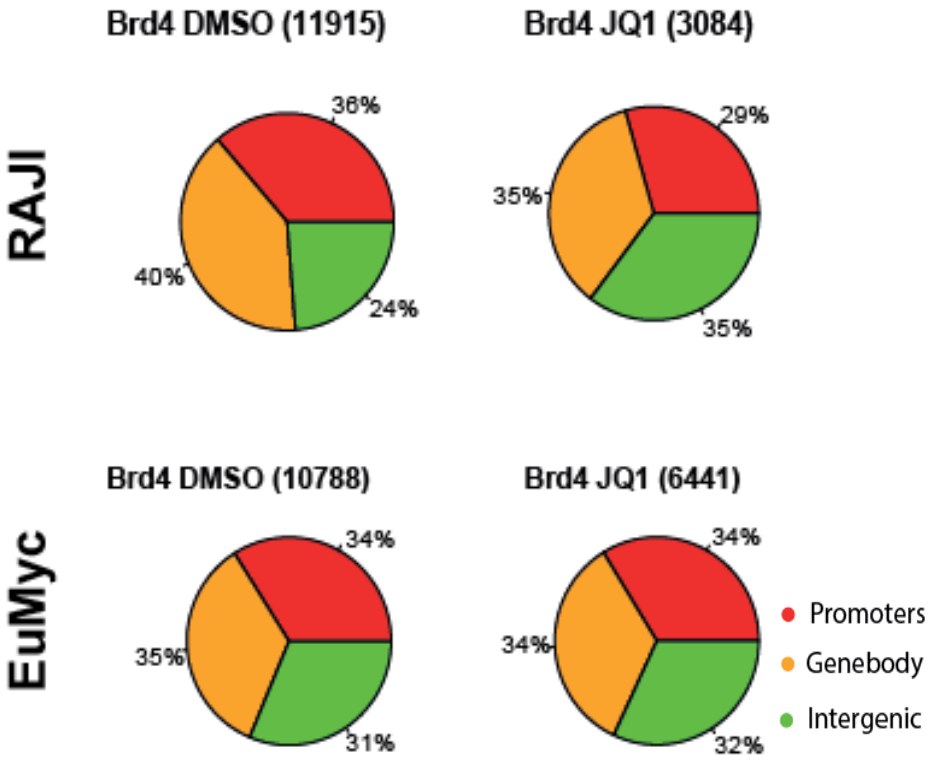

Fig. 38 BETs inhibition does not affect BRD4 peaks distribution
Analysis of genomic distribution (promoter: red, genebody: orange, intergenic: green) of BRD4 peaks after 24h of treatment with DMSO (left) or JQ1 (right) in RAJI (upper panel) or Eμ-Myc lymphomas (lower panel). Each ChIP sample was sequenced once.

Overall, the genome wide studies of BRD4 distribution in RAJI and Eμ-Myc cells showed that BRD4 was homogeneously disperse among promoter, intergenic and intragenic regions and that all BRD4 binding sites were sensitive to BETs inhibitor effects, since we noticed a reduction of number and intensity of the peaks regardless of the genomic localization.

BETs inhibition affects Myc and E2F transcriptional programs

Since BET proteins are involved in the regulation of transcription (Jang et al., 2005; Yang et al., 2005), we first investigated the genome wide transcriptional changes caused by JQ1. Using microarray assay, we were able to identify a small subset of genes affected by BETs inhibition; in particular we scored 1017 downregulated and 481 upregulated genes (JQ1-DEGs) in RAJI. RTqPCR analysis on genes selected from the downregulated or not-deregulated classes was used

to efficiently validate the genome wide assay, indeed we were able to confirm respectively the downregulation or the insensitivity to the JQ1 treatment using a different approach, obtaining a good correlation among the two techniques (R^2=0.91) (Fig.39-40). Furthermore, the RTqPCR analysis suggested that genes responsive to BETs inhibition were downregulated in a dose-dependent manner, while not responsive genes were unaffected even at high concentration of JQ1 (Fig.39).

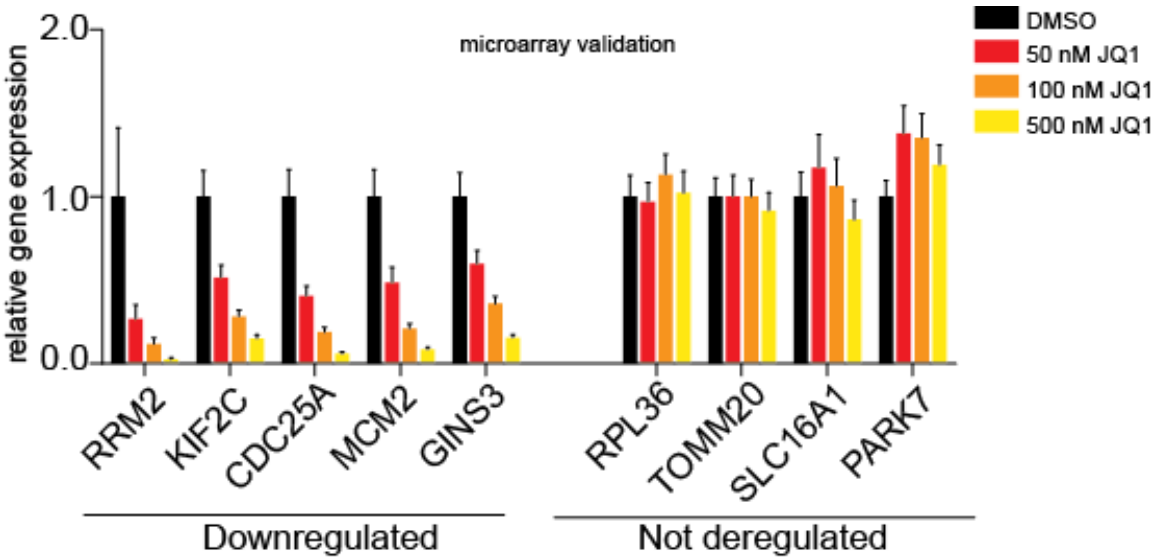

Fig. 39 JQ1 responsive genes are downregulated in a dose-dependent manner, while JQ1 insensitive genes are not affected neither by high concentration of drug
Expression analysis by RTqPCR in RAJI treated for 24h with DMSO or different concentration of JQ1 (black: DMSO, red: 50 nM, orange: 100 nM, yellow: 500 nM) to validate downregulated or not deregulated genes obtained from Microarray assay. The expression levels are normalized on RPP0 and DMSO sample. The mean and the standard deviations of 3 technical replicates are reported.

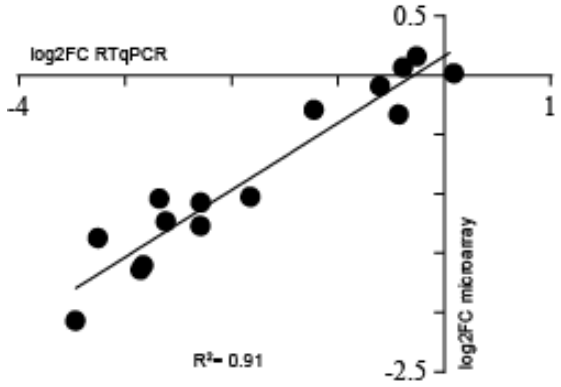

Fig. 40 RTqPCR validates genome wide expression data in RAJI
Correlation plot to validate the genome wide expression data on RAJI treated for 24h with DMSO or JQ1. On the x axis the Log2 Fold Change obtained from RTqPCR is reported, while on the y axis the Log2 Fold Change obtained from Microarray assay is reported.

Similar results were obtained in Eμ-Myc lymphomas, where we investigated, through RNA sequencing (RNAseq), the transcriptional changes caused by BETs inhibition. Also in this system, we were able to identify a subset of JQ1 deregulated genes (608 downregulated and 840 upregulated) that we validated by Nanostring® (Fig.41) and RTqPCR (Fig.42) assays.

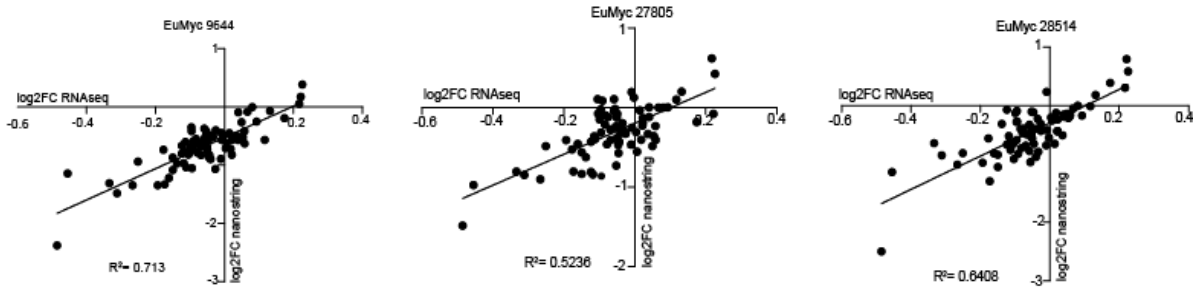

Fig. 41 Nanostring assay validates genome wide expression data in Eμ-Myc lymphomas
Correlation plot to validate the genome wide expression data on Eμ-Myc lymphomas (9644, 27805 and 28514) treated for 24h with DMSO or JQ1. On the x axis the Log2 Fold Change obtained from RNAseq is reported, while on the y axis the Log2 Fold Change obtained from Nanostring assay is reported.

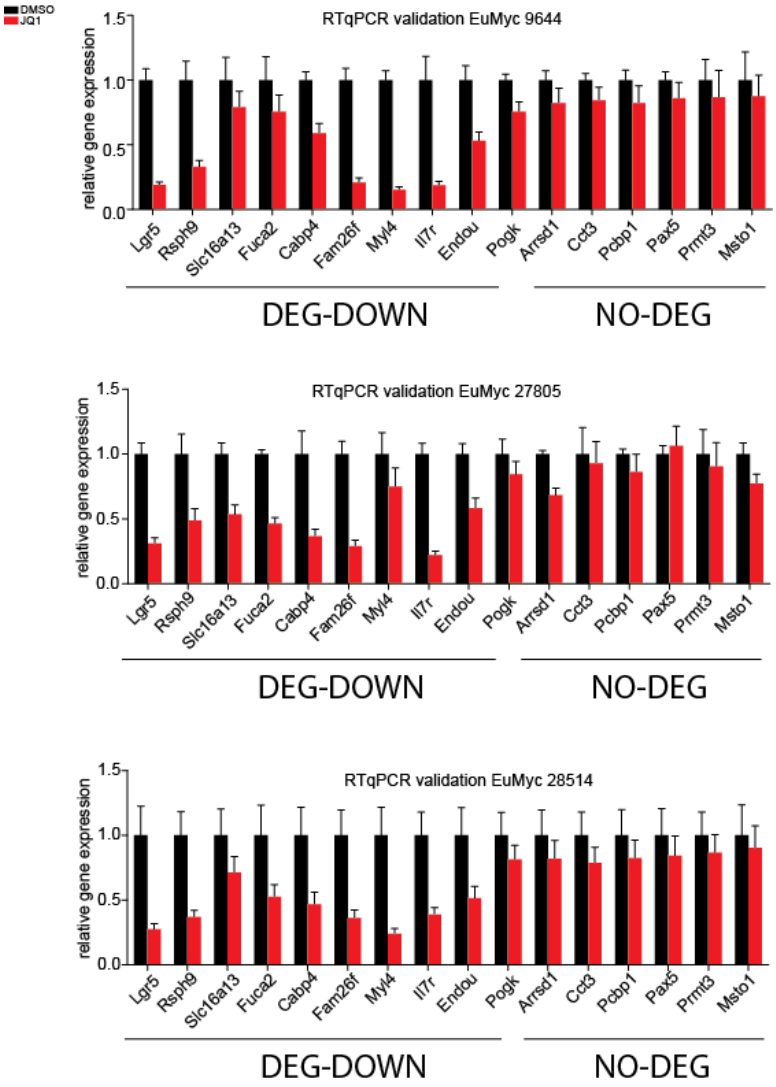

Fig. 42 RTqPCR validates genome wide expression data in Eμ-Myc lymphomas
Expression analysis by RTqPCR to validate downregulated or not deregulated genes identified through RNAseq assay in Eμ-Myc lymphomas (9644, 27805 and 28514) treated with DMSO (black) or 50 nM of JQ1 (red) for 24h. The expression values are normalized on RPP0 and DMSO sample. The mean and the standard deviations of 3 technical replicates are reported.

We functionally annotate JQ1-DEGs by performing Gene Set Enrichment Analysis (GSEA) (Subramanian et al., 2005) using different collections from Molecular Signature Database (MSigDB) (Subramanian et al., 2005) as gene sets of reference. While upregulated genes in RAJI did not show robust enrichment for any gene set, analysis of downregulated genes using MSigDB collection for Gene Ontology (GO) terms (C5) showed strong enrichment for genes involved in the cell cycle control and DNA replication or G2/M checkpoint, as expected since the block in G1 after JQ1 treatment (Fig.43).

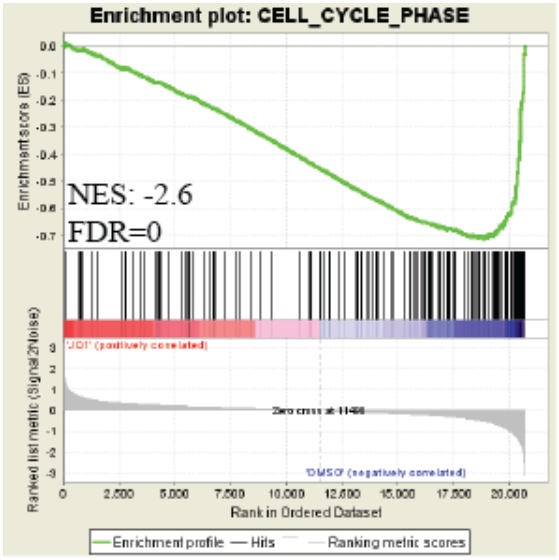

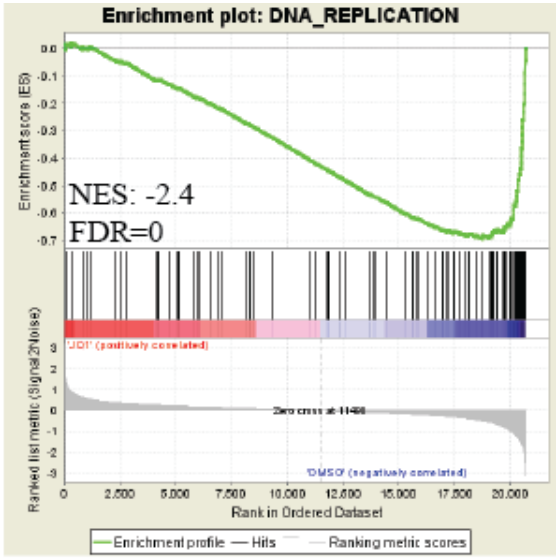

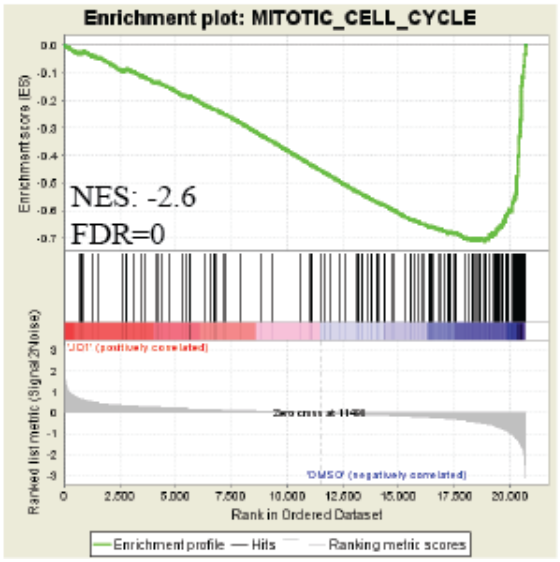

GO_term	SIZE	ES	NES	FDR q-val
CELL_CYCLE_PROCESS	174	-0.7248	-2.74772	0
CELL_CYCLE_PHASE	156	-0.71301	-2.6616	0
MITOTIC_CELL_CYCLE	143	-0.71132	-2.62671	0
DNA_METABOLIC_PROCESS	223	-0.65015	-2.55767	0
M_PHASE	101	-0.71945	-2.52673	0
CHROMOSOME	113	-0.69598	-2.50958	0
CELL_CYCLE_GO_0007049	286	-0.63248	-2.47855	0
MITOSIS	75	-0.72658	-2.47655	0
CHROMOSOMAL_PART	88	-0.71137	-2.46899	0
M_PHASE_OF_MITOTIC_CELL_CYCLE	78	-0.72229	-2.45903	0

Fig. 43 BETs inhibition deregulates genes involved in cell cycle control

Gene Ontology analysis using expression genome wide data, obtained through microarray assay in RAJI treated with DMSO or JQ1 for 24h. The Gone Ontology C5 collection from MSigDB is used. In the upper panel representative enrichment plots are reported. In the lower panel, the top10 GO terms are reported. Normalized Enrichment Score (NES) and False Discovery Rate (FDR) values are reported.

In order to identify the key transcription factors associated to BETs inhibition response, we further characterized the JQ1-DEGs performing GSEA using as gene set of reference already published Myc ChIPseq in RAJI cells and the collections for Oncogenic Signature (C6) from MSigDB. As shown in Fig. 44-45, genes downregulated after JQ1 treatment were enriched for genes bound by Myc (Fig.44) and positively regulated by E2F1 (Fig.45).

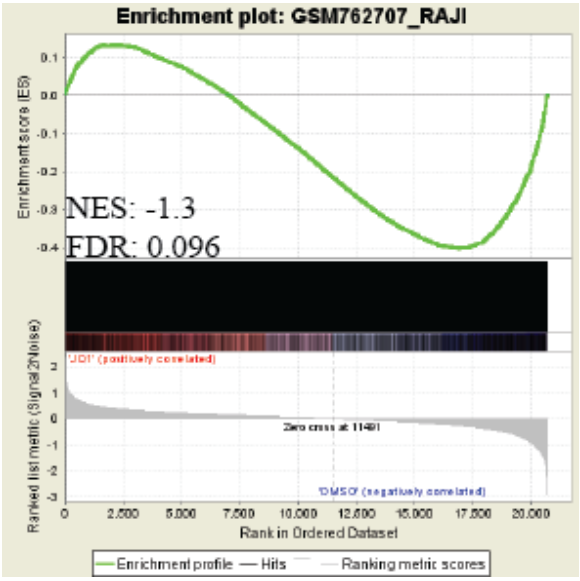

Fig. 44 JQ1 sensitive genes in RAJI were enriched for Myc targets
Gene Set Enrichment Analysis using expression genome wide data, obtained through microarray assay, in RAJI treated with DMSO or JQ1 for 24h using already published Myc ChIPseq on RAJI (Seitz et al., 2011).

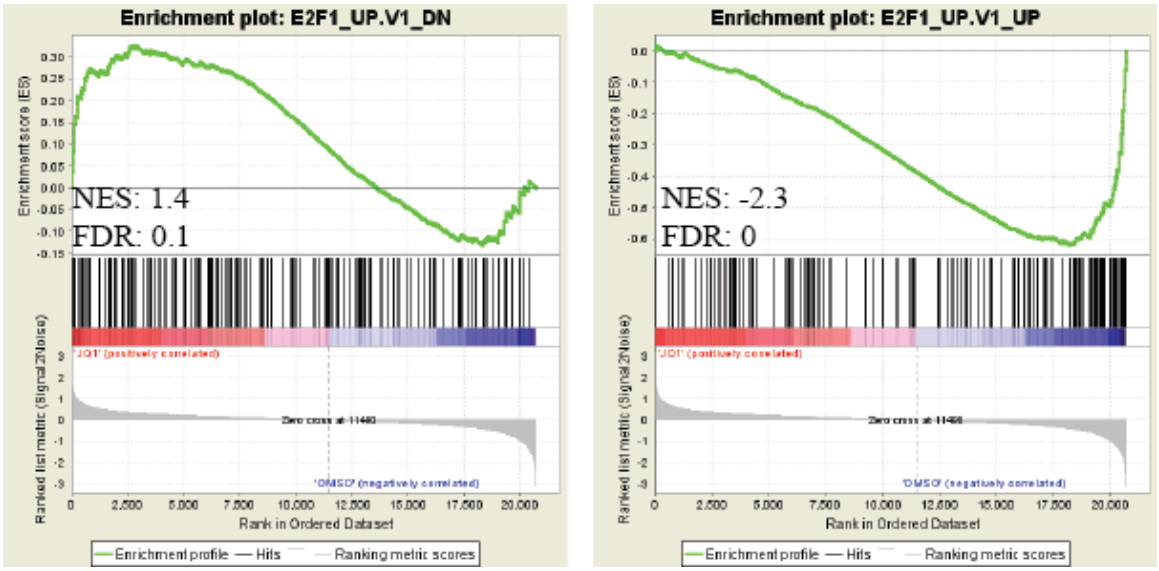

Fig. 45 JQ1 sensitive genes in RAJI were enriched for E2F1 regulated genes
Gene Set Enrichment Analysis using expression genome wide data, obtained through microarray assay, in RAJI treated with DMSO or JQ1 for 24h using Oncogenic Signature Collection (C6 collection) from MSigDB.

The enrichment in the downregulated genes for Myc targets or for genes that contain the recognition elements for Myc-Max binding was also confirmed in the Eμ-Myc system, performing GSEA with Transcription Factor motif or Oncogenic Signature collections (C3 and C6, respectively) (Fig.46).

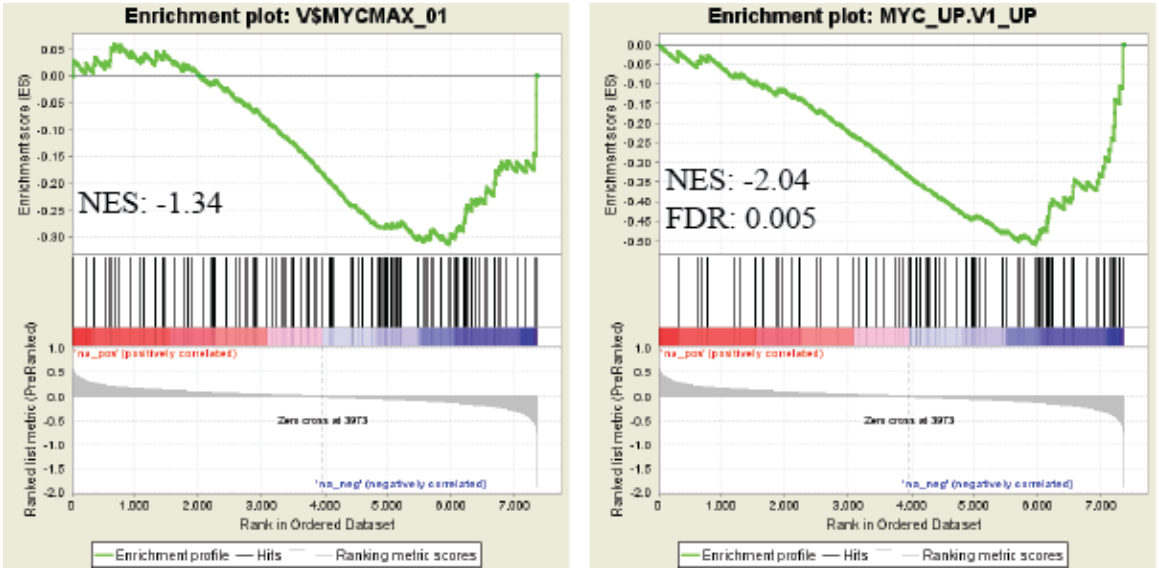

Fig. 46 JQ1 sensitive genes in Eμ-Myc lymphomas were enriched for Myc bound and regulated genes
Gene Set Enrichment Analysis using genome wide expression data, obtained through RNAseq, in Eμ-Myc lymphomas treated with DMSO or JQ1 for 24h. Transcription Factor motif and Oncogenic Signature (C3 and C6, respectively) collections from MSigDB are used as gene set of reference.

Altogether, the genome wide expression analysis on RAJI and Eμ-Myc lymphomas pointed out that genes involved in the cell cycle control and Myc and E2F1 targets were preferentially downregulated after treatment with BETs inhibitor. Since the downregulation of the same classes of genes was already reported in MM cells (Delmore et al., 2011), we tested if there was similarity between the altered transcriptional programs in different contexts. To verify this possibility, we performed GSEA using as gene set of reference the lists of deregulated genes obtained from Delmore et al., (2011). As shown in Fig.47, genes identified as downregulated in MM cells in Delmore et al., (2011) were enriched for genes downregulated in RAJI, while genes upregulated in MM were enriched for upregulated transcripts in RAJI, suggesting that BRD4 inhibition in different lines leads to the alteration of similar pathways.

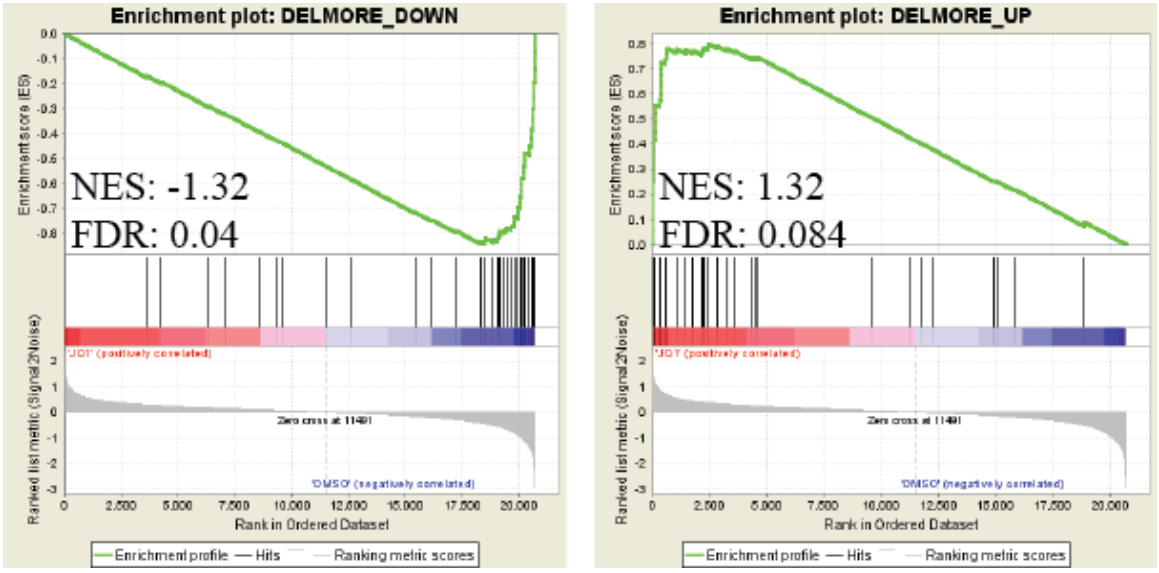

Fig. 47 BETs inhibition altered the similar transcriptional program in different contexts
Gene Set Enrichment Analysis using genome wide expression data on RAJI treated with DMSO or JQ1 for 24h using as gene set of reference the list of deregulated genes in MM.1S cells treated with JQ1already published (Delmore et al., 2011).

Thus, regardless the alteration of Myc levels, the final transcriptional outcome, in response to BRD4 inhibition, is comparable in different cellular contexts and it mainly affects Myc/E2F1 targets thereby accounting for the strong cytostatic effect exerted by JQ1 in these cell lines.

Myc and E2F1 genomic occupancy is not altered by BETs inhibition

Since Myc and E2F1 target genes were downregulated following JQ1 treatment, we asked whether the treatment with BETs inhibitors would affect Myc or E2F1 chromatin distribution.

As a first step in the analysis, we investigated the genomic distribution of the two transcription factors in RAJI cells and asked whether their localization would be altered after BET inhibition. As expected, in the control samples, Myc was equally distributed among either promoters, intergenic and intragenic regions (Fig.48), while E2F1 was preferentially localized in the proximity of promoters (Fig.48). Myc and E2F1 binding was not influenced by JQ1 treatment, since the total number of peaks and their localization were comparable among the two conditions, as displayed in the pie chart for genomic distribution and Venn diagram showing the overlap between peaks identified in the treated versus untreated sample (Fig.48-49).

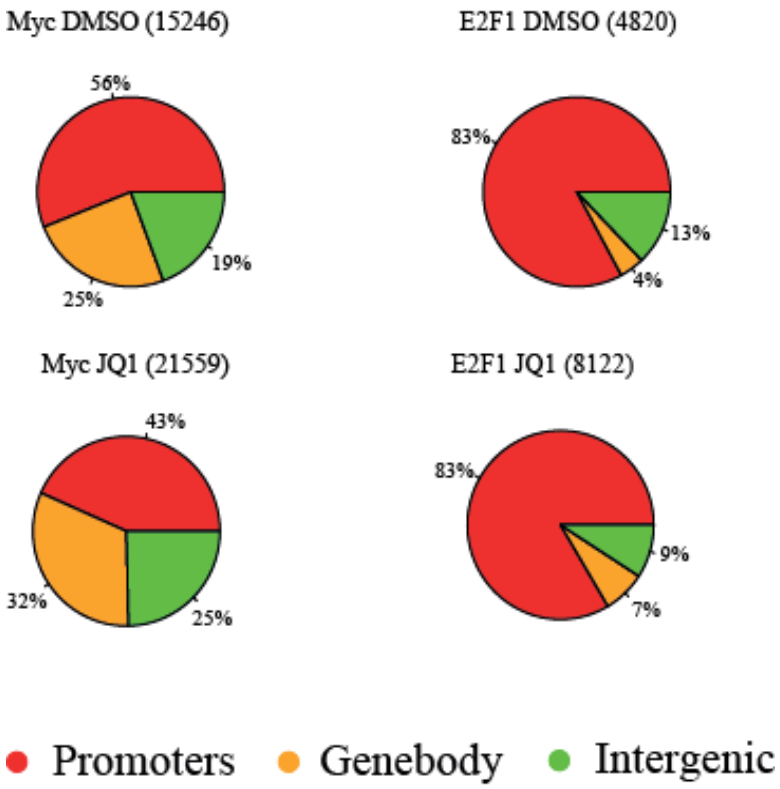

Fig. 48 BETs inhibition does not change genomic localization of Myc or E2F1 binding
Analysis of genomic distribution (promoter: red, genebody: orange, intergenic: green) of Myc (left) or E2F1 (right) ChIPseq peaks in RAJI treated with DMSO (upper panel) or JQ1 (lower panel) for 24h. Each ChIP sample was sequenced once.

Fig. 49 BETs inhibition does not reduce global Myc and E2F1 binding in RAJI
Analysis of BRD4 chromatin binding in RAJI or Eμ-Myc lymphoma after treatment for 24h with DMSO (gray) or JQ1 (red). In the Venn diagram the overlapping regions (gray+red) represent the common BRD4 peaks identified both in DMSO and in JQ1 samples. The gray only and the red only regions represent the number of BRD4 peaks identified uniquely in DMSO and JQ1 sample, respectively. Each ChIP sample was sequenced once.

In order to verify if BETs inhibition affects the intensity of Myc and E2F1 binding, we further analyzed the ChIPseq data, quantifying the reads localized in the proximity of the TSS of Myc or E2F1 targets. The intensity of Myc or E2F1 promoter peaks was not reduced by BETs inhibition,

on the contrary JQ1 treated samples showed a slight increase in the read density around the TSS (Fig.50).

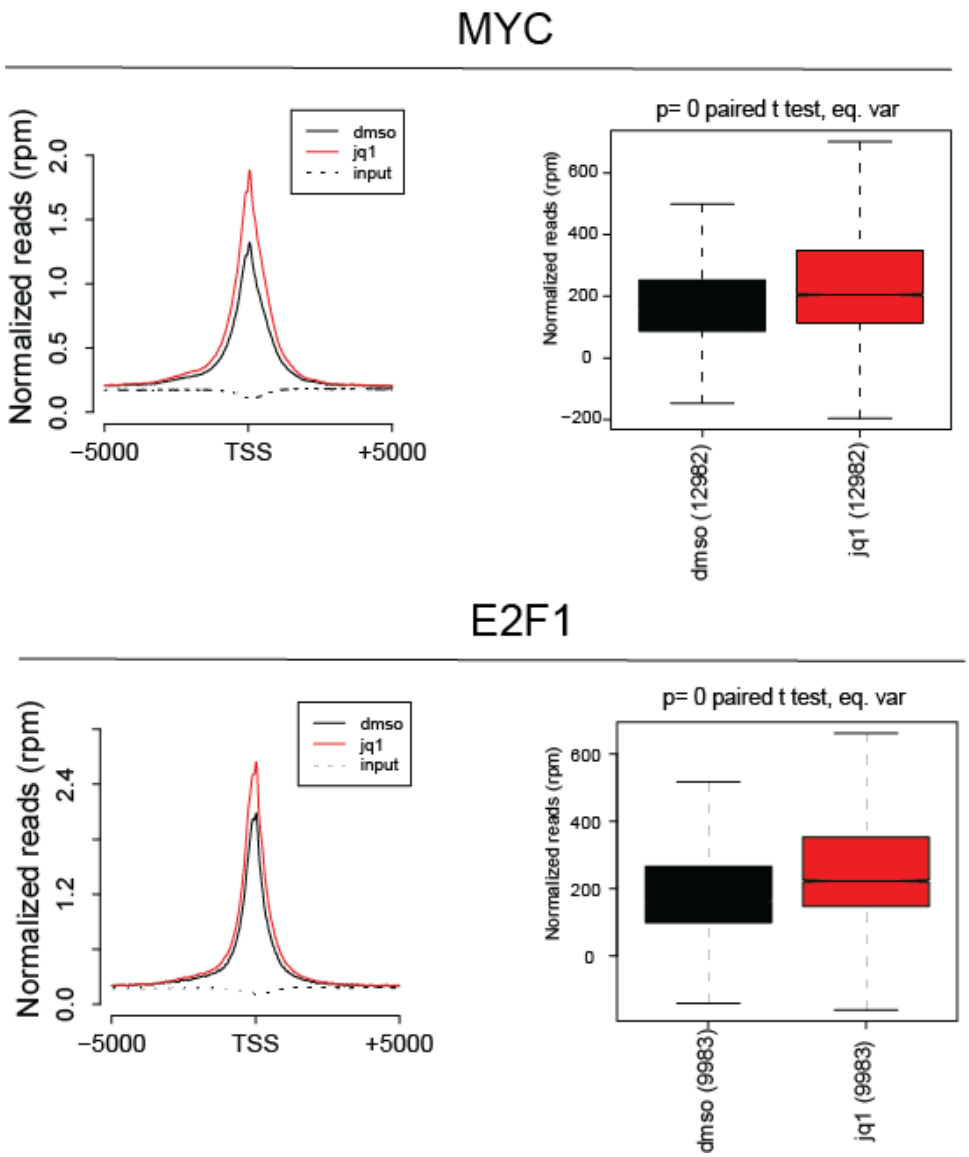

Fig. 50 BETs inhibition does not impair the TSS binding of Myc or E2F1 in RAJI
Reads distribution around the TSSs for Myc (upper panels) or E2F1 (lower panels) ChIPseq in RAJI after DMSO (black line) or JQ1 (red line) treatment for 24h. The input is used to set the background levels. The quantification of the reads distribution is reported in the boxplot on the right. Paired t-test is used to evaluate statistical significant differences. Each ChIP sample was sequenced once.

Therefore, the downregulation of Myc and E2F1 dependent genes observed after JQ1 treatment could not be explained by the displacement of the two TFs from the promoter of their target genes. To gain further confirmation of the lack of alteration of TF binding after BETs inhibition, we performed Myc ChIPseq in Eμ-Myc lymphomas treated with DMSO or JQ1 for 24h. As shown in figures 51-52, neither the total number of Myc peaks (Fig.51) nor its binding intensity on the TSS

(Fig.52) were reduced by JQ1 treatment, on the contrary we noticed a slight increase both in the number of peaks and in the intensity of Myc TSS binding after BETs inhibition.

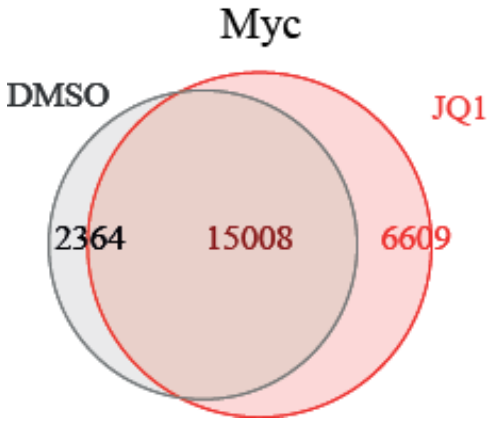

Fig. 51 BETs inhibition does not alter global Myc chromatin occupancy in Eμ-Myc lymphomas
Analysis of Myc chromatin binding in Eμ-Myc lymphomas treated with mock (DMSO: gray) or JQ1 (red). The overlap region (gray+red) in the Venn Diagram represents the number of common peaks between the two conditions. The only gray and only red parts represent the unique peaks in DMSO and JQ1 sample, respectively. Myc ChIPseq was performed in 3 independent Eμ-Myc lymphomas and the merge of the three sequencing was used for the analysis.

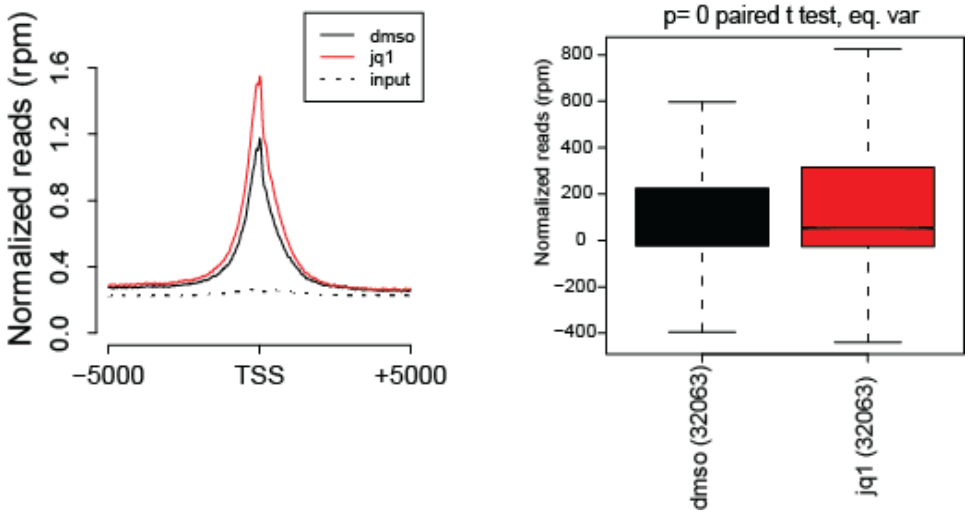

Fig. 52 BETs inhibition does not impair the TSS binding of Myc in Eμ-Myc lymphomas
Analysis of Myc binding on the TSS of its target through quantification of reads distribution around the TSSs for Myc ChIPseq in Eμ-Myc lymphomas after DMSO (black) or JQ1 (red) treatment for 24h. In the left panel, it is shown the TSS profile of Myc ChIPseq. The input is used to set the background level. In the right panel, the boxplot shows the quantification of reads distribution. Paired t-test is used to evaluate statistical significant differences. Myc ChIPseq was performed in 3 independent Eμ-Myc lymphomas and the merge of the three sequencing was used for the analysis.

In order to further verify if the response to BETs inhibitor was independent on the levels of TFs, we tested the JQ1 effects in cells where either Myc or E2F levels and activity could be raised by ectopic overexpression. To modulate the activation of Myc, we took advantage of the Myc-ER system, where Myc is fused to a modified form of the Estrogen Receptor (ER) which is responsive

to 4-Hydroxytamoxyfen (OHT). Once OHT is added to the cell culture, Myc-ER fusion protein is shuttled into the nucleus and free to transcribe its target genes. As a first step, we evaluated cell growth of two independent Myc-ER cell lines cultured in the presence of JQ1. As shown in Fig.53, both control and OHT treated cells were sensitive to BETs inhibition: not only OHT addition (i.e. ectopic Myc activation) did not rescue the cell growth arrest, but cells in which Myc-ER was activated seemed slightly more sensitive to BETs inhibition, in line with previous publication where based on a genome wide screen in Myc overexpressing cells, BRD4 was identified as a gene synthetic lethal with Myc (Toyoshima et al., 2012).

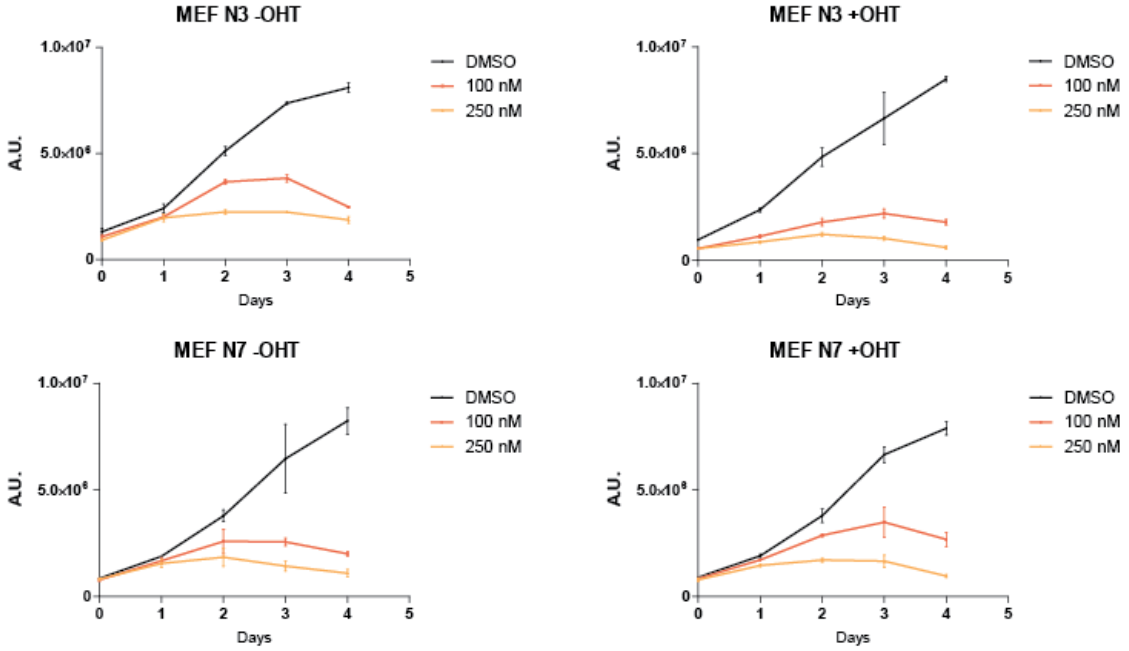

Fig. 53 Enhanced Myc activity is not sufficient to compensate growth arrest caused by BETs inhibition
Cell growth assay using CellTiterGlo on primary Murine Embrionic Fibroblast (MEF) infected with pBabePuro-MycER and treated with OHT (right panel), to induce Myc activation, or EtOH (left panel), as control, in combination with different concentration of JQ1 (black: DMSO, red: 100 nM, orange: 250 nM) for up to 4 days. Two independent MEFs preparations (N3 and N7) are used. The mean and the standard deviations of 3 technical replicates are reported.

As we already verified for cancer cell lines, also in this context BETs inhibition main effect was a block in the cell cycle progression with a consistent decrease in the percentage of cells in S phase, as demonstrated by BrdU incorporation and labeling after 48h of JQ1 treatment in combination with Myc activation (Fig.54).

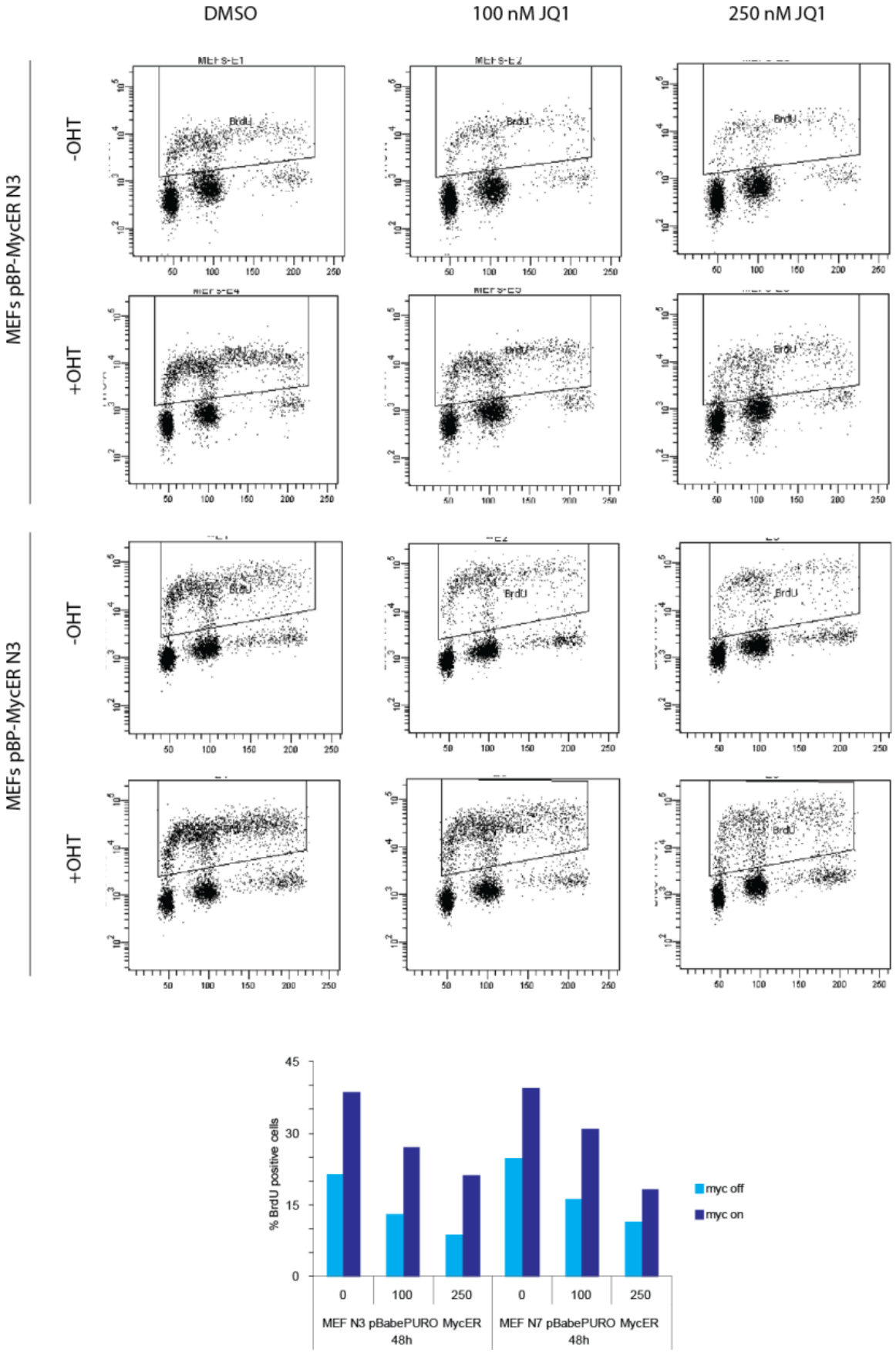

Fig. 54 Myc increased activity is not sufficient to prevent block in the cell cycle progression induced by BETs inhibition

Cell cycle analysis through BrdU incorporation (pulse 20') on primary MEFs infected with pBabePuro-MycER and treated with OHT, to induce Myc activation, or EtOH, as control, in combination with different concentration of JQ1 (0-100-250 nM) for 48h. In the lower panel a barplot depicting the % of BrdU positive cells is reported. Two independent MEFs preparations (N3 and N7) are used.

From this phenotypical analysis, we collected evidences that high Myc activity, rather than rescuing, is actually sensitizing cells to BET inhibition. In order to verify if ectopic activation of Myc could at least prevent the downregulation of Myc target genes after BETs inhibition, we performed RTqPCR on MEFs infected with pBabePuro-Myc-ER after JQ1 treatment and/or OHT administration (Fig.55). The analysis of the expression levels on selected Myc targets clearly demonstrated that BETs inhibition caused a reduction in their expression levels and that Myc enhanced activity was not sufficient to prevent this transcriptional response, suggesting that BRD4 affects transcription of these genes at a level that is downstream Myc binding to its targets.

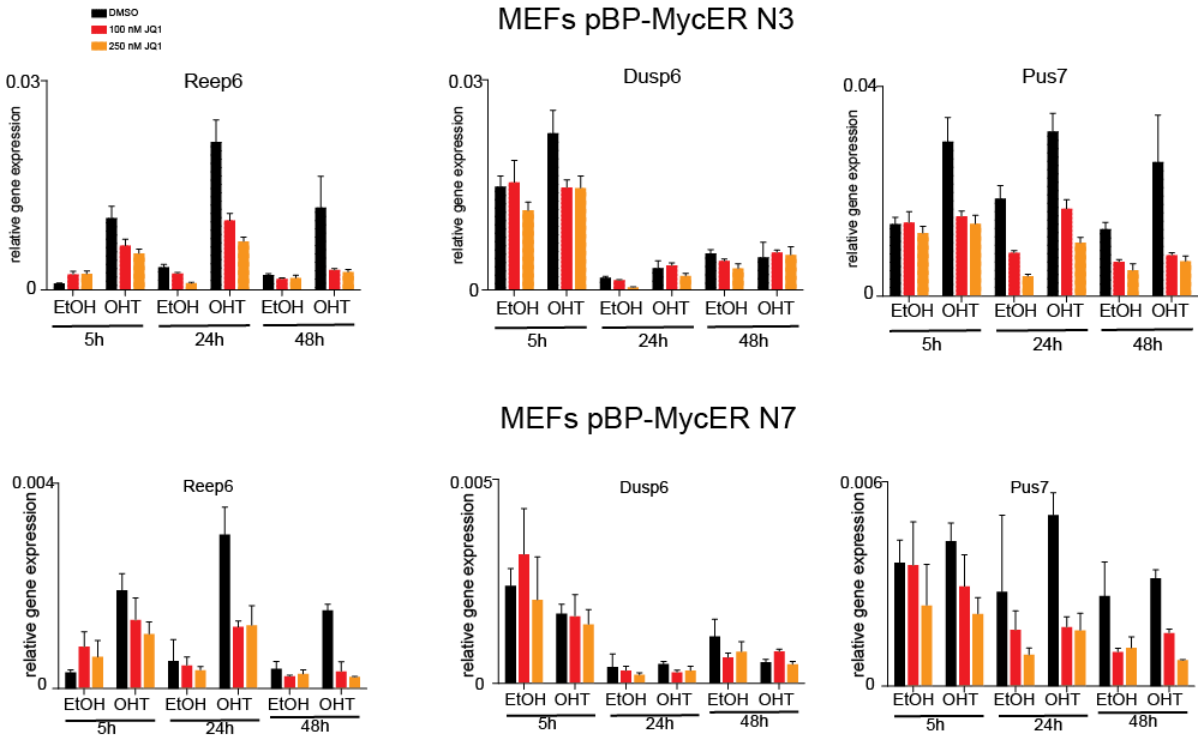

Fig. 55 Myc overexpression is not sufficient to prevent JQ1transcriptional effects on Myc targets
Expression analysis by RTqPCR on Myc target on primary Murine Embrionic Fibroblast (MEF) infected with pBabePuro-MycER and treated with different concentration of JQ1 (black: DMSO, red: 100 nM, orange: 250 nM) in combination with EtOH (mock) or OHT treatment to induce Myc activation. Two independent MEFs preparations (N3 and N7) are used. The expression values are normalized on RPP0 expression. The mean and the standard deviations of 3 technical replicates are reported.

The previously described GSEA on RAJI highlighted the alteration of both Myc and E2F transcriptional program (Fig.44-45). Therefore we decided to test if E2F1 overexpression could be sufficient to bypass BET inhibition. To verify this hypothesis, we infected RAJI cells with a constitutive vector overexpressing E2F1 and we analyzed the effect of JQ1 treatment in terms of

transcriptional response of some E2F1 target genes. As shown in Fig.56, the downregulation of E2F1 targets caused by BET inhibition was not bypassed by the ectopic expression of the transgene.

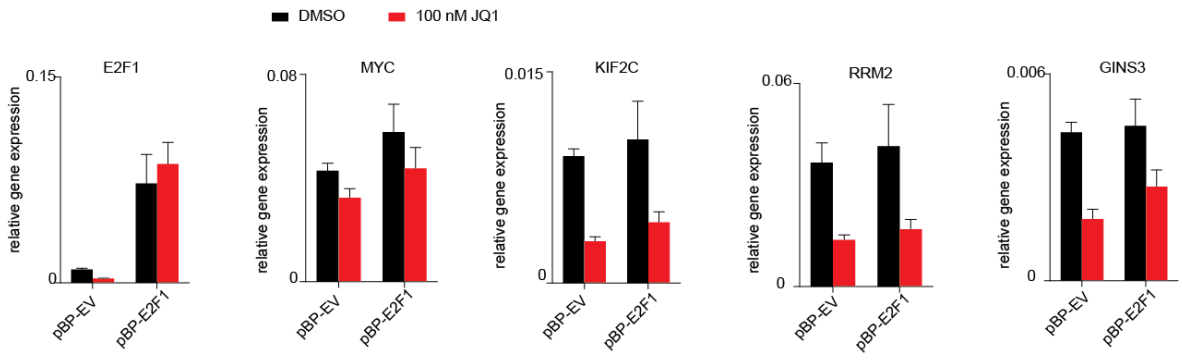

Fig. 56 E2F1 overexpression is not sufficient to prevent JQ1 transcriptional effects on E2F1 targets
Expression analysis by RTqPCR on E2F1 targets on RAJI infected with pBabePuro-EV or pBabePuro-E2F1-HA and treated for 24h with DMSO (black) or 100 nM JQ1 (red). The expression values are normalized to RPP0 expression. The mean and the standard deviations of 3 technical replicates are reported.

In order to rule out the possibility of a cooperation between Myc and E2F1 and the need of the double overexpression to overcome BET inhibition, we performed E2F1 overexpression experiments in MEFs where Myc-ER transgene was knocked in (KI) under the control of the Rosa26 promoter. As it is shown in Fig.57-58, even though we were able to properly overexpressed E2F1, the cell growth response to JQ1 treatment was not rescued by the combination of Myc activation and E2F1 overexpression.

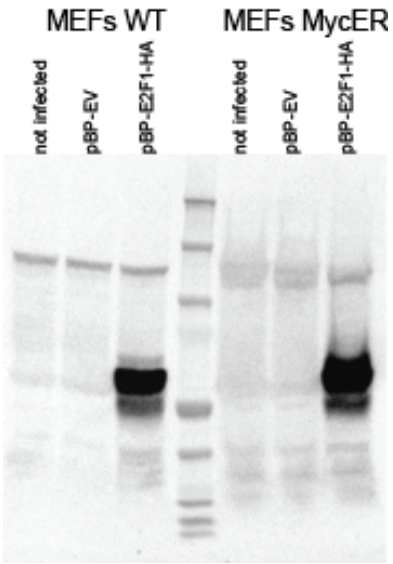

Fig. 57 E2F1 is efficiently overexpressed in MEFs
Analysis of E2F1 protein level by Western Blot on primary MEFs Wilde Type (WT) or MycER Knock-in (KI) not infected or infected with pBabePuro-EV or pBabePuro-E2F1-HA. A single replicate was performed.

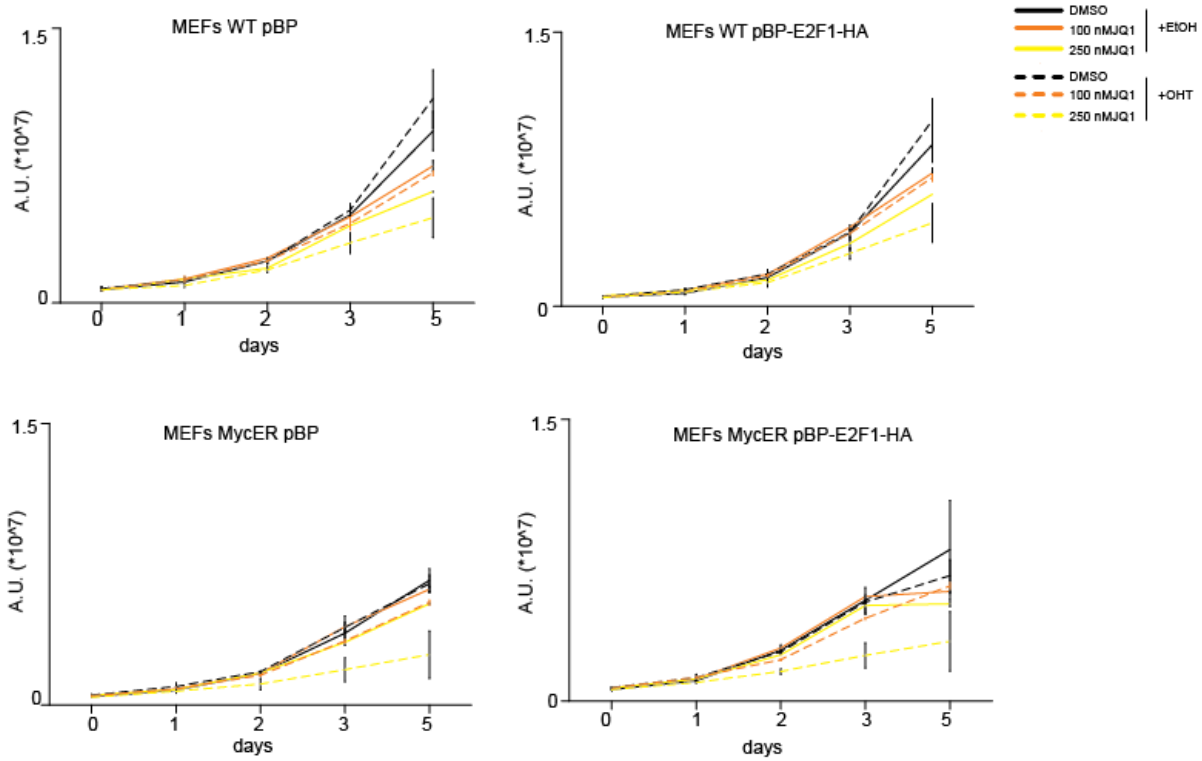

Fig. 58 E2F1 overexpression and Myc activation are not sufficient to overcome BETs inhibition impairment of cell growth

Cell viability assay on primary MEFs Wilde Type (WT) or MycER knock in (KI) infected with pBabePuro-EV (upper panel) or pBabePuro-E2F1-HA (lower panel) and treated for up to 4 days with different concentration of JQ1 (black: DMSO, orange: 100 nM, yellow: 250 nM) and with EtOH (solid lines) or OHT (dashed lines), to induce Myc activation. The mean and the standard deviations of 3 technical replicates are reported.

Characteristics of JQ1 responsive genes

Since BETs inhibition alters the expression of a defined set of genes, shared by different cell lines, we wondered whether we could identify features that specifically characterized these JQ1 responsive genes. With this idea in mind, we performed an integrated analysis of the transcriptome and the chromatin profiles obtained by the ChIPseq. As a first level of investigation, we analyzed if JQ1 responsive genes show differences in their expression levels in comparison to the not deregulated ones. Indeed, quantifying the expression in the DMSO treated samples, we observed that in RAJI cells the class of downregulated genes was characterized by a significant higher level of expression respect to not-deregulated genes (Fig.59).

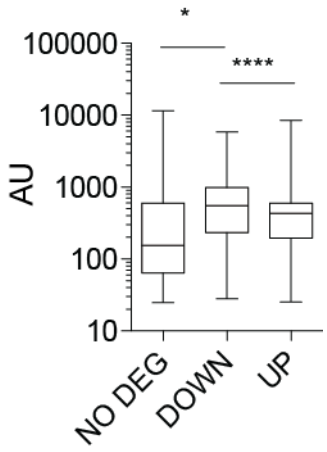

Fig. 59 JQ1 sensitive genes are expressed at high levels
Expression quantification through Microarray assay in RAJI for NO-DEG, DOWN or UP regulated genes identified through Microarray analysis in RAJI after treatment with JQ1. Unpaired t test (two tails) is used. * pvalue=0.0259; **** pvalue<0.0001.

In order to verify if this higher expression level in the downregulated genes could be associated to the presence of specific chromatin features, we investigated the chromatin occupancy of different transcription factors or histone marks (Fig.60) in RAJI. Focusing our attention on downregulated genes, we noticed that the vast majority of the TSS in the DMSO sample was simultaneously bound by BRD4 and by Myc and E2F1, as predicted by the GSEA analysis. On the contrary, only a small fraction of not deregulated genes showed the presence of BRD4 and the transcription factors Myc and E2F1 (Fig.60) on their TSS. Furthermore, it is worth to notice that, regardless of the group identity (downregulated or not-deregulated), the genes characterized by the presence of RNA PolII and by the histone marks for active chromatin (H3K27Ac, H3K4me1, H3K4me3) were also bound by BRD4, that, as expected, is strongly depleted after BETs inhibition. This evidence suggested that, even though BETs inhibition ultimately affects the expression of a limited number of genes, BRD4 is bound to all the promoters of genes actively transcribed (Fig.60).

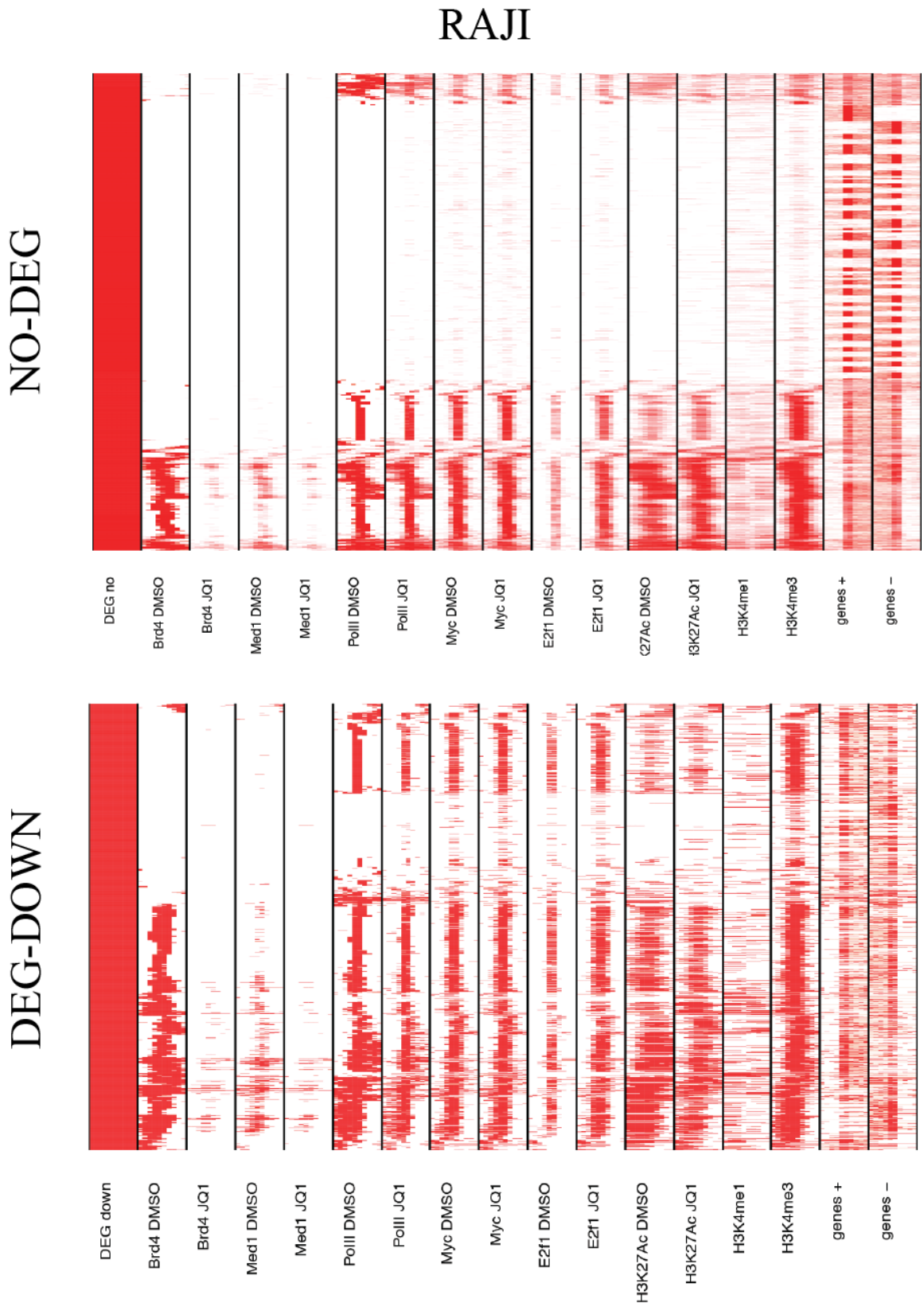

Fig. 60 JQ1 sensitive genes are preferentially bound by BRD4, TFs (Myc and E2F1) and RNA PolII in RAJI

Digital heatmap showing the distribution of BRD4, Med1, TFs (Myc and/or E2F1), RNA PolII and histone marks (H3K27AC, H3K4me1 and H3K4me3) in no-deregulated or downregulated genes in RAJI after the treatment for 24h with DMSO or JQ1. Each ChIP sample was sequenced once.

These results were also confirmed using available ChIPseq data for MM.1S (Delmore et al., 2011) and for a Diffuse Large B Cell Lymphoma cell line (OC-LY1) (Chapuy et al., 2013) after BETs inhibition. In both cell lines, regions marked with histone modifications for open and active chromatin were also bound by BRD4, furthermore there was a strong association between BRD4 binding and RNA PolII/Myc. Moreover, also in these cellular models, downregulated genes were highly enriched for targets of Myc, in contrast to not-deregulated genes (Fig.61-62).

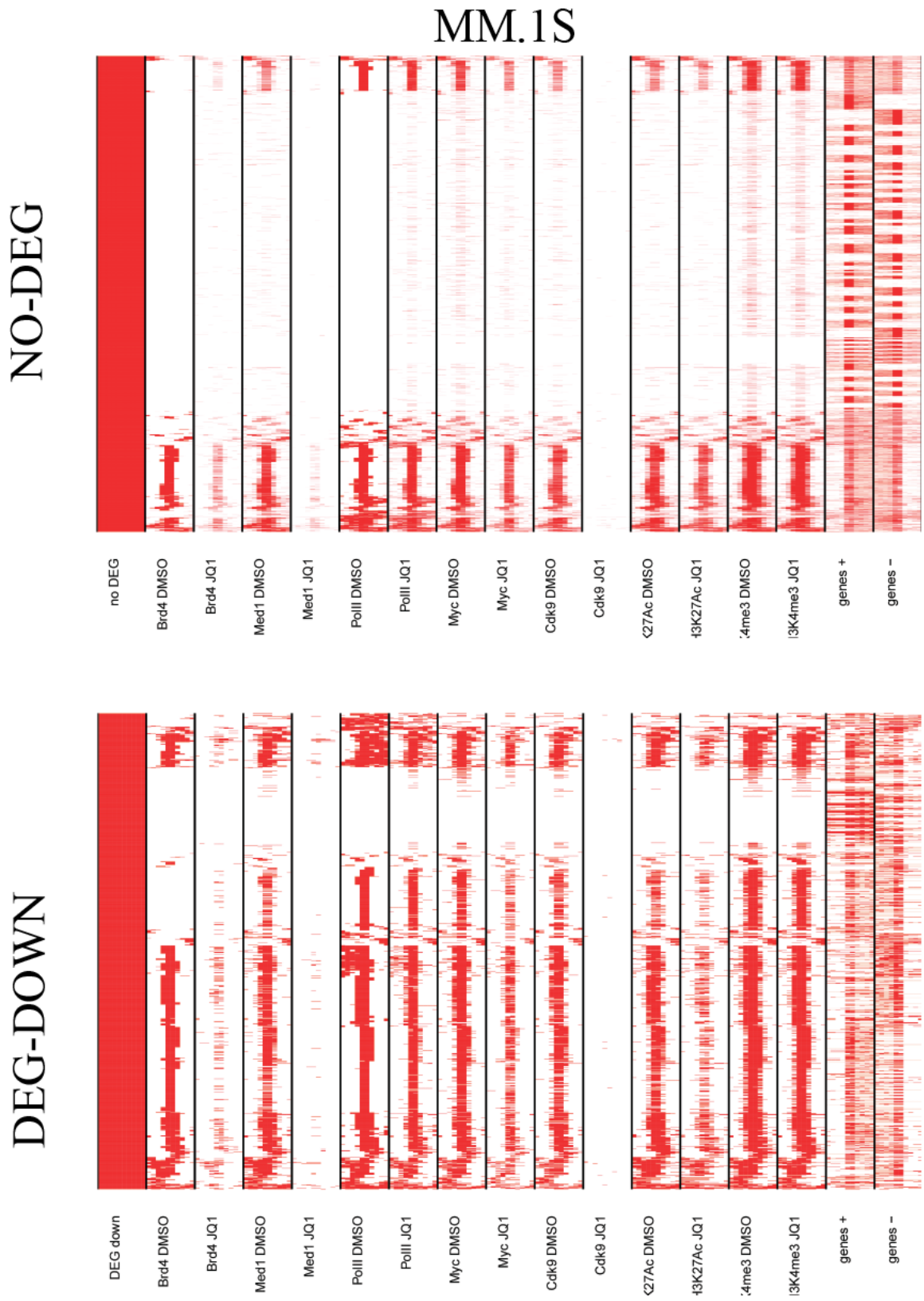

Fig. 61 JQ1 sensitive genes are preferentially bound by BRD4, E2F1 and RNA PolII in MM.1S
Digital Heatmap showing the distribution of BRD4, Med1, RNA PolII, Myc, CDK9 and histone marks (H3K27Ac and H3K4me3) in no-deregulated or downregulated genes after JQ1 treatment in MM.1S. Expression data and ChIPseq data used to perform this analysis were public available (Delmore et al., 2011; Lovén et al., 2013) .

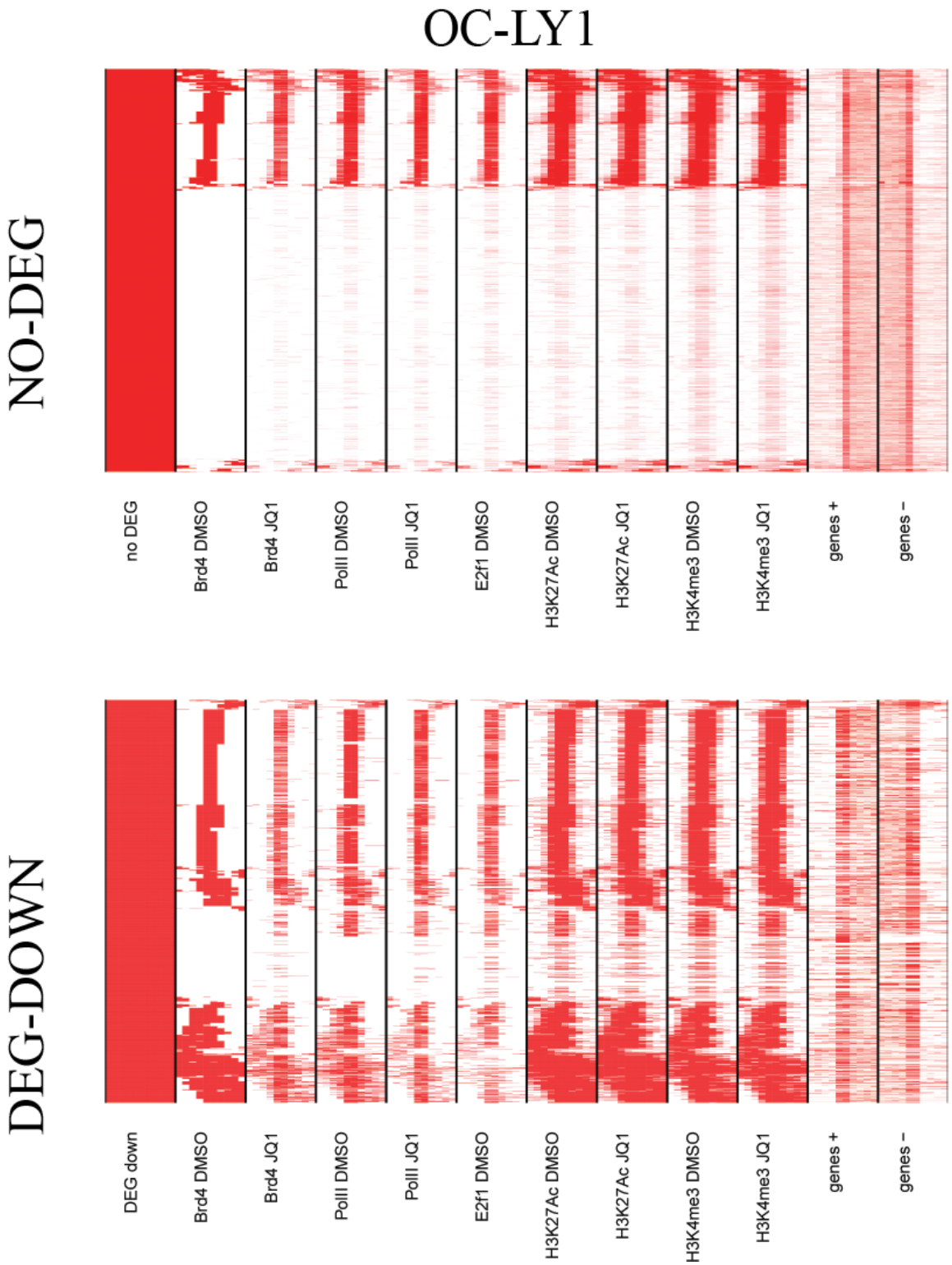

Fig. 62 JQ1 sensitive genes are preferentially bound by BRD4, E2F1 and RNA PolII in OC-LY1
Digital Heatmap showing the distribution of BRD4, RNA PolII, E2F1 and histone marks (H3K27AC, and H3K4me3) in no-deregulated or downregulated genes in OC-LY1 after the treatment for 24h with DMSO or JQ1. Expression data and ChIPseq data used for this analysis were obtained from (Chapuy et al., 2013).

In order to extend these observations, we verified also in the Eμ-Myc lymphomas the chromatin landscape for downregulated or not-regulated genes after BETs inhibition. Also in Eμ-Myc lymphomas, we still observed the strong correlation between TSS marked with transcription

factors/RNA PolII/active histone marks and BRD4, but we were not able to discriminate between responding versus not responding genes based on the binding pattern, since also the latter class of genes was strongly enriched for Myc/RNA PolII bound genes (Fig.63). This difference could be due to the biology of Eμ-Myc lymphomas: in this cellular system, Myc is expressed at very high levels and a phenomenon called "invasion" occurs (Lin et al., 2012; Sabò et al., 2014). Briefly, when Myc is expressed at physiological and low levels, it binds only few targets with the canonical E-box sequences in their promoter; once Myc is overexpressed it will bind also not canonical E-boxes, both at the promoter and at the enhancer regions, invading all the regulatory regions. This phenomenon will explain why we were not able to discriminate among JQ1 sensitive and insensitive genes based on Myc binding.

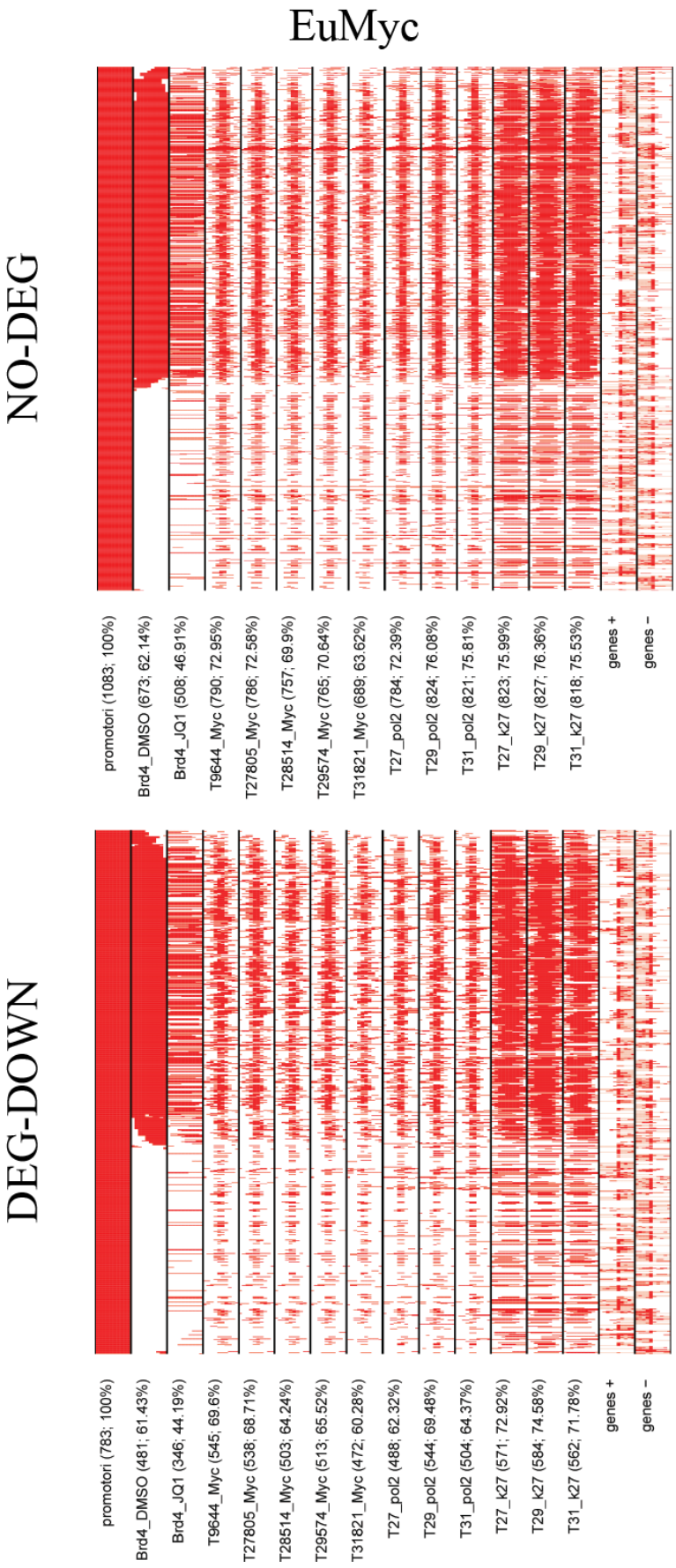

Fig. 63 JQ1 responsive genes are not distinguishable from not deregulated ones based on chromatin occupancy in Eμ-Myc lymphomas

Digital Heatmap showing the distribution of BRD4 (DMSO or JQ1 sample) and Myc, RNA PolII and H3K27Ac in 3 different Eμ-Myc lymphomas.

Since these heatmaps are digital representations of the occupancy of a particular region, we decided to analyze also the binding intensity of each factor on the TSS of the genes belonging to the different classes (Fig.64). From the analysis in RAJI of the reads distribution around the TSS, we noticed a much higher intensity binding of BRD4, Myc & E2F1 and RNA PolII in downregulated genes respect to not-deregulated ones (Fig.64). These data are in line with the results obtained in MM.1S cell line: in fact, also in this cellular system the downregulated genes were characterized by a very high binding of BRD4, Myc and RNA PolII (Fig.64).

This analysis suggested that the promoters of downregulated genes are (over)loaded with BRD4 and other TFs that, attracting more RNA PolII, may ensure a higher expression level in basal conditions.

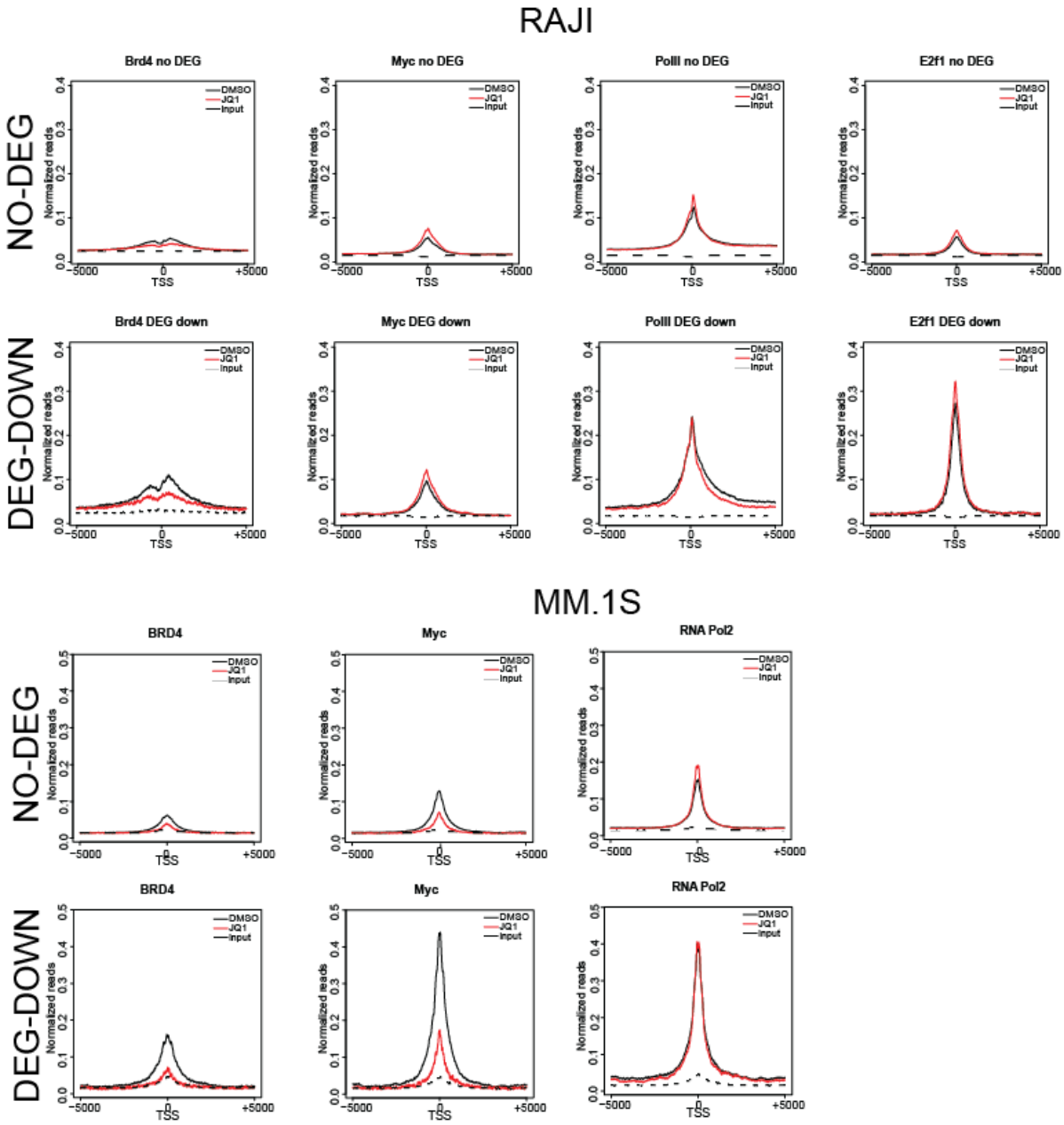

Fig. 64 JQ1 sensitive genes are characterized by high intensity binding of BRD4, TFs and RNA PolII on the TSSs

Reads distribution around the TSSs in no-deregulated or downregulated genes in RAJI (upper panels) or MM.1S (lower panels) after DMSO (black line) or JQ1 (red line) treatment. For RAJI BRD4, Myc, E2F1 and RNA PolII ChIPseq are analyzed. Each ChIP sample was sequenced once. For MM.1S BRD4, Myc and RNA PolII ChIPseq already published are used (Delmore et al., 2011; Lovén et al., 2013).

BRD4 inhibition causes alteration of RNA PolII dynamics

Since the ChIPseq data clearly showed that the deregulation of Myc and E2F1 targets did not correspond to a reduced binding of these TFs on the promoter of their targets, and the overexpression experiments suggested that the BETs inhibitors act downstream the binding of a TF on the promoter of its targets, we wondered whether gene downregulation caused by BETs

inhibition was actually linked to alterations of RNA PolII activity. To address this question, we performed ChIPseq on RNA PolII in RAJI treated with JQ1. Analysis of the RNA PolII peaks distribution (Fig.65) showed that the binding sites were mainly localized in the genebody (around 50%) and on the promoter (30%), while a minority of peaks were localized in the intergenic regions, as expected. Moreover, BETs inhibition did not change the global binding of RNA PolII to the chromatin (Fig.65-66), suggesting no massive alteration of RNA PolII occupancy after BRD4 inhibition.

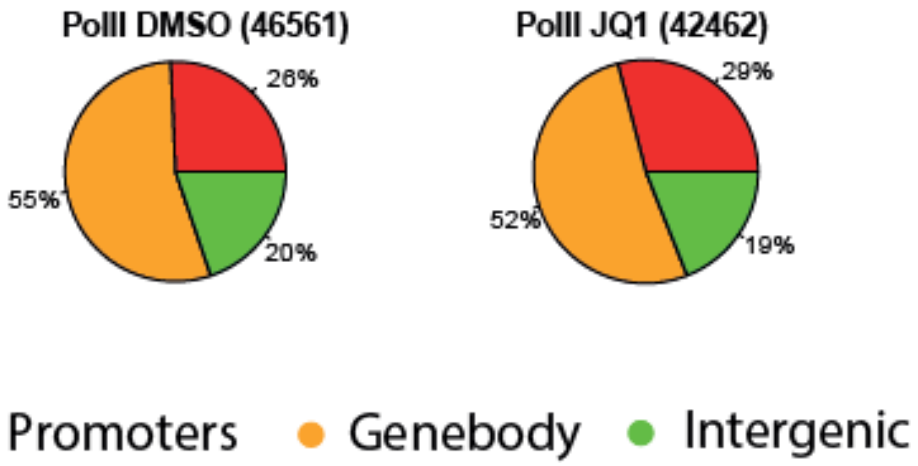

Fig. 65 BETs inhibition does not alter the global genomic distribution of RNA PolII in RAJI
Analysis of genomic distribution in Promoters (red), Genebody (orange) and Intergenic (green) regions of RNA PolII peaks in RAJI treated with DMSO (left) or 100 nM of JQ1 (right) for 24h. Each ChIP sample was sequenced once.

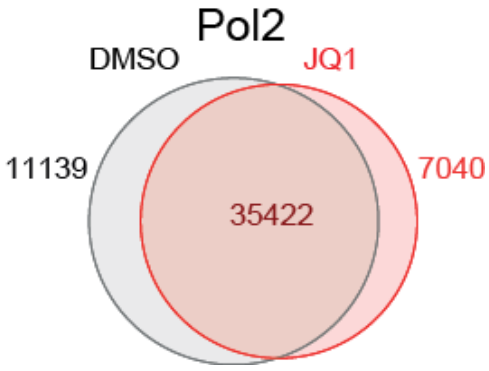

Fig. 66 BETs inhibition does not reduce the number of RNA PolII binding sites in RAJI
Analysis of RNA PolII chromatin binding in RAJI treated with mock (DMSO: gray) or JQ1 (red) for 24h. The overlap region (gray+red) in the Venn Diagram represents the number of common peaks between the two conditions. The only gray and only red parts represent the unique peaks in DMSO and JQ1 samples, respectively. Each ChIP sample was sequenced once.

Nonetheless, the inhibition of BRD4 might affect RNA PolII processivity. To test this hypothesis, we evaluated the Stalling Index (SI). This value takes into account the signal of RNA PolII on the promoter and on the genebody of transcribed genes (Fig.67): usually, an high SI value is

associated to high levels of RNA PolII on promoter (stalled PolII) and/or low level of traveling RNA PolII on the genebody (related to the block in the elongation step). From this analysis, we noticed that the SI associated to RAJI treated with JQ1 was higher than the control (DMSO) sample, regardless of the class of genes analyzed (Fig.67). In particular, the compromised elongation step was evident in JQ1 downregulated genes, in which the RNA PolII signal in the genebody was strongly reduced while the occupancy on the promoter was not affected, as shown by the SI plot and by the RNA PolII profile and reads quantification in Fig.67. On the contrary, the not-deregulated (Fig.67) and upregulated (Fig.67) genes were characterized by a higher RNA PolII signal on the promoter without massive changes on the genebody.

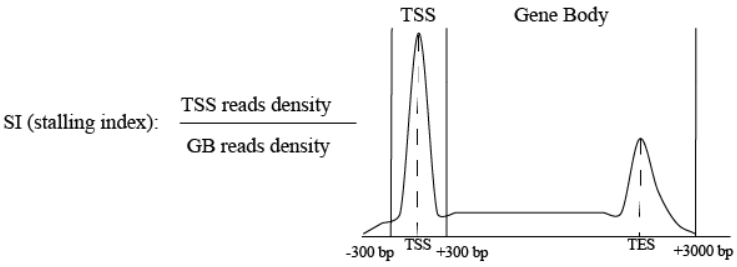

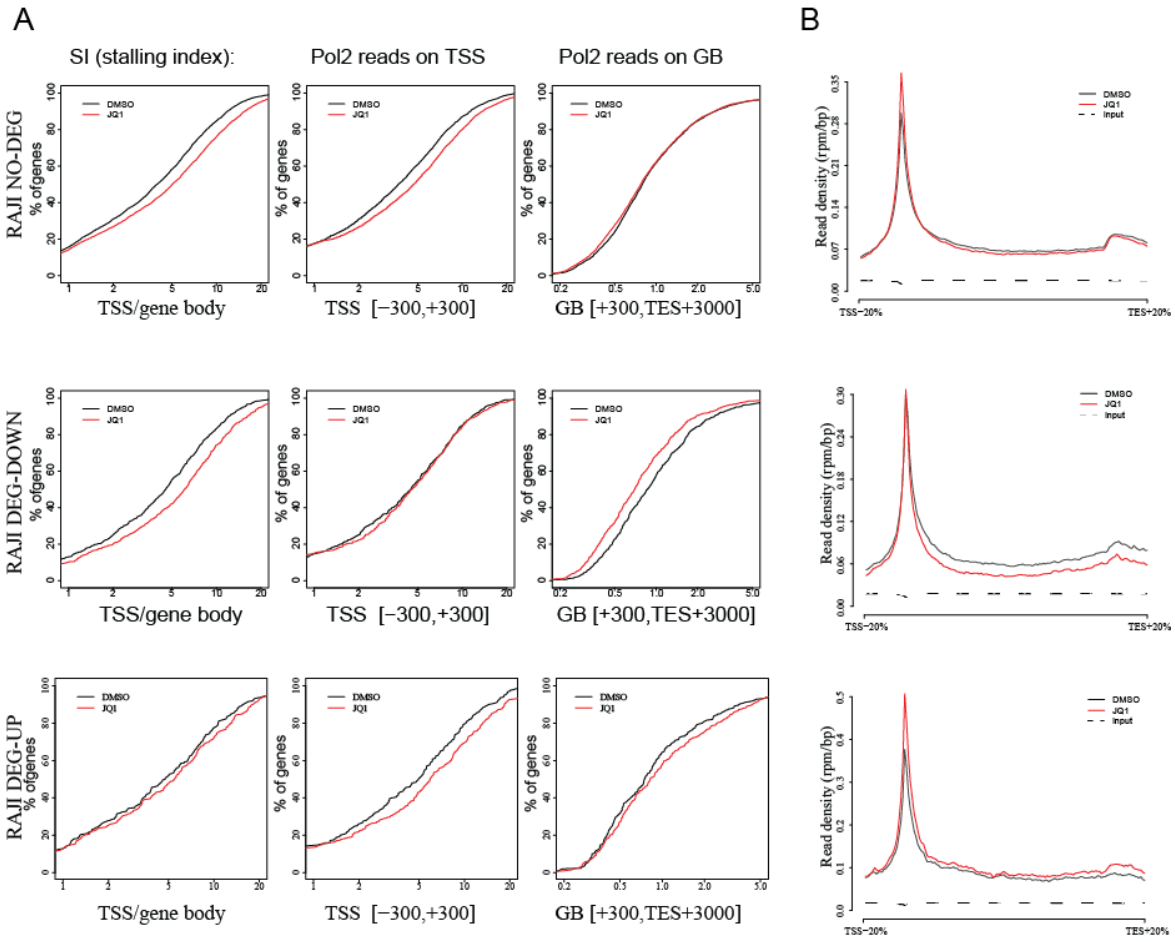

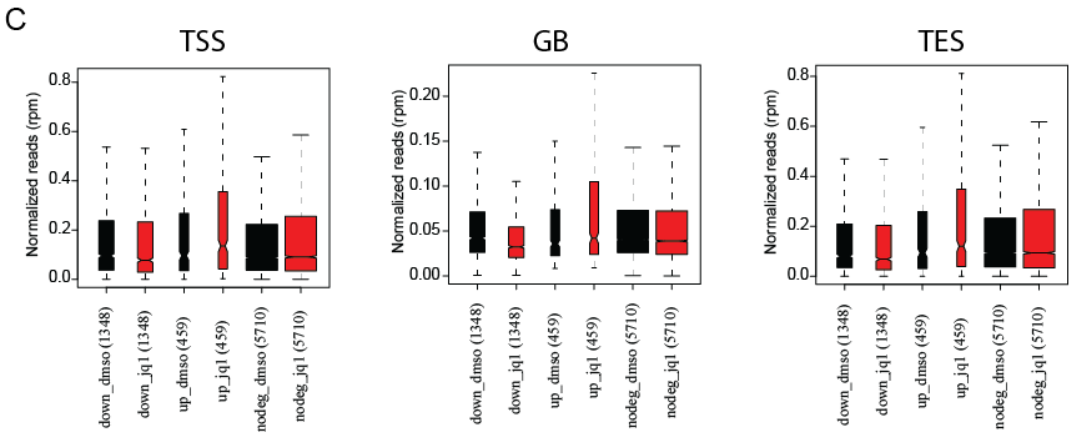

p-value DMSOvs JQ1:
DOWN= 3.17e-05
UP=1.64e-22
NO_DEG=2.07e-103

p-value DMSOvsJQ1:
DOWN=2.08e-69
UP=0.00049
NO_DEG=7.49e-19

p-value DMSOvsJQ1:
DOWN=0.0006
UP=1.06e-22
NO_DEG=2.2e-115

Fig. 67 BETs inhibition strongly affects RNA PolII dynamics in RAJI
Evaluation of the RNA PolII dynamics in RAJI after treatment with DMSO (black) or JQ1 (red) for 24h. In the upper panel a schematic representation of Stalling Index evaluation was reported. (A) Stalling Index is calculated for not-deregulated, downregulated and upregulated genes. The left panel summarizes the global SI, the middle panel shows the quantification of RNA PolII on the TSS, while the right panel shows the quantification of RNA PolII reads on the GeneBody (GB). (B) RNA PolII profiles along the gene. The dashed line represents the background (input) signal. (C) Boxplot to quantify RNA PolII reads on the TSS, on the GB and on the TES. Pair t-test is calculated for each DMSO-JQ1 pair. Each ChIP sample was sequenced once.

In order to verify if the stalling of the RNA PolII on downregulated genes would lead to a reduction in the transcription rate, we performed 4-thioUridine (4-sU) labeling, followed by RTqPCR. This technique, indeed, allows the specific labeling of the newly synthesized mRNA. As shown in Fig.68, downregulated genes showed a 60% reduction in the production of new transcripts after the treatment with JQ1, while no differences were evident in the not-deregulated genes.

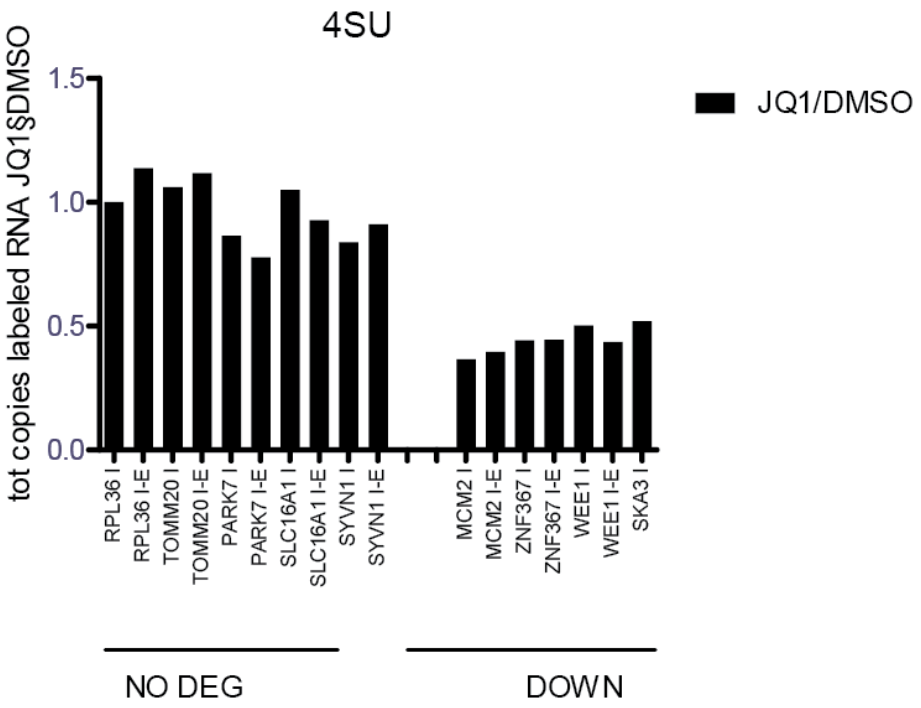

Fig. 68 JQ1 treatment affects the mRNA production of downregulated genes
Quantification by RTqPCR of ongoing transcription in genes not deregulated or downregulated by 24h JQ1 treatment in RAJI. The newly synthesized RNA is labeled with a 30' pulse of 4-sU. The total number of copies of labeled RNA in the JQ1 sample over the DMSO is reported. In order to discriminate the immature from the spliced mRNA, primers are designed at the intro-exon boundary. One technical replicate per two biological replicates were performed and a representative plot is shown.

The analysis on RNA PolII dynamics and the 4-sU labeling results suggested that BRD4 inhibition affected the synthesis of downregulated genes by selectively compromising their transcriptional

elongation. On the contrary, the transcription of not-deregulated genes was not altered, probably because the initial reduction on the elongating RNA PolII was immediately compensated by a higher recruitment of RNA PolII on the promoter, as it is suggested by the higher ChIPseq signal of promoter associated polymerase.

In order to verify if the stalling of the RNA PolII is an effect shared also by other cell lines, we performed the SI evaluation on RNA PolII ChIPseq in MM.1S (Fig.69) or OC-LY1 (Fig.70) cells using published datasets (Chapuy et al., 2013; Lovén et al., 2013). Also in these cell lines, JQ1 treatment strongly affected the RNA PolII rate. In particular, downregulated genes were characterized by a reduction of RNA PolII signal on the genebody, without any change at the promoter level (Fig.69-70); while not-deregulated (Fig.69-70) and upregulated genes (Fig.69-70) were marked with a higher RNA PolII density on their promoter.

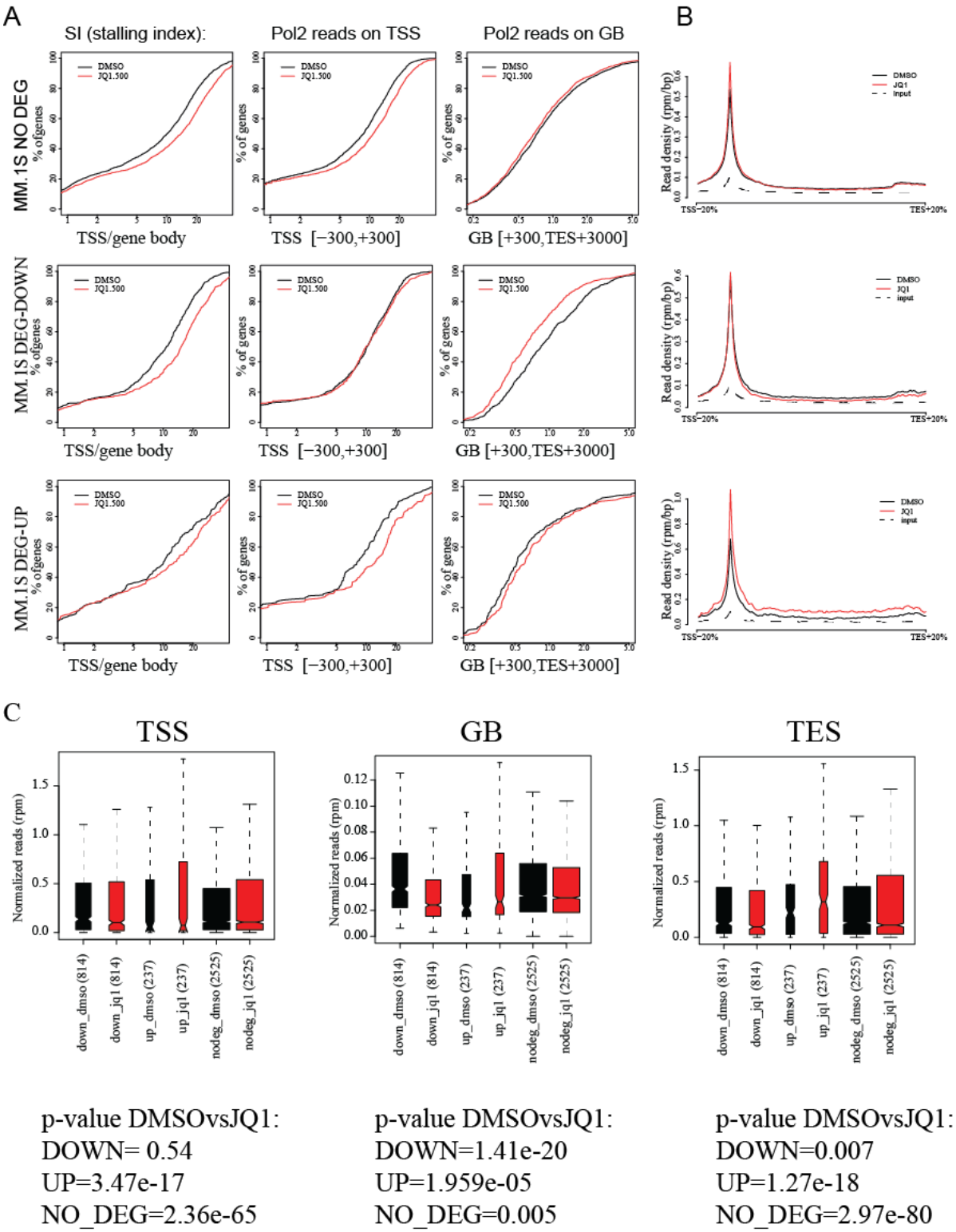

Fig. 69 BETs inhibition strongly affects RNA PolII dynamics in MM.1S

Evaluation of the RNA PolII dynamics in MM.1S after treatment with DMSO (black) or JQ1 (red). (A) Stalling Index is calculated for not-deregulated, downregulated and upregulated genes. The left panel summarizes the global SI, the middle panel shows the quantification of RNA PolII on the TSS, while the right panel shows the quantification of RNA PolII reads on the GeneBody (GB). (B) RNA PolII profiles along the gene for not-deregulated, downregulated and upregulated genes. The dashed line represents the background (input) signal. (C) Boxplot to quantify RNA PolII reads on the TSS, on the GB and on the TES. Pair t-test is calculated for each DMSO-JQ1 pair. For this analysis already published data are used (Delmore et al., 2011; Lovén et al., 2013)

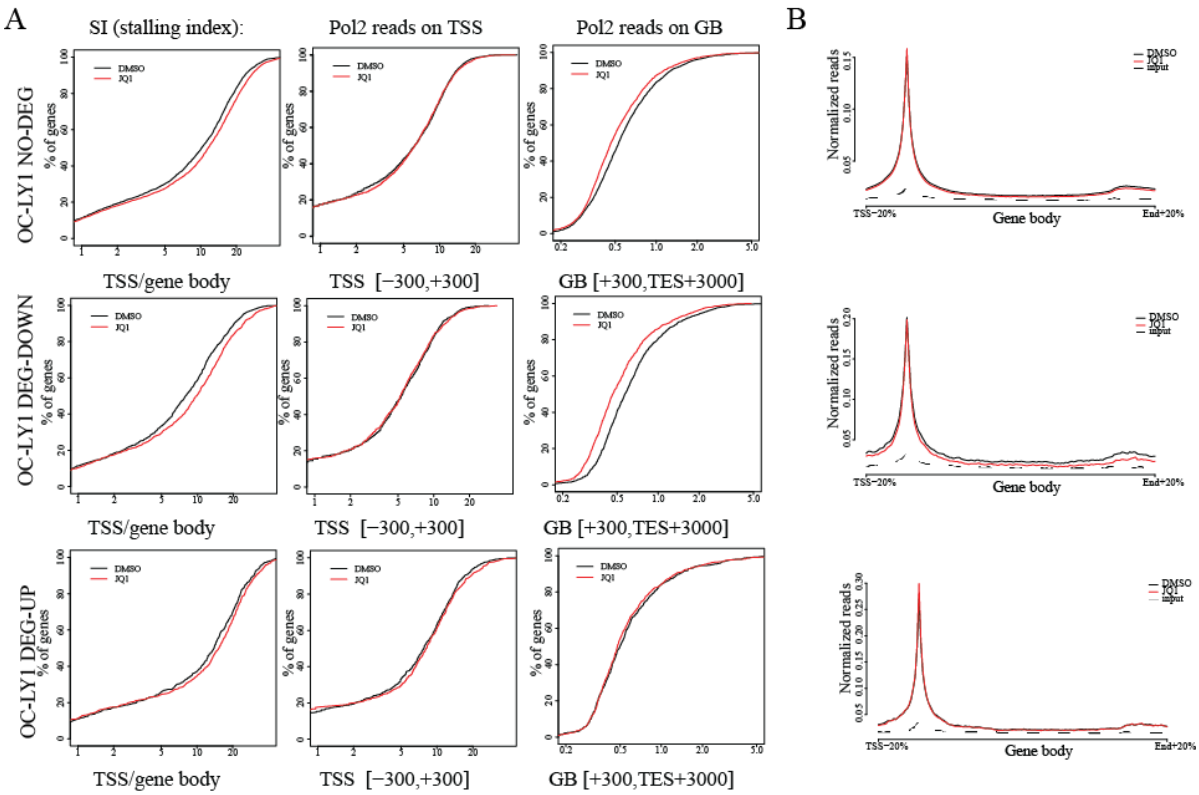

Fig. 70 BETs inhibition strongly affects RNA PolII dynamics in OC-LY1
Evaluation of the RNA PolII dynamics in OC-LY1 after treatment with DMSO (black) or JQ1 (red). (A) Stalling Index is calculated for not-deregulated, downregulated and upregulated genes. The left panel summarized the global SI, the middle panel shows the quantification of RNA PolII on the TSS, while the right panel shows the quantification of RNA PolII reads on the GeneBody (GB). (B) RNA PolII profiles along the gene for not-deregulated, downregulated and upregulated genes. The dashed line represents the background (input) signal. For this analysis already published data are used (Chapuy et al., 2013)

Further indications of alteration of RNA PolII dynamics and processivity derived from analysis of its phosphorylation status. After the recruitment on the promoter, RNA PolII needs to be phosphorylated on Serine5 (Ser5) and Serine 2 (Ser2) of its CTD in order to be active and to start gene transcription (Kwak and Lis, 2013). In particular, the phosphorylation on Ser5 of RNA PolII CTD is mediated by CDK7 during the initiation step of the transcription process and it is characteristic of primed and promoter-paused RNA PolII. Instead, the modification of Ser2 is mediated by CDK9, the kinase of the positive elongation factor pTEFb, and it is necessary for the transition from the initiation to the elongation step. In order to verify if the treatment with JQ1 caused global alteration of the phosphorylation status, we checked by Western Blot the level of phosphorylated RNA PolII with specific antibodies, previously tested, and that recognize exclusively the RNA PolIIS5p or RNA PolIIS2p forms. After the treatment with JQ1, neither RNA

PolIIS5p nor RNA PolIIS2p levels were decreased (Fig.71), suggesting the absence of a global alteration in RNA PolII phosphorylation status.

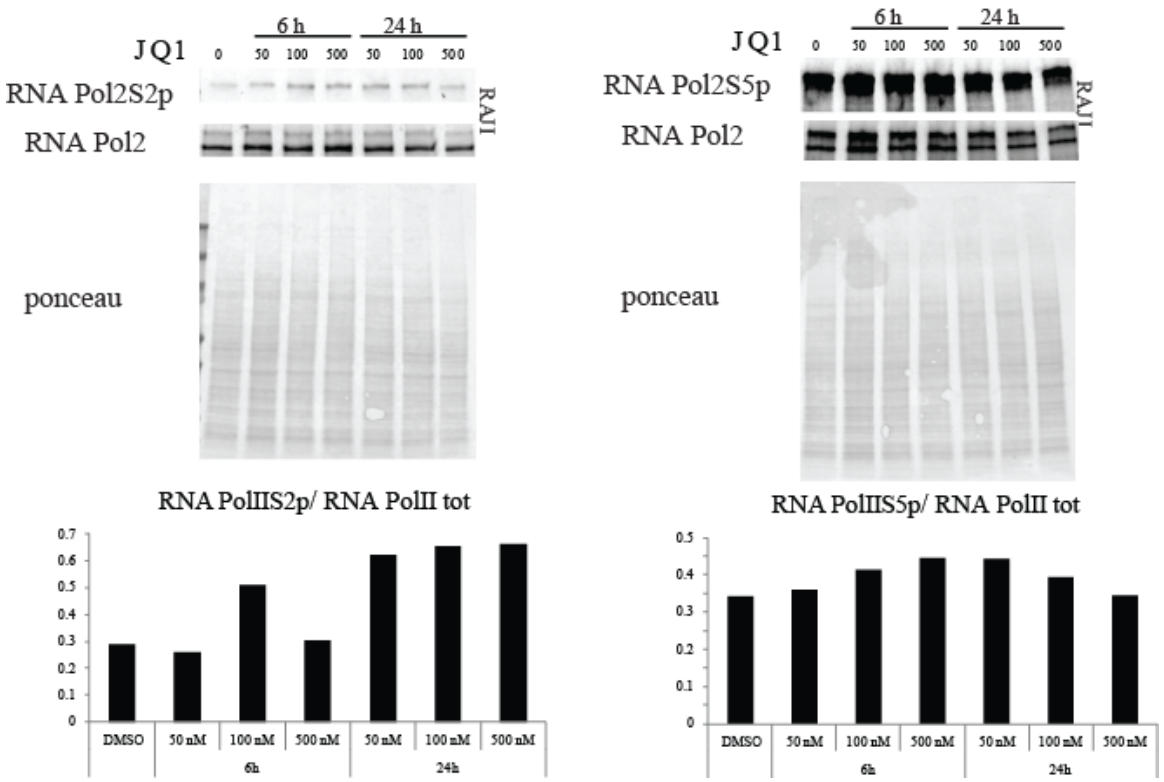

Fig. 71 BETs inhibition does not cause a global reduction in RNA PolII phosphorylated forms
Analysis of RNA PolIIS2p and RNA PolIIS5p levels by Western Blot in RAJI treated with different concentration of JQ1 (0-50-100-500 nM) for 6 or 24h. Total RNA PolII was used to monitor eventual alteration in the levels of total RNA PolII. Ponceau is used as loading control. Two technical replicates were performed and a representative blot is shown. In the lower panels, the barplots show the quantification of the phosphor RNA PolII over the total.

In order to assess differences in RNA PolII phosphorylation that could be characteristic and restricted to JQ1 responsive genes, we performed ChIPseq on phosphorylated RNA PolII forms (RNA PolIIS2p and RNA PolIIS5p) and we analyzed their distribution along the genes of the different classes of genes. This analysis showed that the distribution of RNA PolIIS2p was strongly affected by BETs inhibition, in particular the JQ1 responsive genes were characterized by a strong decrease in the levels of RNA PolIIS2p both in the genebody and on the Transcriptional End Site (TES), as shown both in the gene profile and in the quantification of the intensity of the phosphorylated RNA PolII respect to the total form (Fig.72), supporting the hypothesis that BET inhibition led to a decrease in the elongating RNA PolII in this class of genes. On the contrary, both upregulated and not affected genes showed a global increase in the RNA PolIIS2 phosphorylated forms (Fig.72). While for the upregulated genes this result was expected, since

they responded to BET inhibition with an increase in transcription, the results for the not deregulated genes was a further support to our hypothesis of a compensatory mechanism that can counterbalance the effect of JQ1 by recruiting more RNA PolII on the TSS of the genes and thus leading to an increase in the elongating RNA PolII.

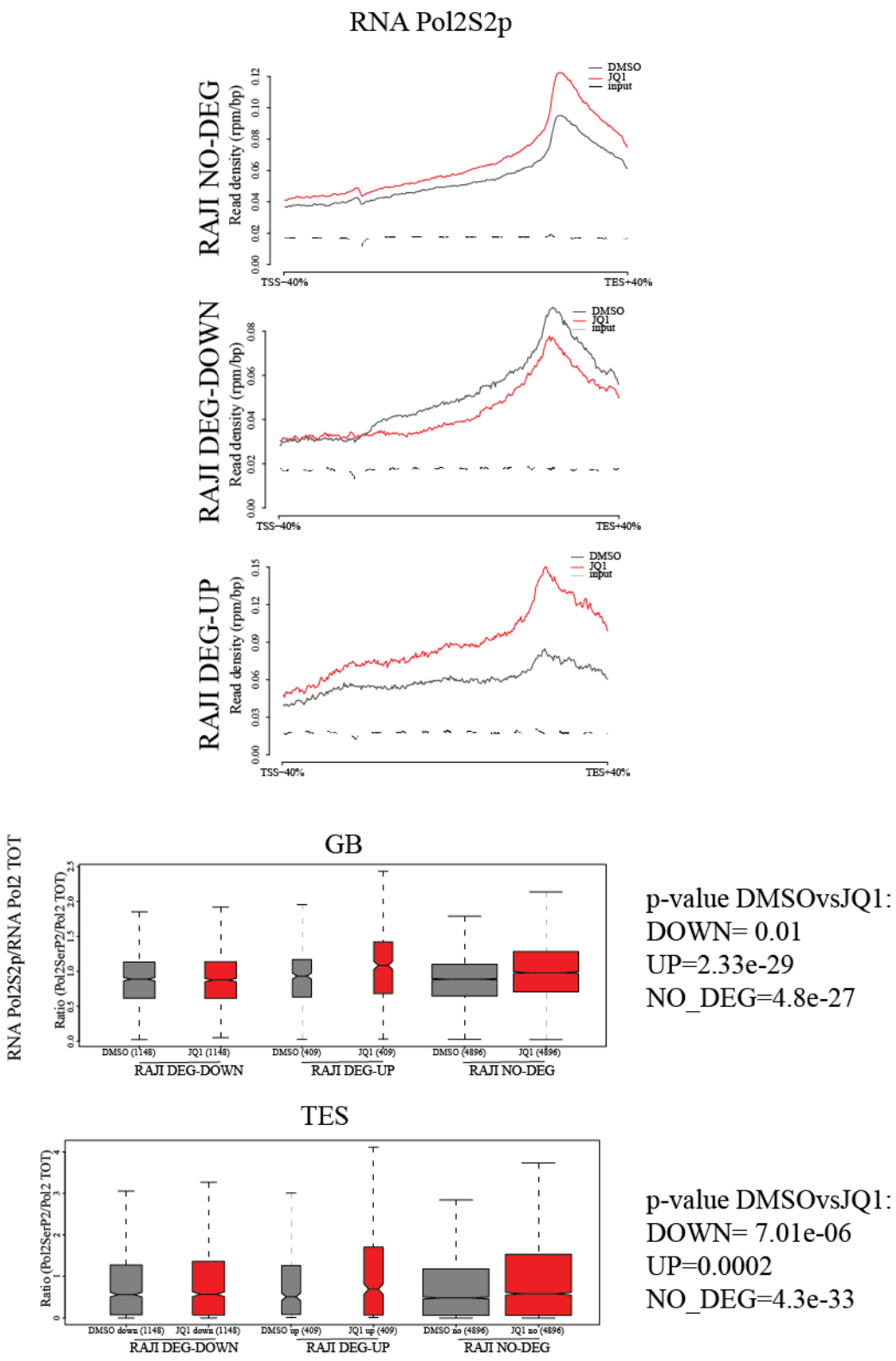

Fig. 72 BETs inhibition strongly affects elongating RNA PolII (S2p)

Analysis of RNA PolIIS2p in not deregulated (NO-DEG), downregulated (DEG-DOWN) or upregulated (DEG-UP) genes after 24h JQ1 treatment in RAJI. In the upper panel the analysis of RNA PolIIS2p distribution along the genes in DMSO (black) or JQ1 (red) is reported. The dashed line represents the background level (input).
In the lower panel, the amount of phosphorylated Ser2 RNA PolII over the total form in the Genebody (GB) or Transcription End Site (TES) is evaluated. Pair t-test is performed to evaluate statistical significant differences among DMSO (gray) and JQ1 (red) samples. Each ChIPseq sample was sequenced once.

Moreover, from the analysis of RNA PolIIS5 phosphorylated form, we noticed that downregulated genes showed a strong decrease in the RNA PolIIS5p along the genebody, with no significant changes at the TSS (Fig. 73), supporting the idea that less initiating RNA PolII is able to escape from the TSS in order to complete the transcription. The not deregulated and upregulated genes showed a clear increase in the Ser5 phosphorylated form both at the TSS and on the genebody (Fig.73). Furthermore, the increased Ser5p/Tot ratio (Fig.57) both in not-deregulated and upregulated genes denoted an enhancement of the phosphorylation mediated by CDK7 after BETs inhibition, suggesting that the compensatory effect may be mediated also by an active recruitment and priming of RNA PolII, rather than a simple release from the TSS of RNA PolII molecules already present.

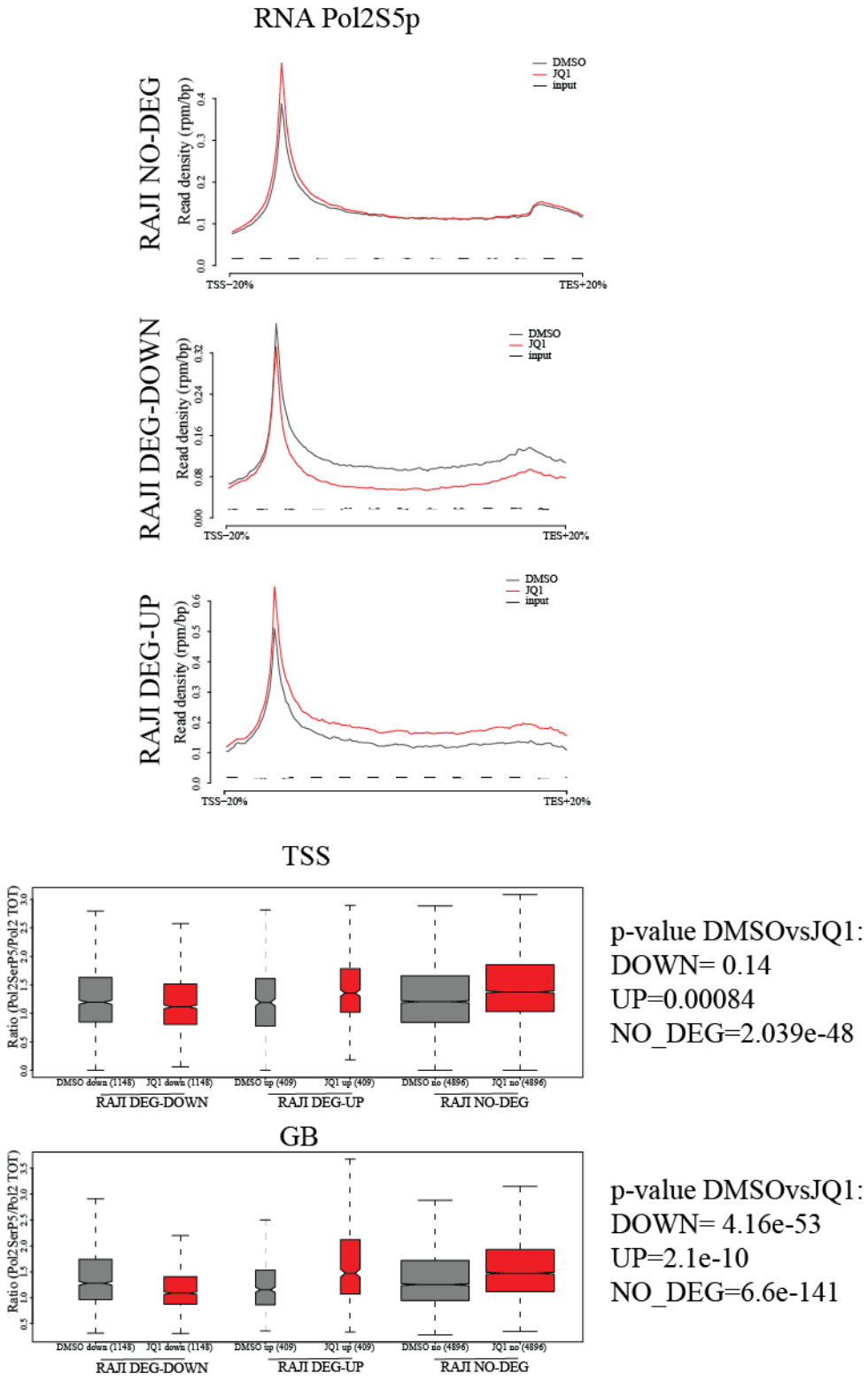

Fig. 73 BETs inhibition induces phosphorylation of RNA PolII on the Serine 5

Analysis of RNA PolIIS5p in not deregulated (NO-DEG), downregulated (DEG-DOWN) or upregulated (DEG-UP) genes after 24h JQ1 treatment in RAJI. In the upper panel the analysis of RNA PolIIS2p distribution along the genes in DMSO (black) or JQ1 (red) is reported. The dashed line represents the background level (input).

In the lower panel, the amount of phosphorylated Ser5 RNA PolII over the total form in the Genebody (GB) or Transcription End Site (TES) is evaluated. Pair t-test is performed to evaluate statistical significant differences among DMSO (gray) and JQ1 (red) samples. Each ChIPseq sample was sequenced once.

These observations suggested that BRD4 regulates RNA PolII elongation, while this is a general effect that will likely concern any transcribed gene, the decrease in the transcription rate will specifically affect a subset of expressed genes which will be unable to compensate the drop in elongation rate with the increase in RNA PolII recruitment.

Cdk9 inhibition preferentially downregulates JQ1 sensitive genes

Several experimental evidences suggest that BRD4 is a positive co-factor in the regulation of gene transcription, since it is necessary for the recruitment of Positive Elongation Factor (pTEFb composed by CDK9 and Cyc T1) on the promoter of target genes, allowing the phosphorylation on Serine 2 of RNA PolII (Jang et al., 2005; Yang et al., 2005). Since our data showed that JQ1 responsive genes are particularly sensitive to alteration in RNA PolII elongation, we wondered whether this class of genes would be similarly sensitive to other inhibitors of RNA PolII elongation. To answer to this question, we analyzed the transcriptional response after inhibition of CDK9, using two well-known CDK9 inhibitors (e.g. DRB and PHA-767491) on both JQ1 responsive and not responsive genes. As shown in Fig.74, genes sensitive to BET inhibition were preferentially downregulated by CDK9 inhibitors. As expected, high concentration of CDK9 inhibitors, which will globally blunt elongation preventing any compensatory effect at the promoter level, affected the expression of all the tested genes.

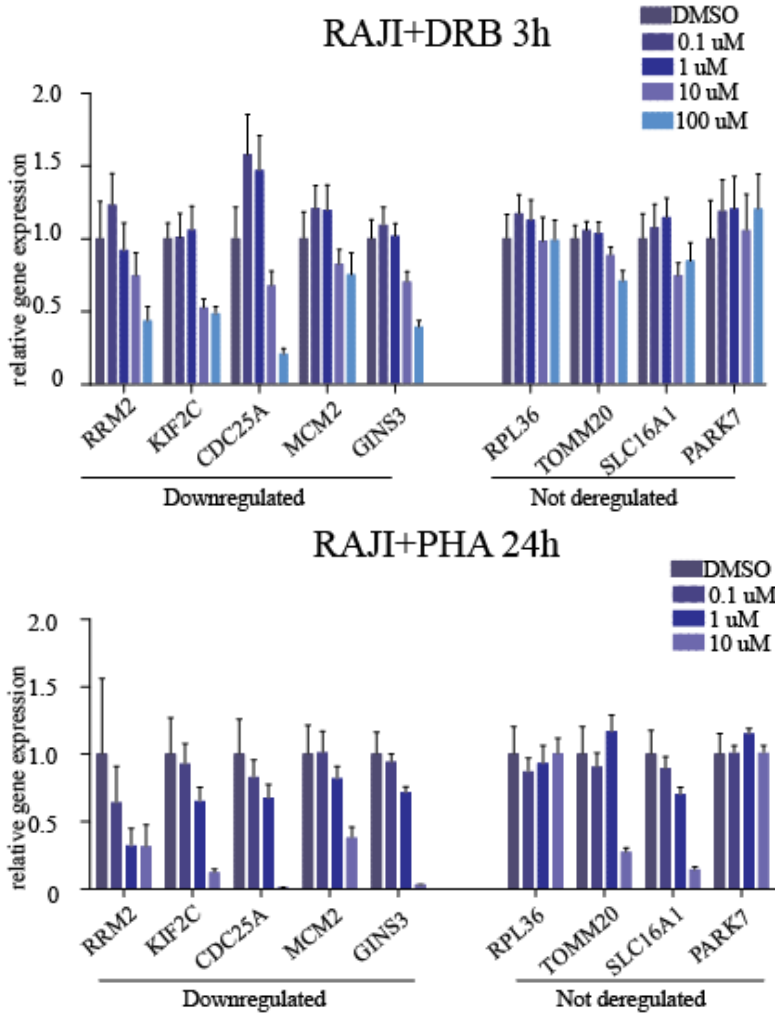

Fig. 74 JQ1 responsive genes are more sensitive to CDK9i
Expression analysis by RTqPCR on JQ1 responsive or not-deregulated genes in RAJI in response to two different CDK9 inhibitors: in the upper panel, RAJI cells are treated for 3h with different concentration of DRB (Mountbatten pink: DMSO, indaco: 0.1 μM, blu persia: 1 μM, lavender: 10 μM, periwinkle: 100 μM), in the lower panel RAJI are treated for 24h with different concentration of PHA (Mountbatten pink: DMSO, indaco: 0.1 μM, blu persia: 1 μM, lavender: 10 μM). The expression values are normalized on RPP0 expression and on the DMSO sample. The mean and the standard deviations of 3 technical replicates are reported.

Taking advantage of already published data, we analyzed also the RNA PolII dynamics on MM.1S cells treated with CDK9 inhibitor (Anders et al., 2014) using the (Delmore et al., 2011) expression data to define the classes of JQ1 sensitive or insensitive genes. As shown in Fig.75, CDK9 inhibitors had a stronger effect respect to BRD4 inhibition in terms of stalling of RNA PolII, indeed we observed a decrease in the elongating RNA PolII also in genes classified as not responding to BRD4 inhibition. Nonetheless, JQ1 targets showed a greater stalling index with a higher reduction in the travelling RNA PolII on the genebody compared to the others, consistent with the hypothesis that these genes are intrinsically less capable to compensate for drops in elongation rates.

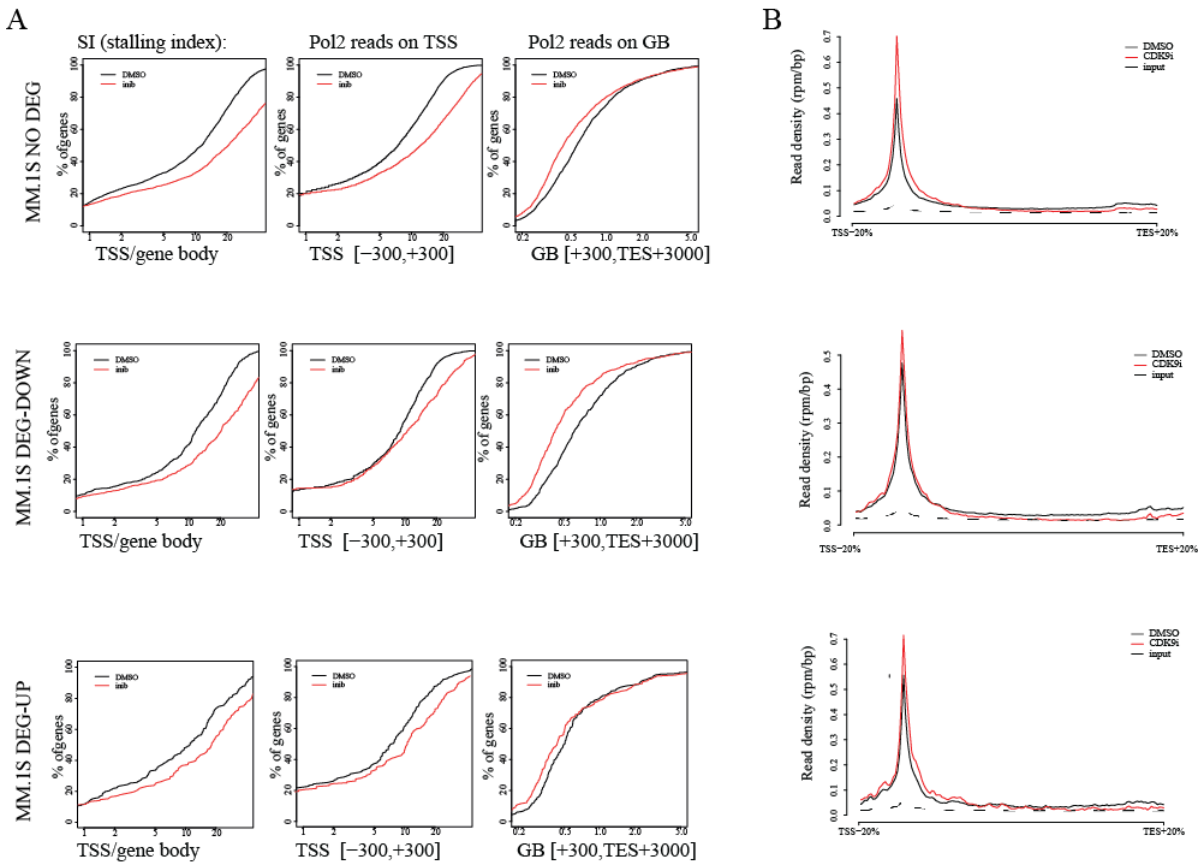

Fig. 75 JQ1 responding genes are also more sensitive to CDK9 inhibition
Evaluation of the RNA PolII dynamics in MM.1S after treatment with DMSO (black) or CDK9 inhibitor (red) on genes identified as not-deregulated (NO-DEG), downregulated (DEG-DOWN) or upregulated (DEG-UP) after BETs inhibition. (A) Stalling Index is calculated for NO-DEG, DEG-DOWN or DEG-UP genes. The left panel summarizes the global SI, the middle panel shows the quantification of RNA PolII on the TSS, while the right panel shows the quantification of RNA PolII reads on the GeneBody (GB). (B) RNA PolII profiles along the gene for NO-DEG, DEG-DOWN, DEG-UP genes. The dashed line represents the background (input) signal. For this analysis already published data are used (Anders et al., 2014; Delmore et al., 2011).

The elongation dependency of the genes downregulated by BETs inhibition was further verified in CDK9 overexpression experiments. Indeed, ectopic expression of CDK9 (Fig.76) was sufficient to slightly increase the expression levels of genes sensitive to JQ1 treatment, while genes insensitive to the drug were not altered by CDK9 overexpression (Fig.77).

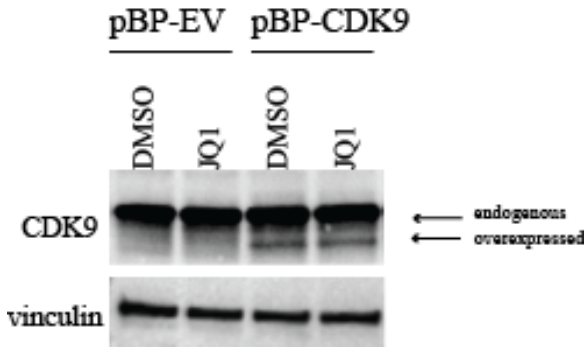

Fig. 76 CDK9 overexpression in RAJI
Analysis of CDK9 protein level by Western Blot analysis to evaluate CDK9 overexpression in RAJI cells infected with either pBabe-PURO-EV or pBabe-PURO-CDK9. Vinculin is used as loading control. One technical replicate per each of the two biological replicates was performed and a representative blot is shown.

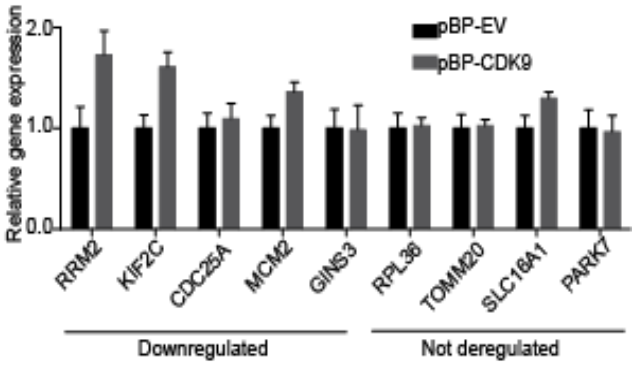

Fig. 77 CDK9 overexpression slightly induces the expression of JQ1 sensitive genes
Expression analysis by RTqPCR to evaluate the expression levels of genes responsive (downregulated) or insensitive (not deregulated) to JQ1 in RAJI infected with either pBabe-Puro-EV (black) or pBabe-Puro-CDK9 (gray). The expression values are normalized to RPP0 expression levels and pBabe-Puro-EV sample. The mean and the standard deviations of 3 technical replicates are reported.

These data suggested that the limiting step in the control of BRD4 targets expression is the elongation of RNA PolII. Once this process is perturbed the genes cannot compensate it and their transcription will be decreased. On the contrary, the regulation of JQ1 insensitive genes could be multilayer allowing to buffer eventual mild perturbation, only heavy alteration of the elongation step, as in the case of high concentration of CDK9 inhibitors, will end up with a decrease in their expression level.

Super-Enhancers

Recent publications have highlighted the presence of new distal regulatory elements, called Super-enhancers (SEs), characterized by their unusual length and by high levels of BRD4, Med1 and H3K27 acetylation (Lovén et al., 2013). These SE regions are associated to genes that confers cell identity or that are necessary for tumor maintenance (Chapuy et al., 2013; Dowen et al., 2014; Hnisz et al., 2013; Lovén et al., 2013; Whyte et al., 2013). The presence and the characteristics of those regions were used to support and rationalize the specific downregulation caused by BETs inhibitors of some genes associated to tumor progression as *c-myc* (Lovén et al., 2013). In order to verify if also in RAJI we could identify these regions, we analyzed our BRD4 ChIPseq data according to the parameter used in the paper mentioned above (Fig.78).

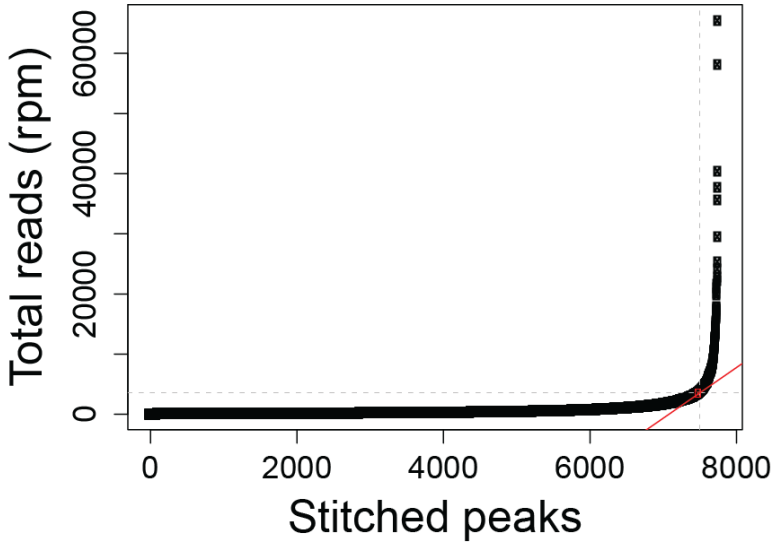

Fig. 78 Super-enhancers identification in RAJI
Identification of super-enhancers ranking BRD4 stitched peaks according to BRD4 intensity signal (rpm: reads per million). Each ChIPseq sample was sequenced once.

This analysis allowed us to identify in RAJI around 270 Super-enhancers that share features of the canonical active enhancers, such as high ratio H3K4me1/H3K4me3 and H3K27Ac (Fig.79).

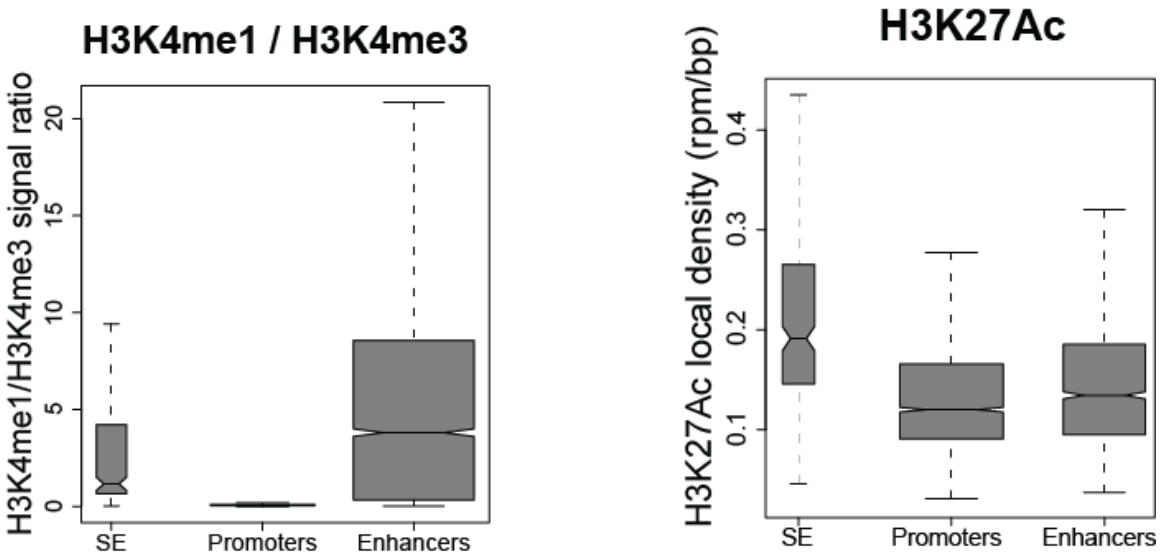

Fig. 79 SEs shows characteristics of distal regulatory regions and they are highly acetylated
Analysis of histone modifications signal in Super-enhancers (SE), promoters or enhancers. H3K4me1/H3K4me3 ratio is used to identify active enhancers, while H3K27Ac is a mark of active and open chromatin on SE, promoters or canonical enhancers. The local read density (reads per million/ base pair: rpm/bp) is reported. Each ChIPseq sample was sequenced once.

Compared to canonical enhancers, Super-enhancers were particularly enriched for BRD4 binding and acetylation on the H3K27 (Fig.80).

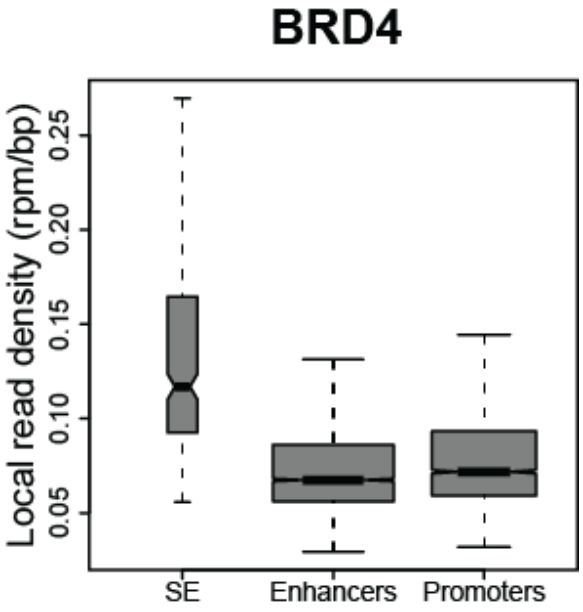

Fig. 80 SEs are strongly bound by BRD4
Analysis of BRD4 intensity binding on Super-enhancers (SE), canonical enhancers or promoters. The local read density (reads per million/ base pair: rmp/bp) is reported.

Moreover, SEs were highly sensitive to BETs inhibition, since the treatment with JQ1 caused a much stronger BRD4 depletion on SE compared to canonical enhancers (Fig.81).

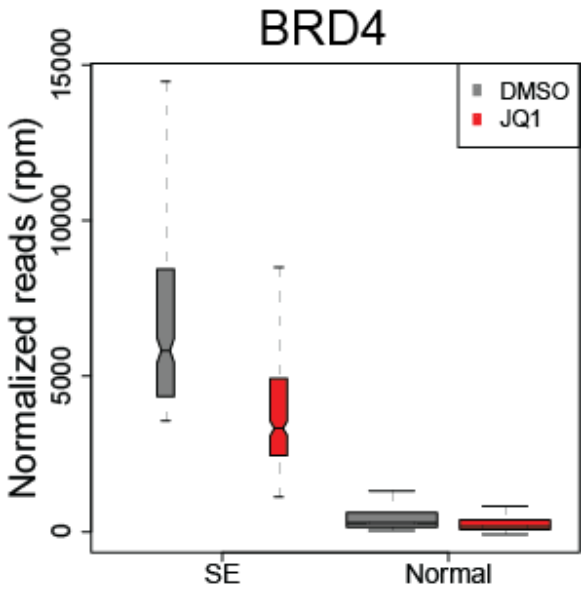

Fig. 81 SEs are highly sensitive to BRD4 displacement mediated by JQ1
Analysis of BRD4 intensity binding on Super-enhancers (SE) or canonical enhancers (normal) after 24h of treatment with DMSO (gray) or 100 nM of JQ1 (red) in RAJI.

Super-enhancers were occupied by Myc and RNA PolII and also in this case, as for canonical enhancers and promoters, BETs inhibition caused a local increase of Myc and RNA PolII binding (Fig.82).

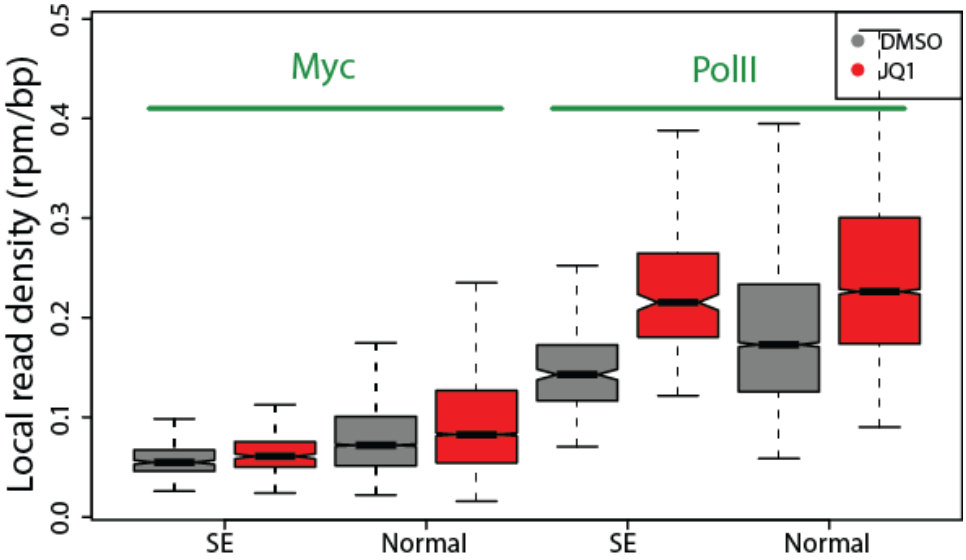

Fig. 82 SEs are bound by Myc and RNA PolII in RAJI
Analysis of Myc or RNA PolII intensity binding on Super-enhancers (SE) or canonical enhancers (normal) after 24h of treatment with DMSO (gray) or 100 nM of JQ1 (red) in RAJI. Each ChIPseq sample was sequenced once.

Since Super-enhancers have been proposed to regulate either cell type specific genes or key oncogenes in tumor cell lines and they are particularly sensitive to the treatment with JQ1, we wondered whether they were also associated to genes that were downregulated after BETs

inhibition in RAJI. To answer to this question, we first associated the Super-enhancers to the closest gene and we performed the overlap between the associated Super-enhancers genes and the DEGs identified after microarray analysis. None of the classes that we defined as DEGs were enriched for genes associated to Super-enhancers (Fig.83).

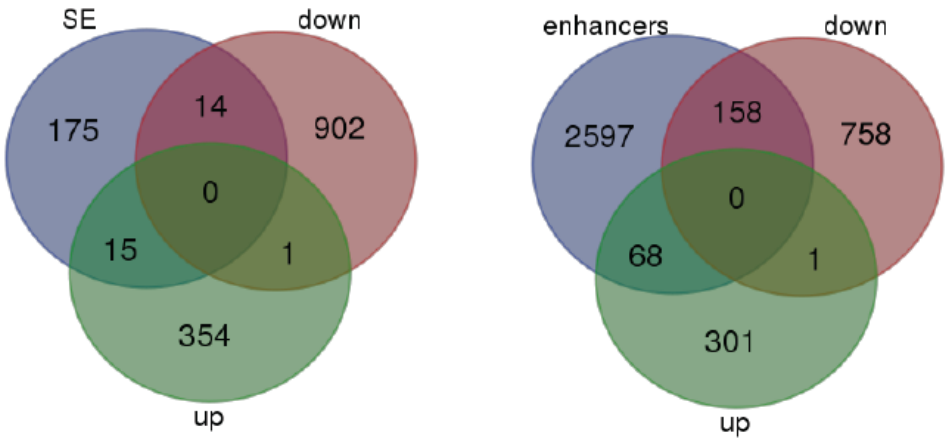

Fig. 83 SEs associated genes are not enriched for JQ1 responsive genes
Comparison of Super-Enhancer (SE) associated genes and genes deregulated (DOWN or UP) by JQ1 treatment in RAJI. The comparison of canonical enhancer associated genes and JQ1 responsive genes is used as control.

While we did not find any direct association between genes differentially expressed upon BETs inhibition and SE, based on proximity analysis, long-range transcriptional control exerted by SE will merit further assessment.

V. Discussion

The *c-myc* gene encodes for a transcription factor involved in different aspects of cellular life and, in particular, in cell cycle control and apoptosis, cell differentiation, cell metabolism, energy production and RNA synthesis (Ponzielli et al., 2005). The crucial role of Myc in the regulation of cell cycle and cell proliferation was demonstrated shortly after its discovery as a viral oncogene in avian leukemia (Sheiness and Bishop, 1979). Hitherto, Myc oncogenic activity has been associated not only to the onset of the vast number of human tumors (Dang, 2012), but also to tumor maintenance (Pelengaris et al., 2002b; Shachaf et al., 2004; Soucek et al., 2008). Thus, the development of inhibitory strategies aimed at modulating or switching off Myc expression represents "the promise land" in cancer treatment. Different strategies have been proposed to impair Myc expression or activity (Ponzielli et al., 2005), among these, in the last years the possibility to target chromatin readers has been explored. Indeed, different reports in 2011 demonstrated that the use of BETs inhibitors led to cell cycle arrest *in vitro* and tumor regression *in vivo* (Dawson et al., 2011; Delmore et al., 2011; Mertz et al., 2011; Zuber et al., 2011). Moreover, in these publications, Myc downregulation was proposed as the main target of BETs inhibitors (Dawson et al., 2011; Delmore et al., 2011; Mertz et al., 2011; Zuber et al., 2011).

BET proteins are crucial mediators in gene transcription, since, after the recognition and the binding of acetylated histones through the bromodomains, they recruit activators of transcription, as pTEFb (Jang et al., 2005; Yang et al., 2005).

Different working models have been proposed to explain how BETs inhibition triggers Myc downregulation. Indeed when the *c-myc* gene is translocated under the control of the IgH enhancer, its transcription is regulated by broad regulatory distal regions located in the IgH locus, called IgH-Super Enhancers (SE), that are highly enriched for BRD4. In

this context, Myc downregulation could be explained by the displacement of BRD4 from the IgH-SE (Delmore et al., 2011; Lovén et al., 2013). When *c-myc* is not translocated, its expression can be regulated by oncogenic transcription factors, as MLL/AF9 in the Acute Myeloid Leukemia, recruited on chromatin by BET proteins. Also in this system the treatment with BETs inhibitors prevents BET proteins binding to chromatin and switch off Myc transcription (Dawson et al., 2011).

Subsequent publications, as well as our work, called into question the idea that Myc downregulation is a *conditio sine qua non* BETs inhibitors can exert their therapeutic functions. Indeed, we were able to identify different Burkitt's lymphoma cell lines and Eμ-Myc lymphomas that do not show any alteration of Myc levels (Fig.22-23), even if highly sensitive to drug treatment in terms of decrease in cell growth (Fig.17) and block in G1/S progression (Fig.18). Moreover, our results suggest that, despite the final effect on Myc expression, BETs inhibition leads to a deregulation of a restricted class of genes, enriched for targets of Myc (Fig.44) and E2F (Fig.45) and involved in cell cycle progression (Fig.43). It is worth to highlight that similar classes of genes are downregulated in response to BETs inhibitors in different hematological tumors (Burkitt's Lymphomas and Multiple Myeloma), independently from the alteration of Myc levels (Fig.47). Indeed, both RAJI (Myc no change) and MM.1S (Myc downregulated) showed a strong downregulation of genes involved in the cell cycle progression in response to BETs inhibitors. This similarity in the global transcriptional changes in BL and MM, regardless the effect on Myc transcription, further reinforces the idea that, beside the already proposed Myc-dependent mechanisms, a more general mechanism should exist.

Despite the growing literature on BET proteins and the use of BETs inhibitors in different cellular models, a clear characterization of genes sensitive to BETs inhibition is still missing. In our work, we identify an association that may lead to *a priori* prediction of JQ1 responsive genes. Indeed, our results suggest that downregulated genes in RAJI are characterized by a high expression level, compared to the not deregulated ones (Fig.59).

Moreover, JQ1 responsive genes, not only are enriched for Myc and E2F1 targets, as demonstrated by GSEA (Fig.44-45) and ChIPseq (Fig.60-61-62), but also they show the strongest intensity binding of those TFs (Myc and E2F1) and RNA PolII on the TSS (Fig.64), suggesting an high transcriptional activity.

Beside the deep characterization of JQ1 responsive genes, our work demonstrates that in hematological malignancies (BL, MM, DLBCL) BETs inhibition alters the dynamics of RNA PolII both in JQ1 sensitive and insensitive genes. Previous publications already showed the involvement of BRD4 in the regulation of RNA PolII rate in different cellular systems (Di Micco et al., 2014; Anand et al., 2013; Kanno et al., 2014; Liu et al., 2014, 2013). Indeed, it was demonstrated that BRD4 inhibition or silencing are associated to an impairment of RNA PolII rate not only in JQ1 responsive genes, but also in the remaining active transcripts (Anand et al., 2013; Liu et al., 2013; Di Micco et al., 2014). While some reports associate the regulation of RNA PolII rate mediated by BRD4 to its capacity to recruit and activate pTEFb (Liu et al., 2014), in Ozato's lab this possibility was excluded and the BRD4 control of the elongation rate was connected to its histone chaperone activity (Kanno et al., 2014). In our work, we mainly focused our attention on the analysis of the transcriptional consequences to BETs inhibition rather than on the mechanistic dissection of BRD4 involvement in the control of the elongation step. Indeed, our results add an additional layer of information, thanks to a deeper analysis of RNA PolII dynamics: our work, in line with already published reports, demonstrates an increase in the Stalling Index (SI) in all active genes as well as in JQ1 sensitive ones (Fig.67-69-70). Furthermore we demonstrate that, while not sensitive genes are characterized by an increase in the promoter-proximal RNA PolII with no changes on the elongating RNA PolII on the genebody, JQ1 responsive genes show a strong decrease in the RNA PolII associated to genebody (Fig.67-69-70). It is worth to remember at this point that the SI takes into account the amount of RNA PolII both on the TSS and on the genebody, consequently an increase in the SI value could be associated to either an increase in the

TSS associated RNA PolII or to a decrease in the elongating polymerase. Our work suggests that BETs inhibition causes a genome wide alteration of RNA PolII dynamics with an increase in the SI value: while JQ1 sensitive genes experience a drop in the elongating RNA PolII, JQ1 insensitive genes actively recruit more RNA PolII on the TSS. Furthermore, our results suggest that the active recruitment of total RNA PolII on the TSS of JQ1 insensitive genes is followed by an active phosphorylation on the polymerase CTD, since we observed an increase of both S5p TSS associated (Fig.73) and S2p elongating RNA PolII (Fig.72). On the contrary, JQ1 sensitive genes were characterized by the absence of additional phosphorylation after BETs inhibition, since the amount of RNA PolII phosphorylated forms over the total was comparable among DMSO and JQ1 sample (Fig.72-73).

Overall, the analysis of RNA PolII clearly demonstrated that two different responses are possible after BETs inhibition: while JQ1 insensitive genes recruit more RNA PolII on the promoter and respond to BETs inhibition increasing the phosphorylation of the polymerase, JQ1 sensitive genes show a strong reduction in the elongating RNA PolII without any further recruitment or phosphorylation of new RNA PolII molecules.

Comprehensively, our work proposes a novel mechanism of action for BETs inhibitors. Indeed our data show that, beside the already proposed direct downregulation of key Transcription Factors as Myc, another JQ1 effect is the alteration of RNA PolII dynamics: while JQ1 responsive genes transcription is strongly reduced after drug treatment due to a drop in the elongating RNA PolII, JQ1 not responsive genes are able to compensate the alteration of the polymerase distribution increasing both the total amount of TFs and RNA PolII on the promoter and the phosphorylation of polymerase in order to enhance its processivity. Probably this compensatory mechanism is not possible in the class of JQ1 sensitive genes because they are already expressed at their maximum level. Furthermore, our work suggests that for highly transcribed genes the elongation step is a rate limiting step, since they are highly sensitive to any alteration of RNA PolII elongating fraction and

they are not able to compensate this change. In this light, our work not only suggests a novel BETs inhibitor mechanism of action but highlights the possibility to use the elongation step as an additional potential therapeutic target.

VI. References

Adams, J.M., Harris, A.W., Pinkert, C.A., Corcoran, L.M., Alexander, W.S., Cory, S., Palmiter, R.D., and Brinster, R.L. (1985). The c-myc oncogene driven by immunoglobulin enhancers induces lymphoid malignancy in transgenic mice. Nature *318*, 533–538.

Alekseyenko, A.A., Walsh, E.M., Wang, X., Grayson, A.R., Hsi, P.T., Kharchenko, P.V., Kuroda, M.I., and French, C.A. (2015). The oncogenic BRD4-NUT chromatin regulator drives aberrant transcription within large topological domains. Genes Dev. *29*, 1507–1523.

Amati, B., Dalton, S., Brooks, M.W., Littlewood, T.D., Evan, G.I., and Land, H. (1992). Transcriptional activation by the human c-Myc oncoprotein in yeast requires interaction with Max. Nature *359*, 423–426.

Anand, P., Brown, J.D., Lin, C.Y., Qi, J., Zhang, R., Artero, P.C., Alaiti, M.A., Bullard, J., Alazem, K., Margulies, K.B., et al. (2013). BET bromodomains mediate transcriptional pause release in heart failure. Cell *154*, 569–582.

Anders, L., Guenther, M.G., Qi, J., Fan, Z.P., Marineau, J.J., Rahl, P.B., Lovén, J., Sigova, A.A., Smith, W.B., Lee, T.I., et al. (2014). Genome-wide localization of small molecules. Nat. Biotechnol. *32*, 92–96.

Belkina, A.C., Blanton, W.P., Nikolajczyk, B.S., and Denis, G.V. (2014). The double bromodomain protein Brd2 promotes B cell expansion and mitogenesis. J. Leukoc. Biol. *95*, 451–460.

Bentley, D.L., and Groudine, M. (1986). A block to elongation is largely responsible for decreased transcription of c-myc in differentiated HL60 cells. Nature *321*, 702–706.

Berman, D.M., Karhadkar, S.S., Hallahan, A.R., Pritchard, J.I., Eberhart, C.G., Watkins, D.N., Chen, J.K., Cooper, M.K., Taipale, J., Olson, J.M., et al. (2002). Medulloblastoma growth inhibition by hedgehog pathway blockade. Science *297*, 1559–1561.

Blackwood, E.M., and Eisenman, R.N. (1991). Max: a helix-loop-helix zipper protein that forms a sequence-specific DNA-binding complex with Myc. Science *251*, 1211–1217.

Bromberg, J.F., Wrzeszczynska, M.H., Devgan, G., Zhao, Y., Pestell, R.G., Albanese, C., and Darnell, J.E. (1999). Stat3 as an oncogene. Cell *98*, 295–303.

Buratowski, S. (2009). Progression through the RNA polymerase II CTD cycle. Mol. Cell *36*, 541–546.

Chapuy, B., McKeown, M.R., Lin, C.Y., Monti, S., Roemer, M.G., Qi, J., Rahl, P.B., Sun, H.H., Yeda, K.T., Doench, J.G., et al. (2013). Discovery and characterization of super-enhancer-associated dependencies in diffuse large B cell lymphoma. Cancer Cell *24*, 777–790.

Chen, C.-R.R., Kang, Y., Siegel, P.M., and Massagué, J. (2002). E2F4/5 and p107 as Smad cofactors linking the TGFbeta receptor to c-myc repression. Cell *110*, 19–32.

Corcoran, L.M., Cory, S., and Adams, J.M. (1985). Transposition of the immunoglobulin heavy chain enhancer to the myc oncogene in a murine plasmacytoma. Cell *40*, 71–79.

Dang, C.V. (2012). MYC on the path to cancer. Cell *149*, 22–35.

Dawson, M.A., Prinjha, R.K., Dittmann, A., Giotopoulos, G., Bantscheff, M., Chan, W.-I.I., Robson, S.C., Chung, C.W., Hopf, C., Savitski, M.M., et al. (2011). Inhibition of BET recruitment to chromatin as an effective treatment for MLL-fusion leukaemia. Nature *478*, 529–533.

Delmore, J.E., Issa, G.C., Lemieux, M.E., Rahl, P.B., Shi, J., Jacobs, H.M., Kastritis, E., Gilpatrick, T., Paranal, R.M., Qi, J., et al. (2011). BET bromodomain inhibition as a therapeutic strategy to target c-Myc. Cell *146*, 904–917.

Devaiah, B.N., Lewis, B.A., Cherman, N., Hewitt, M.C., Albrecht, B.K., Robey, P.G., Ozato, K., Sims, R.J., and Singer, D.S. (2012). BRD4 is an atypical kinase that phosphorylates serine2 of the RNA polymerase II carboxy-terminal domain. Proc. Natl. Acad. Sci. U.S.A. *109*, 6927–6932.

Dey, A., Nishiyama, A., Karpova, T., McNally, J., and Ozato, K. (2009). Brd4 marks select genes on mitotic chromatin and directs postmitotic transcription. Mol. Biol. Cell *20*, 4899–4909.

Dowen, J.M., Fan, Z.P., Hnisz, D., Ren, G., Abraham, B.J., Zhang, L.N., Weintraub, A.S., Schuijers, J., Lee, T.I., Zhao, K., et al. (2014). Control of cell identity genes occurs in insulated neighborhoods in mammalian chromosomes. Cell *159*, 374–387.

Eberhardy, S.R., and Farnham, P.J. (2002). Myc recruits P-TEFb to mediate the final step in the transcriptional activation of the cad promoter. J. Biol. Chem. *277*, 40156–40162.

Farina, A., Hattori, M., Qin, J., Nakatani, Y., Minato, N., and Ozato, K. (2004). Bromodomain protein Brd4 binds to GTPase-activating SPA-1, modulating its activity and subcellular localization. Mol. Cell. Biol. *24*, 9059–9069.

Fellmann, C., Hoffmann, T., Sridhar, V., Hopfgartner, B., Muhar, M., Roth, M., Lai, D.Y., Barbosa, I.A.A., Kwon, J.S., Guan, Y., et al. (2013). An optimized microRNA backbone for effective single-copy RNAi. Cell Rep *5*, 1704–1713.

Filippakopoulos, P., and Knapp, S. (2014). Targeting bromodomains: epigenetic readers of lysine acetylation. Nat Rev Drug Discov *13*, 337–356.

Filippakopoulos, P., Qi, J., Picaud, S., Shen, Y., Smith, W.B., Fedorov, O., Morse, E.M., Keates, T., Hickman, T.T., Felletar, I., et al. (2010). Selective inhibition of BET bromodomains. Nature *468*, 1067–1073.

Floyd, S.R., Pacold, M.E., Huang, Q., Clarke, S.M., Lam, F.C., Cannell, I.G., Bryson, B.D., Rameseder, J., Lee, M.J., Blake, E.J., et al. (2013). The bromodomain protein Brd4 insulates chromatin from DNA damage signalling. Nature *498*, 246–250.

Frederick, J.P., Liberati, N.T., Waddell, D.S., Shi, Y., and Wang, X.-F.F. (2004). Transforming growth factor beta-mediated transcriptional repression of c-myc is dependent on direct binding of Smad3 to a novel repressive Smad binding element. Mol. Cell. Biol. *24*, 2546–2559.

French, C.A., Miyoshi, I., Kubonishi, I., Grier, H.E., Perez-Atayde, A.R., and Fletcher, J.A. (2003). BRD4-NUT fusion oncogene: a novel mechanism in aggressive carcinoma. Cancer Res. *63*, 304–307.

French, C.A., Ramirez, C.L., Kolmakova, J., Hickman, T.T., Cameron, M.J., Thyne, M.E., Kutok, J.L., Toretsky, J.A., Tadavarthy, A.K., Kees, U.R., et al. (2008). BRD-NUT oncoproteins: a family of closely related nuclear proteins that block epithelial differentiation and maintain the growth of carcinoma cells. Oncogene *27*, 2237–2242.

Gabay, M., Li, Y., and Felsher, D.W. (2014). MYC activation is a hallmark of cancer initiation and maintenance. Cold Spring Harb Perspect Med *4*.

Grandori, C., Cowley, S.M., James, L.P., and Eisenman, R.N. (2000). The Myc/Max/Mad network and the transcriptional control of cell behavior. Annu. Rev. Cell Dev. Biol. *16*, 653–699.

Greenwald (2003). E -BRD2 transgenic mice develop B-cell lymphoma and leukemia. Blood *103*.

He, T.C., Sparks, A.B., Rago, C., Hermeking, H., Zawel, L., da Costa, L.T., Morin, P.J., Vogelstein, B., and Kinzler, K.W. (1998). Identification of c-MYC as a target of the APC pathway. Science *281*, 1509–1512.

Hemann, M.T., Bric, A., Teruya-Feldstein, J., Herbst, A., Nilsson, J.A., Cordon-Cardo, C., Cleveland, J.L., Tansey, W.P., and Lowe, S.W. (2005). Evasion of the p53 tumour surveillance network by tumour-derived MYC mutants. Nature *436*, 807–811.

Hnisz, D., Abraham, B.J., Lee, T.I., Lau, A., Saint-André, V., Sigova, A.A., Hoke, H.A., and Young, R.A. (2013). Super-enhancers in the control of cell identity and disease. Cell *155*, 934–947.

Houzelstein, D., Bullock, S.L., Lynch, D.E., Grigorieva, E.F., Wilson, V.A., and Beddington, R.S. (2002). Growth and early postimplantation defects in mice deficient for the bromodomain-containing protein Brd4. Mol. Cell. Biol. *22*, 3794–3802.

Huang, B., Yang, X.-D.D., Zhou, M.-M.M., Ozato, K., and Chen, L.-F.F. (2009). Brd4 coactivates transcriptional activation of NF-kappaB via specific binding to acetylated RelA. Mol. Cell. Biol. *29*, 1375–1387.

Jang, M.K., Mochizuki, K., Zhou, M., Jeong, H.-S.S., Brady, J.N., and Ozato, K. (2005). The bromodomain protein Brd4 is a positive regulatory component of P-TEFb and stimulates RNA polymerase II-dependent transcription. Mol. Cell *19*, 523–534.

Jonkers, I., and Lis, J.T. (2015). Getting up to speed with transcription elongation by RNA polymerase II. Nat. Rev. Mol. Cell Biol. *16*, 167–177.

Kanno, T., Kanno, Y., LeRoy, G., Campos, E., Sun, H.-W.W., Brooks, S.R., Vahedi, G., Heightman, T.D., Garcia, B.A., Reinberg, D., et al. (2014). BRD4 assists elongation of both coding and enhancer RNAs by interacting with acetylated histones. Nat. Struct. Mol. Biol. *21*, 1047–1057.

Kiuchi, N., Nakajima, K., Ichiba, M., Fukada, T., Narimatsu, M., Mizuno, K., Hibi, M., and Hirano, T. (1999). STAT3 is required for the gp130-mediated full activation of the c-myc gene. J. Exp. Med. *189*, 63–73.

Koch, H.B., Zhang, R., Verdoodt, B., Bailey, A., Zhang, C.-D.D., Yates, J.R., Menssen, A., and Hermeking, H. (2007). Large-scale identification of c-MYC-associated proteins using a combined TAP/MudPIT approach. Cell Cycle *6*, 205–217.

Kress, T.R., Sabò, A., and Amati, B. (2015). MYC: connecting selective transcriptional control to global RNA production. Nat. Rev. Cancer.

Krumm, A., Meulia, T., Brunvand, M., and Groudine, M. (1992). The block to transcriptional elongation within the human c-myc gene is determined in the promoter-proximal region. Genes Dev. *6*, 2201–2213.

Kwak, H., and Lis, J.T. (2013). Control of transcriptional elongation. Annu. Rev. Genet. *47*, 483–508.

Li, Q., Peterson, K.R., Fang, X., and Stamatoyannopoulos, G. (2002). Locus control regions. Blood *100*, 3077–3086.

Lin, C.Y., Lovén, J., Rahl, P.B., Paranal, R.M., Burge, C.B., Bradner, J.E., Lee, T.I., and Young, R.A. (2012). Transcriptional amplification in tumor cells with elevated c-Myc. Cell *151*, 56–67.

Liu, L., Xu, Y., He, M., Zhang, M., Cui, F., Lu, L., Yao, M., Tian, W., Benda, C., Zhuang, Q., et al. (2014). Transcriptional pause release is a rate-limiting step for somatic cell reprogramming. Cell Stem Cell *15*, 574–588.

Liu, W., Ma, Q., Wong, K., Li, W., Ohgi, K., Zhang, J., Aggarwal, A.K., and Rosenfeld, M.G. (2013). Brd4 and JMJD6-associated anti-pause enhancers in regulation of transcriptional pause release. Cell *155*, 1581–1595.

Lovén, J., Hoke, H.A., Lin, C.Y., Lau, A., Orlando, D.A., Vakoc, C.R., Bradner, J.E., Lee, T.I., and Young, R.A. (2013). Selective inhibition of tumor oncogenes by disruption of super-enhancers. Cell *153*, 320–334.

Maruyama, T., Farina, A., Dey, A., Cheong, J., Bermudez, V.P., Tamura, T., Sciortino, S., Shuman, J., Hurwitz, J., and Ozato, K. (2002). A Mammalian bromodomain protein, brd4, interacts with replication factor C and inhibits progression to S phase. Mol. Cell. Biol. *22*, 6509–6520.

McMahon, S.B., Van Buskirk, H.A., Dugan, K.A., Copeland, T.D., and Cole, M.D. (1998). The novel ATM-related protein TRRAP is an essential cofactor for the c-Myc and E2F oncoproteins. Cell *94*, 363–374.

McMahon, S.B., Wood, M.A., and Cole, M.D. (2000). The essential cofactor TRRAP recruits the histone acetyltransferase hGCN5 to c-Myc. Mol. Cell. Biol. *20*, 556–562.

Meng, F.-L.L., Du, Z., Federation, A., Hu, J., Wang, Q., Kieffer-Kwon, K.-R.R., Meyers, R.M., Amor, C., Wasserman, C.R., Neuberg, D., et al. (2014). Convergent transcription at intragenic super-enhancers targets AID-initiated genomic instability. Cell *159*, 1538–1548.

Mertz, J.A., Conery, A.R., Bryant, B.M., Sandy, P., Balasubramanian, S., Mele, D.A., Bergeron, L., and Sims, R.J. (2011). Targeting MYC dependence in cancer by inhibiting BET bromodomains. Proc. Natl. Acad. Sci. U.S.A. *108*, 16669–16674.

Meyer, N., and Penn, L.Z. (2008). Reflecting on 25 years with MYC. Nat. Rev. Cancer *8*, 976–990.

Di Micco, R., Fontanals-Cirera, B., Low, V., Ntziachristos, P., Yuen, S.K., Lovell, C.D., Dolgalev, I., Yonekubo, Y., Zhang, G., Rusinova, E., et al. (2014). Control of embryonic stem cell identity by BRD4-dependent transcriptional elongation of super-enhancer-associated pluripotency genes. Cell Rep *9*, 234–247.

Mochizuki, K., Nishiyama, A., Jang, M.K., Dey, A., Ghosh, A., Tamura, T., Natsume, H., Yao, H., and Ozato, K. (2008). The bromodomain protein Brd4 stimulates G1 gene transcription and promotes progression to S phase. J. Biol. Chem. *283*, 9040–9048.

Molyneux, E.M., Rochford, R., Griffin, B., Newton, R., Jackson, G., Menon, G., Harrison, C.J., Israels, T., and Bailey, S. (2012). Burkitt's lymphoma. Lancet *379*, 1234–1244.

Nepveu, A., and Marcu, K.B. (1986). Intragenic pausing and anti-sense transcription within the murine c-myc locus. EMBO J. *5*, 2859–2865.

Nicodeme, E., Jeffrey, K.L., Schaefer, U., Beinke, S., Dewell, S., Chung, C.-W.W., Chandwani, R., Marazzi, I., Wilson, P., Coste, H., et al. (2010). Suppression of inflammation by a synthetic histone mimic. Nature *468*, 1119–1123.

Obaya, A.J., Mateyak, M.K., and Sedivy, J.M. (1999). Mysterious liaisons: the relationship between c-Myc and the cell cycle. Oncogene *18*, 2934–2941.

Oster, S., Ho, C., Soucie, E., and Penn, L. (2002). The myc oncogene: MarvelouslY Complex. Advances in Cancer Research *84*, 81–154.

Palomero, T., Lim, W.K., Odom, D.T., Sulis, M.L., Real, P.J., Margolin, A., Barnes, K.C., O'Neil, J., Neuberg, D., Weng, A.P., et al. (2006). NOTCH1 directly regulates c-MYC and activates a feed-forward-loop transcriptional network promoting leukemic cell growth. Proc. Natl. Acad. Sci. U.S.A. *103*, 18261–18266.

Pelengaris, S., Khan, M., and Evan, G. (2002a). c-MYC: more than just a matter of life and death. Nat Rev Cancer *2*, 764–776.

Pelengaris, S., Khan, M., and Evan, G.I. (2002b). Suppression of Myc-induced apoptosis in beta cells exposes multiple oncogenic properties of Myc and triggers carcinogenic progression. Cell *109*, 321–334.

Plet, A., Eick, D., and Blanchard, J.M. (1995). Elongation and premature termination of transcripts initiated from c-fos and c-myc promoters show dissimilar patterns. Oncogene *10*, 319–328.

Ponzielli, R., Katz, S., Barsyte-Lovejoy, D., and Penn, L.Z. (2005). Cancer therapeutics: targeting the dark side of Myc. Eur. J. Cancer *41*, 2485–2501.

Porrua, O., and Libri, D. (2015). Transcription termination and the control of the transcriptome: why, where and how to stop. Nat. Rev. Mol. Cell Biol. *16*, 190–202.

Pott, S., and Lieb, J.D. (2015). What are super-enhancers? Nat. Genet. *47*, 8–12.

Qian, J., Wang, Q., Dose, M., Pruett, N., Kieffer-Kwon, K.-R.R., Resch, W., Liang, G., Tang, Z., Mathé, E., Benner, C., et al. (2014). B cell super-enhancers and regulatory clusters recruit AID tumorigenic activity. Cell *159*, 1524–1537.

Rabani, M., Levin, J.Z., Fan, L., Adiconis, X., Raychowdhury, R., Garber, M., Gnirke, A., Nusbaum, C., Hacohen, N., Friedman, N., et al. (2011). Metabolic labeling of RNA uncovers principles of RNA production and degradation dynamics in mammalian cells. Nat. Biotechnol. *29*, 436–442.

Rahl, P.B., Lin, C.Y., Seila, A.C., Flynn, R.A., McCuine, S., Burge, C.B., Sharp, P.A., and Young, R.A. (2010). c-Myc regulates transcriptional pause release. Cell *141*, 432–445.

Rahman, S., Sowa, M.E., Ottinger, M., Smith, J.A., Shi, Y., Harper, J.W., and Howley, P.M. (2011). The Brd4 extraterminal domain confers transcription activation independent of pTEFb by recruiting multiple proteins, including NSD3. Mol. Cell. Biol. *31*, 2641–2652.

Rasmussen, E.B., and Lis, J.T. (1993). In vivo transcriptional pausing and cap formation on three Drosophila heat shock genes. Proc. Natl. Acad. Sci. U.S.A. *90*, 7923–7927.

Rougvie, A.E., and Lis, J.T. (1988). The RNA polymerase II molecule at the 5' end of the uninduced hsp70 gene of D. melanogaster is transcriptionally engaged. Cell *54*, 795–804.

Sabò, A., and Amati, B. (2014). Genome recognition by MYC. Cold Spring Harbor Perspectives in Medicine *4*.

Sabò, A., Kress, T.R., Pelizzola, M., de Pretis, S., Gorski, M.M., Tesi, A., Morelli, M.J., Bora, P., Doni, M., Verrecchia, A., et al. (2014). Selective transcriptional regulation by Myc in cellular growth control and lymphomagenesis. Nature *511*, 488–492.

Sainsbury, S., Bernecky, C., and Cramer, P. (2015). Structural basis of transcription initiation by RNA polymerase II. Nat. Rev. Mol. Cell Biol. *16*, 129–143.

Sansom, O.J., Meniel, V.S., Muncan, V., Phesse, T.J., Wilkins, J.A., Reed, K.R., Vass, J.K., Athineos, D., Clevers, H., and Clarke, A.R. (2007). Myc deletion rescues Apc deficiency in the small intestine. Nature *446*, 676–679.

Schmidt, S.F.F., Larsen, B.D.D., Loft, A., Nielsen, R., Madsen, J.G., and Mandrup, S. (2015). Acute TNF-induced repression of cell identity genes is mediated by NFκB-directed redistribution of cofactors from super-enhancers. Genome Res. *25*, 1281–1294.

Seitz, V., Butzhammer, P., Hirsch, B., Hecht, J., Gütgemann, I., Ehlers, A., Lenze, D., Oker, E., Sommerfeld, A., von der Wall, E., et al. (2011). Deep sequencing of MYC DNA-binding sites in Burkitt lymphoma. PLoS ONE *6*, e26837.

Shachaf, C.M., Kopelman, A.M., Arvanitis, C., Karlsson, A., Beer, S., Mandl, S., Bachmann, M.H., Borowsky, A.D., Ruebner, B., Cardiff, R.D., et al. (2004). MYC inactivation uncovers pluripotent differentiation and tumour dormancy in hepatocellular cancer. Nature *431*, 1112–1117.

Shang, E., Wang, X., Wen, D., Greenberg, D.A., and Wolgemuth, D.J. (2009). Double bromodomain-containing gene Brd2 is essential for embryonic development in mouse. Dev. Dyn. *238*, 908–917.

Sharma, V.M., Calvo, J.A., Draheim, K.M., Cunningham, L.A., Hermance, N., Beverly, L., Krishnamoorthy, V., Bhasin, M., Capobianco, A.J., and Kelliher, M.A. (2006). Notch1 contributes to mouse T-cell leukemia by directly inducing the expression of c-myc. Mol. Cell. Biol. *26*, 8022–8031.

Sheiness, D., and Bishop, J.M. (1979). DNA and RNA from uninfected vertebrate cells contain nucleotide sequences related to the putative transforming gene of avian myelocytomatosis virus. J. Virol. *31*, 514–521.

Shi, J., and Vakoc, C.R. (2014). The mechanisms behind the therapeutic activity of BET bromodomain inhibition. Mol. Cell *54*, 728–736.

Shi, J., Wang, Y., Zeng, L., Wu, Y., Deng, J., Zhang, Q., Lin, Y., Li, J., Kang, T., Tao, M., et al. (2014). Disrupting the interaction of BRD4 with diacetylated Twist suppresses tumorigenesis in basal-like breast cancer. Cancer Cell *25*, 210–225.

Sicklick, J.K., Li, Y.-X.X., Jayaraman, A., Kannangai, R., Qi, Y., Vivekanandan, P., Ludlow, J.W., Owzar, K., Chen, W., Torbenson, M.S., et al. (2006). Dysregulation of the Hedgehog pathway in human hepatocarcinogenesis. Carcinogenesis *27*, 748–757.

Soucek, L., Helmer-Citterich, M., Sacco, A., Jucker, R., Cesareni, G., and Nasi, S. (1998). Design and properties of a Myc derivative that efficiently homodimerizes. Oncogene *17*, 2463–2472.

Soucek, L., Jucker, R., Panacchia, L., Ricordy, R., Tatò, F., and Nasi, S. (2002). Omomyc, a potential Myc dominant negative, enhances Myc-induced apoptosis. Cancer Res. *62*, 3507–3510.

Soucek, L., Whitfield, J., Martins, C., Finch, A., Murphy, D., Sodir, N., Karnezis, A., Swigart, L., Nasi, S., and Evan, G. (2008). Modelling Myc inhibition as a cancer therapy. Nature *455*, 679–683.

Soufi, A., Donahue, G., and Zaret, K.S. (2012). Facilitators and impediments of the pluripotency reprogramming factors' initial engagement with the genome. Cell *151*, 994–1004.

Strasser, A., Harris, A.W., Bath, M.L., and Cory, S. (1990). Novel primitive lymphoid tumours induced in transgenic mice by cooperation between myc and bcl-2. Nature *348*, 331–333.

Strobl, L.J., and Eick, D. (1992). Hold back of RNA polymerase II at the transcription start site mediates down-regulation of c-myc in vivo. EMBO J. *11*, 3307–3314.

Subramanian, A., Tamayo, P., Mootha, V.K., Mukherjee, S., Ebert, B.L., Gillette, M.A., Paulovich, A., Pomeroy, S.L., Golub, T.R., Lander, E.S., et al. (2005). Gene set enrichment analysis: a knowledge-based approach for interpreting genome-wide expression profiles. Proc. Natl. Acad. Sci. U.S.A. *102*, 15545–15550.

Sun, Y., Wang, Y., Toubai, T., Oravecz-Wilson, K., Liu, C., Mathewson, N., Wu, J., Rossi, C., Cummings, E., Wu, D., et al. (2015). BET bromodomain inhibition suppresses graft-versus-host disease after allogeneic bone marrow transplantation in mice. Blood *125*, 2724–2728.

Toyoshima, M., Howie, H.L., Imakura, M., Walsh, R.M., Annis, J.E., Chang, A.N., Frazier, J., Chau, B.N., Loboda, A., Linsley, P.S., et al. (2012). Functional genomics identifies therapeutic targets for MYC-driven cancer. Proc. Natl. Acad. Sci. U.S.A. *109*, 9545–9550.

Vennstrom, B., Sheiness, D., Zabielski, J., and Bishop, J.M. (1982). Isolation and characterization of c-myc, a cellular homolog of the oncogene (v-myc) of avian myelocytomatosis virus strain 29. J. Virol. *42*, 773–779.

Vervoorts, J., Lüscher-Firzlaff, J.M., Rottmann, S., Lilischkis, R., Walsemann, G., Dohmann, K., Austen, M., and Lüscher, B. (2003). Stimulation of c-MYC transcriptional activity and acetylation by recruitment of the cofactor CBP. EMBO Rep. *4*, 484–490.

Vervoorts, J., Lüscher-Firzlaff, J., and Lüscher, B. (2006). The ins and outs of MYC regulation by posttranslational mechanisms. J. Biol. Chem. *281*, 34725–34729.

Vita, M., and Henriksson, M. (2006). The Myc oncoprotein as a therapeutic target for human cancer. Semin. Cancer Biol. *16*, 318–330.

Wang, F., Liu, H., Blanton, W.P., Belkina, A., Lebrasseur, N.K., and Denis, G.V. (2010). Brd2 disruption in mice causes severe obesity without Type 2 diabetes. Biochem. J. *425*, 71–83.

Wang, R., Li, Q., Helfer, C.M., Jiao, J., and You, J. (2012). Bromodomain protein Brd4 associated with acetylated chromatin is important for maintenance of higher-order chromatin structure. J. Biol. Chem. *287*, 10738–10752.

Weng, A.P., Millholland, J.M., Yashiro-Ohtani, Y., Arcangeli, M.L., Lau, A., Wai, C., Del Bianco, C., Rodriguez, C.G., Sai, H., Tobias, J., et al. (2006). c-Myc is an important direct target of Notch1 in T-cell acute lymphoblastic leukemia/lymphoma. Genes Dev. *20*, 2096–2109.

Whyte, W.A., Orlando, D.A., Hnisz, D., Abraham, B.J., Lin, C.Y., Kagey, M.H., Rahl, P.B., Lee, T.I., and Young, R.A. (2013). Master transcription factors and mediator establish super-enhancers at key cell identity genes. Cell *153*, 307–319.

Wierstra, I., and Alves, J. (2008). The c-myc promoter: still MysterY and challenge. Adv. Cancer Res. *99*, 113–333.

Xie, W., Schultz, M.D., Lister, R., Hou, Z., Rajagopal, N., Ray, P., Whitaker, J.W., Tian, S., Hawkins, R.D., Leung, D., et al. (2013). Epigenomic analysis of multilineage differentiation of human embryonic stem cells. Cell *153*, 1134–1148.

Yang, Z., Yik, J.H., Chen, R., He, N., Jang, M.K., Ozato, K., and Zhou, Q. (2005). Recruitment of P-TEFb for stimulation of transcriptional elongation by the bromodomain protein Brd4. Mol. Cell *19*, 535–545.

Zeitlinger, J., Stark, A., Kellis, M., Hong, J.-W.W., Nechaev, S., Adelman, K., Levine, M., and Young, R.A. (2007). RNA polymerase stalling at developmental control genes in the Drosophila melanogaster embryo. Nat. Genet. *39*, 1512–1516.

Zhang, Y., Liu, T., Meyer, C.A., Eeckhoute, J., Johnson, D.S., Bernstein, B.E., Nusbaum, C., Myers, R.M., Brown, M., Li, W., et al. (2008). Model-based analysis of ChIP-Seq (MACS). Genome Biol. *9*, R137.

Zhao, R., Nakamura, T., Fu, Y., Lazar, Z., and Spector, D.L. (2011). Gene bookmarking accelerates the kinetics of post-mitotic transcriptional re-activation. Nat. Cell Biol. *13*, 1295–1304.

Zuber, J., Shi, J., Wang, E., Rappaport, A.R., Herrmann, H., Sison, E.A., Magoon, D., Qi, J., Blatt, K., Wunderlich, M., et al. (2011). RNAi screen identifies Brd4 as a therapeutic target in acute myeloid leukaemia. Nature *478*, 524–528.

Acknowledgments

I would like to thank Chiara, Serena, Marieta, Manuel and Francesca for scientific and, especially, not scientific discussions, for everyday life in the lab and outside the lab and for supporting me during these 4 years.

I would like to thank also Arianna, Andrea, Bobo, Paola and Matteo for helping me when I needed it and for supporting me and spurring me on.

I would like to thank Ottavio for the great help with the genome wide data and for his “R for dummies” lessons.

I would like to thanks Sara, Alessandra and Lucia for sharing the good times and the bad during all these 4 years.

I would like to thanks also all the campus facilities (kitchen, warehouse, cell culture, animal house and sequencing) for making our liver easier.

Finally, I thank Stefano for the great experience and opportunity, for challenging me and making me go beyond my limits and for believing in me since the beginning.